UNIL | Université de Lausanne
Faculté de biologie
et de médecine

Département de Physiologie
Département de Biologie Cellulaire et de Morphologie

Study of the physiological role of RasGAP cleavage

Thèse de doctorat ès sciences de la vie (PhD)

Présentée à la Faculté de biologie et de médecine de l'Université de Lausanne par

Joël Walicki

Licence en biologie moleculaire de
L'Université de San Luis,
Argentine

Jury

Prof. Olivier Staub, President of the Jury
Prof. Christian Widmann, Thesis Director
Prof. Jean-Claude Martinou, Expert
Prof. Thomas Brunner, Expert

Lausanne 2007

UNIL | Université de Lausanne
Faculté de biologie
et de médecine

Ecole Doctorale

Imprimatur

Vu le rapport présenté par le jury d'examen, composé de

Président	Monsieur Prof.	Olivier **Staub**
Directeur de thèse	Monsieur Prof.	Christian **Widmann**
Experts	Monsieur Prof.	Thomas **Brunner**
	Monsieur Prof.	Jean-Claude **Martinou**

le Conseil de Faculté autorise l'impression de la thèse de

Monsieur Joël Walicki

Licence en biologie moléculaire de l'Université San Luis, Argentine

intitulée

Study of the physiological role of RasGAP cleavage

Lausanne, le 18 janvier 2008

pour Le Doyen
de la Faculté de Biologie et de Médecine

Prof. Olivier Staub

Acknowledgments

First I would like to express my gratitude to ALL my family, without them this adventure would have never started. A special consideration goes to my parents Miguel and Françoise, their constant support and their multiple efforts made this possible.

I would like to thank my supervisor, Christian Widmann, who opened to me the doors of his laboratory. I want to show my appreciation for all lab members (past and present). Science is teamwork; they were always available and collaborated to generate a great ambient in the lab.

I don't want to forget all the members of the department, specially the persons with whom I shared the floor and office. For all the discussions and coffees that we shared, these moments constitute the human side of science.

I would like to show my indebtedness to the many people around the university that gave me a hand when I was stacked in a problem.

Last but not least, I want to show my deep gratitude to Simona. You were there when I most needed it.

Résume

Les caspases sont un groupe de protéases à cystéine qui s'activent lors de l'apoptose. Leur activation induit le clivage de nombreuses cibles intracellulaires, conduisant à l'activation de voies pro-apoptotiques et finalement au démantèlement des cellules. Cependant, des caspases ont été décrites dans de nombreux autres processus indépendants de l'apoptose, notamment dans la physiologie des cellules hématopoïétiques, des cellules musculaires, des cellules de la peau et des neurones.

Comment est-ce que les cellules réconcilient-elles ces deux fonctions distinctes? Une partie de la réponse réside dans la nature des substrats qu'elles clivent. Certains substrats, une fois clivées, deviennent anti-apoptotiques. RasGAP est une cible des caspases et contient deux sites spécifiques de clivage par les caspases. Lorsque le niveau d'activité des caspases est faible le clivage de RasGAP produit un fragment N-terminal qui active un signal anti-apoptotique, relayé par la voie de Ras/PI3K/Akt. Lorsque le niveau d'activité des caspases est plus élevé le fragment RasGAP N-terminal est à nouveau clivé, perdant de ce fait ses propriétés anti-apoptotiques.

Dans cette étude, nous avons mis en évidence que l'activation de la voie Ras/PI3K/Akt induite par le fragment RasGAP N-terminal dépend de RasGAP lui-même. Par ailleurs, dans le but d'étudier l'importance du clivage de RasGAP dans un contexte physiologique, nous avons développé un modèle animal exprimant une gêne mutée de RasGAP de sorte que la protéine est devenu insensible a l'action de caspases. Les données préliminaires obtenues montrent que le clivage de RasGAP n'est pas indispensable pour le développement et l'homéostasie chez la souris. Finalement, nous avons développé une souris transgénique surexprimant le fragment de RasGAP N-terminal dans les cellules ß du pancréas. Les animaux obtenus ne montrent pas de symptômes dans les conditions basales bien qu'ils soient plus résistants au diabète induit expérimentalement. Ces résultats montrent que la surexpression du fragment N-terminal de RasGAP protége efficacement les cellules ß du pancréas de l'apoptose induite par le stress sans pourtant affecter d'autres paramètres physiologiques des Ilot de Langerhans.

Summary

Caspases are a series of proteases that are activated during apoptosis. Their activation causes the cleavage of numerous intracellular targets, which leads to cell dismantling and activation of pro-apoptotic pathways. Caspases have been found to be involved in the physiology of numerous cell types including haematopoietic cells, muscle cells, skin cells and neurons.

How cells conciliate these two opposite functions? Part of the answer lies in the nature of the substrates they cleave. Some substrates become anti-apoptotic once cleaved by caspases. RasGAP is a caspase substrate that possesses two conserved caspase-cleavage sites. At low caspase activity, RasGAP is first cleaved and the generated N-terminal fragment activates a potent anti-apoptotic signal, mediated by the Ras/PI3K/Akt pathway. At higher caspase activity, the N-terminal fragment is further cleaved thereby losing its anti-apoptotic properties.

In the present study we show that the activation of the Ras/PI3K/Akt pathway mediated by RasGAP N-terminal fragment is dependent on RasGAP itself. Moreover, to study the role of RasGAP cleavage in a physiological model, we have developed a knock-in mouse model expressing a RasGAP mutant that is not cleavable by caspases. Preliminary data shows that RasGAP cleavage is not required for normal development and homeostasis in mice. Finally, we have developed a transgenic mouse model overexpressing RasGAP N-terminal fragment in the ß-cell of the pancreas. In basal conditions, these mice show no difference with their wt counterparts. However, they are protected against experimentally induced diabetes. These results indicate that fragment N can protect β cells from stress-induced apoptosis without affecting other physiological parameters of the Islets.

Index

Chapter 1 – Introduction

1 INTRODUCTION

1.1 Cell death

In the middle of the nineteenth century, soon after the discovery that organisms are composed of cells, cell death was found to play an important role in animal development. Cell death was first discovered during amphibian metamorphosis [1] and later found to occur in developing tissues of both vertebrates and invertebrates [2, 3]. In 1969 Lockshin coined the expression Programmed Cell Death (PCD) after observing that cell death occurred at predictable times and places during development [4]. In 1972, after a detailed analysis of morphological evidence, Kerr and colleagues proposed to distinguish between cells dying after acute lesions and cells dying during animal development or tissue homeostasis. In the first case, cells tend to swell and rupture, inducing inflammation, in a process called necrosis. By contrast, cells dying during development or tissue homeostasis shrink and condense keeping their integrity, in a process named by Kerr and colleagues Apoptosis (from the Greek *apoptōsis* (αποπτωσισ) 'falling off' of petals from a flower, or leaves from a tree) [5]. Robert Horvitz and colleagues used *Caenorhabditis Elegans* as a model organism and 20 years later discovered that all cells have an in-built suicide program and started to characterize its building blocks (reviewed in [6]).

Ever since, cell death has typically been discussed as either apoptosis or necrosis. The finding that other forms of cell death are also programmed is gradually changing this notion, figure 1. According to a recent classification, eight different types of cell death were delineated [7], and some researchers describe as many as 11 pathways of cell death in mammals, 10 of which appear to be programmed [8]. These pathways can be broadly divided into two main groups: apoptotic and non-apoptotic.

Apoptotic cell death is biochemically defined as a form of programmed cell death executed by the activation of the caspase cascade. Non-apoptotic cell death includes autophagy, necrosis (sometimes called oncosis), mitotic cell death (mitotic catastrophe) and caspase independent cell death (CICD).

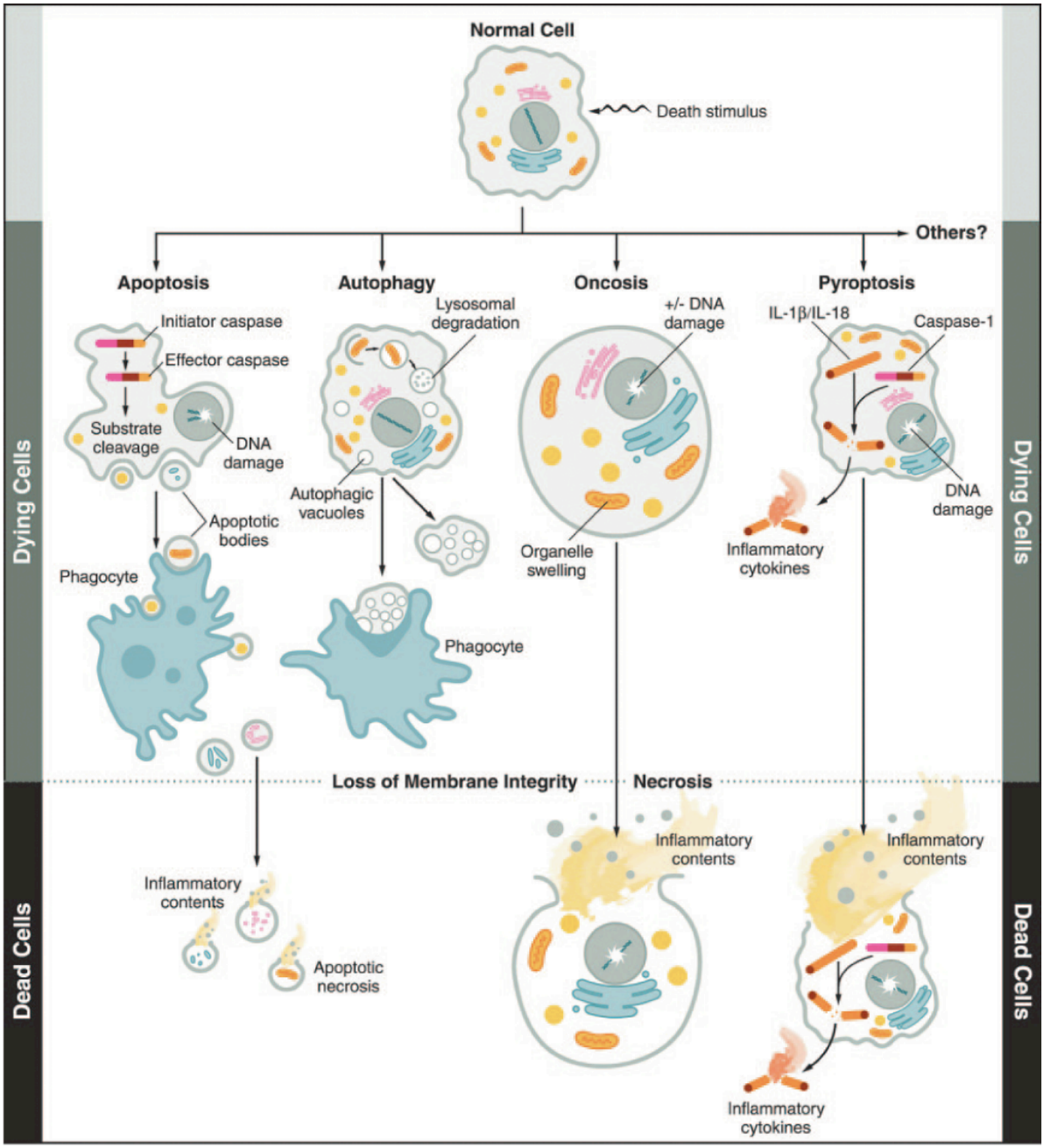

Figure 1. Different pathways leading to cell death.
Schematic representation of some of the different forms of cell death. *Adapted from Fink SL et al Infect Immun 2005 vol. 73 pp. 1907-16.*

1.1.1 Apoptotic cell death.

Apoptotic cell death comprises apoptosis, which will be discussed later, and *anoikis*.

Anoikis is a form of apoptosis induced by loss of attachment to the surrounding extracellular matrix or to other cells. Besides its specific form of induction, the molecular mechanisms appear to be classic apoptosis. Resistance to *anoikis* seems to be an important step in the development of cancer [9].

1.1.2 Non-apoptotic cell death.

Autophagy is based on an evolutionary conserved and genetically controlled turnover of cellular constituents that occurs in all eukaryotic cells [10]. This process is activated in response to nutrient starvation, during differentiation, and following developmental triggers. It is an adaptive process responding to metabolic stress that results in degradation of intracellular proteins and organelles [11].

Mitotic catastrophe occurs during or shortly after a dysregulated or failed mitosis and can be accompanied by morphological alterations such as micronuclei (which often are chromosomes or chromosome fragments that have not been distributed evenly between the daugther nuclei) and multinucleation (the presence of two or more nuclei with similar or heterogeneous sizes, resulting from deficient separation during cytokinesis) [7].

Necrosis/Oncosis is usually a consequence of pathophysiological conditions such as infection, inflammation or ischemia. The prominent features are cellular energy depletion, damage to membrane lipids with cell membrane swelling and rupture, loss of function of homeostatic ion pumps/channels, and activation of non-apoptotic proteases [11]. Although necrosis has been considered to be a passive process, some recent findings suggest it could be a regulated process [12-14].

Caspase-independent cell death shares features with classical apoptosis (e.g., mitochondrial outher membrane permeabilization (MOMP) induction, diffusion of some proteins from the

intermembrane space of the mitochondria and DNA fragmentation). As it does not rely on activation of the caspase cascade, it is therefore classified as a non-apoptotic form of death [15].

1.2 Apoptosis

According to the Nomenclature Committee on Cell Death, apoptosis is a type of cell death that is accompanied by rounding-up of the cell, retraction of pseudopodes, reduction of cellular volume (*pyknosis*), condensation of the chromatin, fragmentation of the nucleus (*karyorhexis*), little or no ultrastructural modification of cytoplasmic organelles, plasma membrane blebbing, and maintenance of an intact plasma membrane until late stages of the process [7]. The biochemical hallmark of apoptosis is the activation of a series of zymogenic cystein proteases that cut after aspartic residues, the caspases.

Apoptosis is involved in the normal physiology, including elimination of damaged or virally infected cells, negative selection in the thymus and during development, elimination of temporary structures and tissue remodelling (e.g. bud limb development). A careful control of cell death mechanisms is fundamental. Aberrant activation may contribute to different diseases (e.g. neurodegenerative disorders, AIDS, ischemic injury, etc). In contrast, deficient cell death is a major factor in the aetiology of cancer and autoimmune disorders, among others [16].

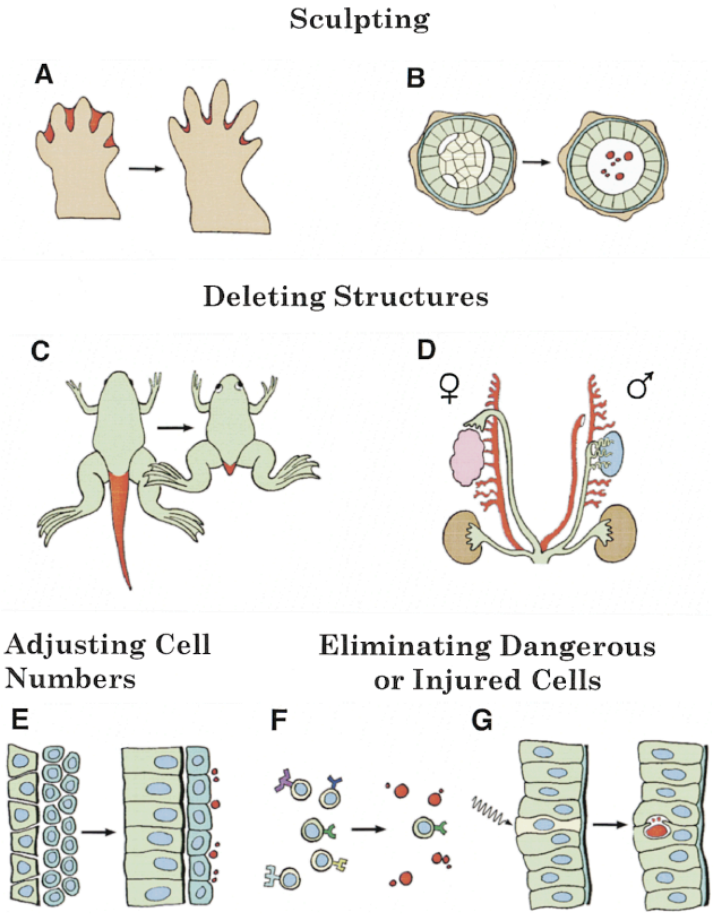

Figure 2. Physiological roles of apoptosis.
A and B sculpting, C and D, deleting unwanted structures, E controlling cell number, F and G eliminating non-functional harmful abnormal, or misplaced cells. Adapted from *Jacobson MD, Cell, 1997 vol. 88 pp. 347-54.*

1.2.1 Physiological apoptosis.

In the human body about one hundred thousand cells are produced every second by mitosis and a similar number dies by apoptosis to maintain homeostasis and for specific tasks such as the regulation of immune cell selection and activity [17]. Most cells produced during embryonic development undergo programmed cell death before the end of the perinatal period. Some of the more important physiological processes, in which apoptosis is involved, are described below, figure 2.

1.2.1.1 Development and Morphogenesis

During development many cells are produced in excess which eventually undergo programmed cell death and thereby contribute to sculpturing many organs and tissues [18]. A good example of this process is the formation of free and independent digits by massive

cell death in the interdigital mesenchymal tissue [19-21]. Furthermore, during the development of the brain, half of the neurons that are initially created die in later stages when the adult brain is formed [22].

A classic example of morphogenesis is seen in amphibian tadpoles, where an increase in thyroid hormone in the blood induces cells in the tail to undergo programmed cell death, facilitating the resorption of the developing tail [23].

Programmed cell death also occurs wherever epithelial sheets invaginate and pinch off to form tubes or vesicles, as in the formation of the vertebrate neural tube or lens, and it is observed when two epithelial sheets come together and fuse, as in the formation of the mammalian palate [2].

1.2.1.2 Homeostasis.

A paradigm of apoptosis involvement in maintaining homeostasis is the immune system. The majority of the developing lymphocytes die either during genetic rearrangement events during formation of the antigen receptor, during negative selection or in the periphery, thereby tightly controlling the pool of highly efficient and functional but not self-reactive immune cells and at the same time keeping lymphocyte numbers relatively constant [24].

1.2.2 Apoptosis in disease.

Involvement of apoptosis in development of disease can be due to both decreased or increased cell death.

Diseases characterized by the accumulation of cells include cancer, autoimmune diseases, and certain viral illnesses. Cell accumulation can result from either increased proliferation or the failure of cells to undergo apoptosis in response to appropriate stimuli. Even if involvement of increased cell proliferation in these disorders has been investigated, increasing evidence suggests that failure to undergo apoptosis, rather than increased proliferation, is involved in these diseases.

1.2.2.1 Cancer

Failure to complete apoptosis is a hallmark of cancer and the main target for anticancer therapies. Survival of neoplasic cells beyond their normally intended lifespan requires to overcome the need for exogenous survival factors, to acquire resistance to the necessity of cell-cell contacts [9] and to provide protection from hypoxia and oxidative stress as the tumor mass expands [25, 26]. Similarly, tumours are resistant to apoptosis induced by DNA damage or abnormal chromosomal segregation. These apoptosis defects permit survival of genetically unstable cells, providing opportunities for selection of progressively more aggressive clones [27]. In this context, it is not surprising that p53, commonly named "the guardian of the genome" [28], is mutated in the majority of human tumours and is often associated with advance tumor stage and poor patient prognosis [29]

Several members of the Inhibitor of Apoptosis Proteins family have been involved in apoptosis. For example, survivin is prominently expressed in most cancers [30] and XIAP overexpression is a negative prognosis marker in acute myelogenous leukaemia (ALM) [31].

1.2.2.2 Autoimmunity

Autoimmune diseases can be due to the failure to remove autoimmune cells that arise during development or that develop because of somatic mutation during an immune response. Inadequate clearance of apoptotic cells has been linked to autoimmune and persistent inflammatory diseases [32]. Defective removal of apoptotic cells by macrophages leads to secondary necrosis, release of danger signals and engulfment by dendritic cells. Uptake of apoptotic cells by dendritic cells can lead to autoimmunity because protein cleavage in dying cells can lead to the generation of neo-autoantigens [33]. Patients suffering from systemic lupus erythematosus might have some uncharacterized defects in the ability of macrophages to eliminate apoptotic cells [34].

1.2.2.3 Viral infection.

A number of viruses have developed strategies to disrupt normal regulation of cell death within the infected cell. For example, the first member of the IAP family has been found in baculorivus [35]. Viral homologues of cellular FLICE-inhibitory protein (cFLIP), known as viral FLIPs (vFLIPs), are contained in several poxvirus and herpes virus genomes. vFLIP seems to inhibit caspase-8 activation by binding to it and FADD and thus inhibiting the formation of the death-inducing signalling complex (DISC)[36-38].

1.2.2.4 AIDS

AIDS is generated by the infection of the human immunodeficiency virus (HIV) and is correlated with apoptosis-mediated depletion of $CD4^+$ T cells [39, 40]. Expression of the viral envelope gp120-gp41 complex in infected cells mediates onset of apoptosis of both infected and non-infected cells. Thus, chronically HIV-infected cells can serve as effector cells to induce apoptosis in uninfected target $CD4^+$ T cells [41, 42].

1.2.2.5 Neurodegenerative disorders.

Wide variety of neurodegenerative disorders are characterized by the loss of a specific population of neurons [43] (e.g. Alzheimer's disease, Parkinson's disease, amyotrophic lateral sclerosis (ALS), retinitis pigmentosa, spinal muscular atrophy, etc).

1.2.2.6 Diabetes.

Excess of apoptosis has been linked to the pathophysiology of both, type 1 and type 2 diabetes. While in type 1 diabetes ß-cell death is caused by autoimmune attack of both $CD4^+$ and $CD8^+$ lymphocytes [44], in type 2 diabetes apoptosis is induced as a result of hyperglycemia [45], hyperlipidemia [46, 47] and the presence of inflammatory cytokines [48].

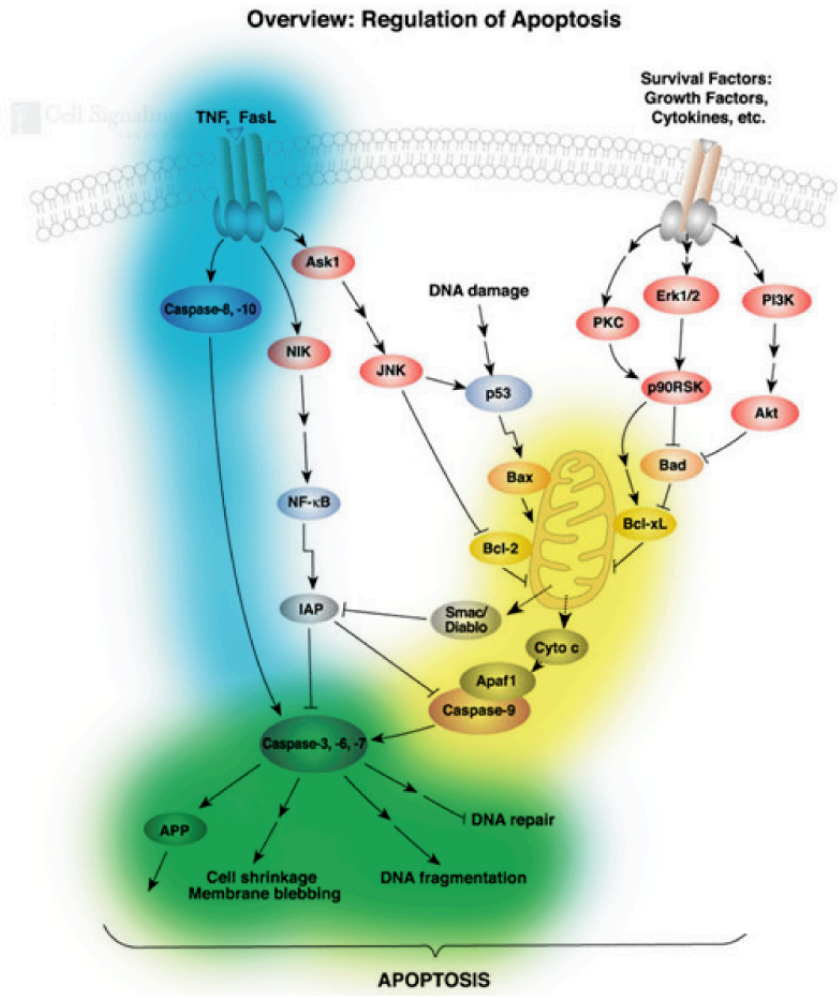

Figure 3. Pathways leading to apoptosis.
Death signals are integrated through death receptors for the extrinsic pathway (indicated in light blue), or through the mitochondria for the intrinsic pathway (indicated in yellow). Both pathways converge on downstream effector caspases (indicated in green), initiating the activation of a cascade of caspases that result in the specific cleavage of substrates, leading to cell dismantling.
Source *Cell Signalling*.

1.2.3 Mechanism of Apoptosis

Apoptosis is characterized by the activation of numerous proteins in a temporally as well as spatially tightly regulated sequence. Initiation is induced by two main stimuli: the binding of ligands to cell surface receptors of the tumor necrosis factor receptor (TNFR) superfamily that activates the "extrinsic pathway" and the damage of DNA integrity by various stress factors, radiation or major changes of the homeostasis of cells that initiate the "intrinsic pathway", figure 3.

1.2.3.1 Extrinsic pathway.

The extrinsic pathway, which leads to caspase activation, is initiated by oligomerization of "death receptors" triggered by the binding of their ligand. Death receptors belong to the tumor necrosis factor receptor (TNFR) superfamily, which includes TNFR-1, Fas/CD95 and the TNF-related apoptosis-inducing ligand (TRAIL) receptors DR-4 and DR-5 [49]. All members of the TNFR family are characterised by an extracellular cysteine rich domain (CRD), responsible for ligand recognition and oligomerization [50]. Subsequent signalling, induced by the oligomerization, is mediated by the intracellular death domains (DD).

The oligomerization of the "death receptors", induced by the binding of their ligands, leads to recruitment of adaptor proteins and to the formation of the death-inducing signalling complex (DISC). Fas-associated death-domain protein (FADD), one of these adaptor proteins, interacts with the death receptors via its own DD and recruits caspase-8 by binding to its death effector domain (DED). In addition to the initiator caspases, the DISC may contain other adaptor and signalling proteins, such as TNF-receptor associated death domain (TRADD), receptor interacting protein (RIP) and RIP-associated Ich-1/CED-3 homologous protein with a death domain (RAIDD). Furthermore, a set of inhibitory proteins, named FLICE-inhibitory proteins (FLIPs), is known to interact with the DISC. FLIPs contain two DED that interact with the DED of FADD and thus inhibit caspase-8 recruitment and activation by the TNFR family members [51, 52].

Recruitment of caspase-8 to the DISC domain is believed to trigger its activation; even tough it is not yet clear whether it is dimerization or autocatalytic cleavage the responsible for pro-caspase activation [53]. Once activated, caspase-8 cleaves downstream effector caspases resulting in cell death. Cells able to directly induce apoptosis upon death receptor stimulation, are known as type 1 cells [54]. In contrast, in type 2 cells, receptor stimulation is not sufficient to induce apoptosis. In these cells, the mithocondrial pathway amplifies the

signal. This is achieved via caspase-8 mediated cleavage of Bcl-2 family member Bid. When Bid is cleaved, its truncated form, tBid, translocates to the mitochondria and together with Bax and Bak induces the release of cytochrome c (Cyt c) and other pro-apoptotic proteins to the cytosol [55].

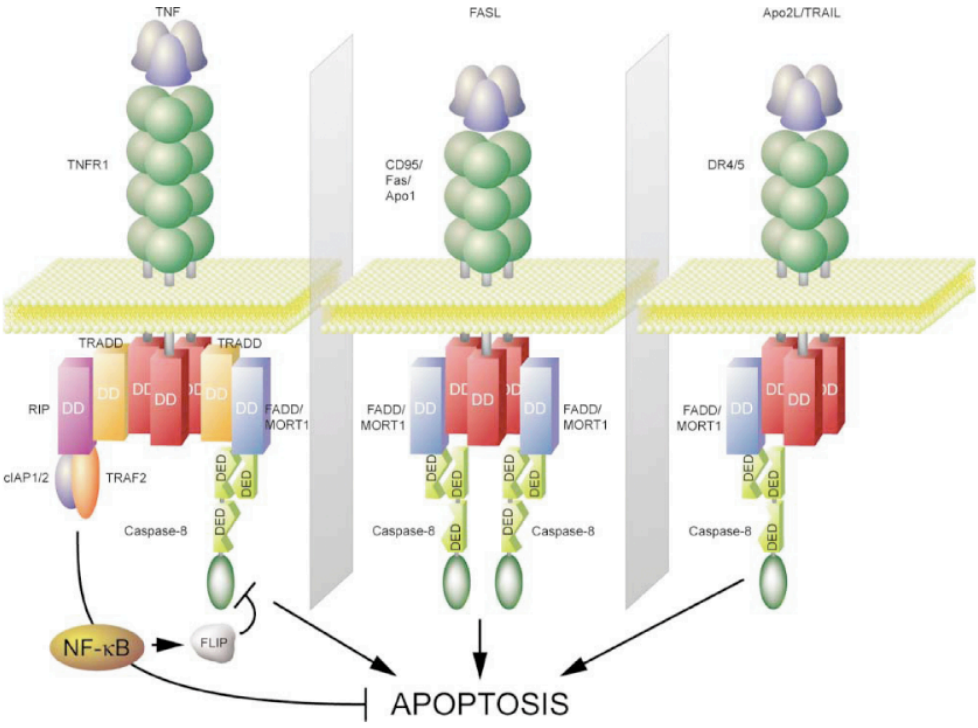

Figure 4. Death receptor induced apoptosis.
Death receptor trimerization induces the formation of the DISC, caspase-8 activation and triggering of apoptosis. Adapted from *Danial et al; Cell; 2004 vol. 116 (2) pp. 205-19.*

1.2.3.2 Intrinsic pathway.

The intrinsic pathway is mediated by the mitochondria and it is responsible for triggering apoptosis in response to cellular stress signals. The critical event that triggers apoptosis by the intrinsic pathway is the release of Cyt c and other mitochondrial proteins mediated by mitochondrial outer membrane permeabilization (MOMP).

Upon apoptotic stimuli, Cyt c is released into the cytosol where, in the presence of ATP, it mediates the allosteric activation and hepta-oligomerization of the adaptor molecule apoptosis-protease activating factor 1 (Apaf-1), generating the complex known as

apoptosome, figure 5. Each apoptosome can recruit seven dimers of caspase-9 and promote their activation leading to proteolytic self-processing.

For a long time, the release of Cyt c has been postulated to be an "all-or-nothing" process. Now cumulative data suggest that Cyt c release is rather biphasic. Accordingly, a first wave of Cyt c release would affect only a small part of the Cyt c pool. The release of this first pool of Cyt c then boosts several different amplification loops, which allow for the complete release of Cyt c. This biphasic Cyt c release adds another layer of regulation for the apoptosis triggering. The release of a small part of the mitochondrial pool of Cyt c would prevent the triggering of apoptosis upon an accidental Cyt c release.

Other proteins released from the mitochondria, together with Cyt c, facilitate apoptosis induction by preventing IAP-mediated caspase inhibition. Good examples are the second mitochondria-derived activator of caspases/direct inhibitor of apoptosis-binding protein with low isoelectric point (Smac/DIABLO) and high temperature requirement protein A2 (HtrA2, also known as Omi) that interact and neutralize inhibitor of apoptosis proteins (IAPs) when released into the cytosol [56, 57]. Another set of proteins released from the mitochondria are the flavoprotein apoptosis-inducing factor (AIF) and endonuclease G (Endo G) which are mainly involved in caspase-independent cell death [58].

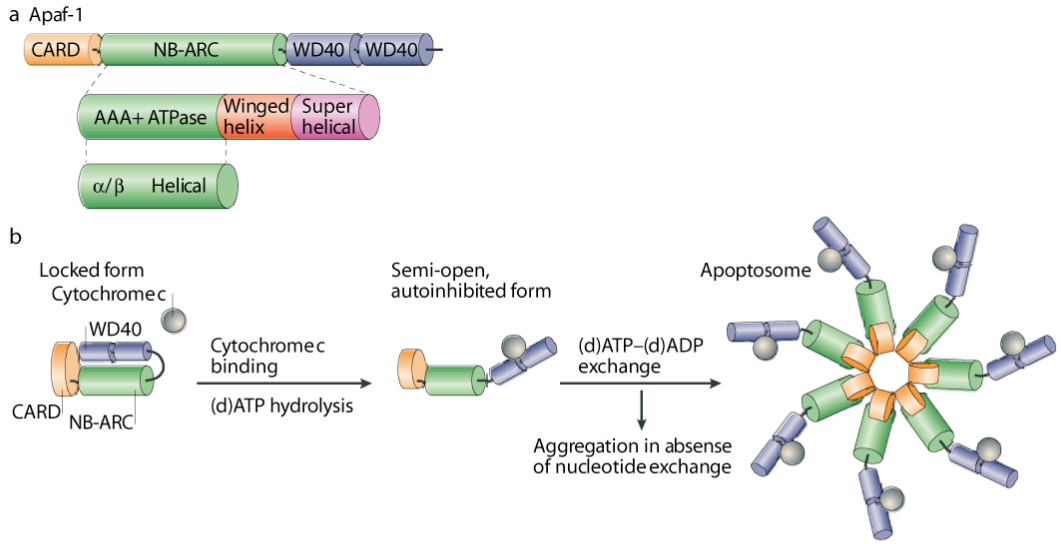

Figure 5. Mechanism of apoptosome formation.
a) Apaf-1 can be divided into three functional units: the N-terminal caspase-recruitment domain (CARD), which is responsible for recruiting caspase-9; a nucleotide-binding and oligomerization domain (NOD), which is responsible for (d)ATP (ATP or 2'-deoxy ATP)-dependent oligomerization, and the WD40 region, which is responsible for binding of cytochrome c.
b) Apoptosome formation. In the absence of an apoptotic signal, Apaf-1 exists in a locked autoinhibited form. Following an apoptotic signal, the binding of cytochrome c to the WD40 region of Apaf-1 releases the lock leading to a semi-open, still autoinhibited, form of Apaf-1. This rearrangement is concurrent with the hydrolysis of the bound nucleotide to (d)ADP. Neither oligomerization nor caspase-9 binding to the CARD domain of Apaf-1 is possible in this conformation. (d)ATP nucleotide exchange leads to oligomerization and apoptosome formation, whereas aggregation occurs in the absence of exchange. The apoptosome adopts a wheel-like structure with the cytochrome-c-bound WD40 regions sticking out like spokes, whereas the NOD regions and CARDs form the central part of the wheel.
Adapted from Riedl SJ and Salvesen Gs, Nat. Rev. Mol. Cell. Biol., 2007, vol. 8 pp. 405-13.

Bcl-2 family.

MOMP is a highly controlled process regulated by the members of the Bcl-2 family. Bcl-2, the founding member of the family, was discovered at the chromosomal breakpoint of translocation t(14;18) bearing human B-cell lymphomas [59, 60]. The Bcl-2 family has expanded significantly and includes both anti- and pro-apoptotic molecules. Members of this family have the ability to form homo- as well as heterodimers, suggesting neutralizing competition between these proteins. It seems that the ratio between pro- and anti-apoptotic subsets helps to determine partially the susceptibility of cells to a death signal [61].

Bcl-2 family members are characterized by the presence of up to four Bcl-2 homology (BH) domains, denominated BH1, BH2, BH3 and BH4, figure 6 [62-64]. Anti-apoptotic members of the Bcl-2 family (Bcl-2, Bcl-xl, A1, Bcl-w, Mcl-1) show sequence conservation in the four BH domains and are initially located at the level of the outer mithocondrial membrane, where they bind and inhibit pro-apoptotic proteins of the Bcl-2 family [65]. They are also found at the level of the endoplasmic reticulum, or nuclear membrane [66-68]. Anti-

apoptotic Bcl-2 family members act by preventing MOMP, and thus inhibit Cyt c release and Apaf-1 activation, figure 6.

Bcl-2 pro-apoptotic family members can be separated in two structurally different subfamilies. The multidomain pro-apoptotic Bcl-2 family is structurally similar to the anti-apoptotic members of the family and shares three of the four BH domains (BH1-3). Bax, Bak and Bok are notable members of this family. In normal conditions they are located in the cytosol but upon apoptotic stimuli they suffer a conformational change and are translocated and inserted into the mitochondria outer membrane. They seem to be necessary [69] and sufficient [70] to induce mitochondrial permeabilization. The BH3-only pro-apoptotic Bcl-2 family members (Puma, Noxa, Bim, Bid, Bad, Bnip3, etc) are structurally heterogenous and share only the BH3 domain with other Bcl-2 family members and therefore are named BH3-only proteins. BH3-only proteins act upstream of multidomain pro-apoptotic Bcl-2 family members. They operate as sensors for death stimuli in the cell, and play a major role in transducing signals from the cytosol to the mitochondria. BH3-only proteins can promote apoptosis by two different mechanisms: some BH3-only proteins preferentially interact with anti-apoptotic Bcl-2 family members, dissociating them from Bcl-2 pro-apoptotic family members, which in turn promote apoptosis; others act through direct activation of Bak and Bax [65].

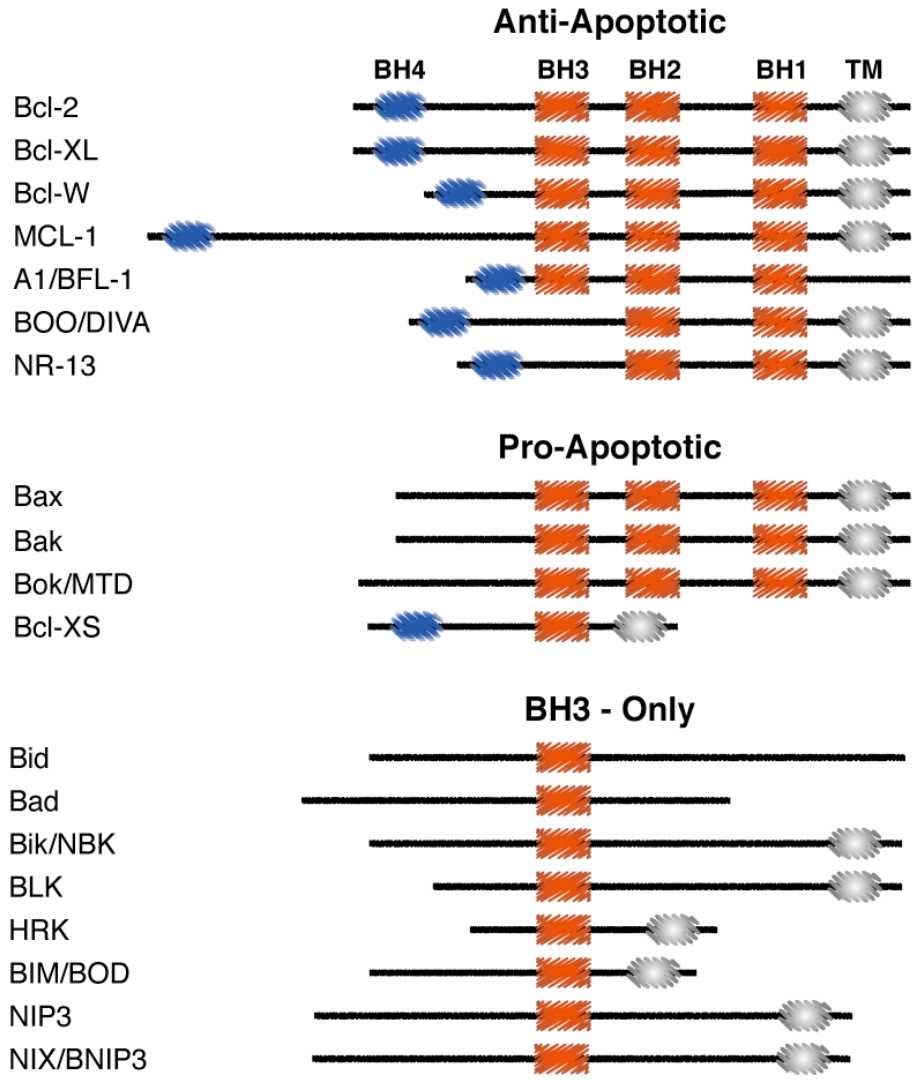

Figure 6. Bcl-2 family members.
Summary of anti-apoptotic and pro-apoptotic BCL-2 members. BCL-2 homology regions (BH1-4) are denoted as is the carboxy-terminal hydrophobic (TM) domain. Adapted from *Gross A et al. Genes. Dev. 1999 vol 13 pp. 1899-911.*

1.3 Caspases

Caspases are an evolutionarily conserved family of aspartate specific cystein-dependent proteases (Cysteine ASPartate-specific proteASES) [71] with central functions in apoptotic and inflammatory signalling pathways. Caspases and their homologues have been reported in species that range from *Caenorhabditis elegans* [72], *Drosophila Melanogaster* [73] and even *Saccharomyces cerevisiae* [74], figure 7. Fourteen caspases have been described until now (caspases 1-14), twelve of which are present in humans (caspases 1–10, caspase 12 and caspase 14). Caspase 11 was identified as the mouse homolog of human caspase 4, while caspase 13 has been shown to be the bovine homolog of human caspase 4 [75].

Caspases can be grouped according to their function. The first group, implicated in the maturation of cytokines, includes caspases 1, 4, 5 and 14 [76]. The involvement of this group of caspases in the process of apoptosis is not straightforward. The second group, which includes caspases 2, 3, 6, 7, 8, 9, 10 and 12, is implicated in apoptosis.

Caspases involved in apoptosis are divided into initiator and executioner caspases. The initiator caspases, which include caspases 2, 8, 9, 10 and 12, have long prodomains with recognisable homotypic protein–protein interaction motifs, such as the death effector domain (DED) or the caspase recruitment domain (CARD) that contribute to the transduction of various signals into proteolytic activity. The two major initiator caspases, 8 and 9, function through distinct pathways, which culminate in the activation of the main effector pro-caspase 3 in the cytosol. Caspases 3, 6 and 7 are known as the effector caspases. The zymogens of these caspases have short prodomains and lack intrinsic enzymatic activity.

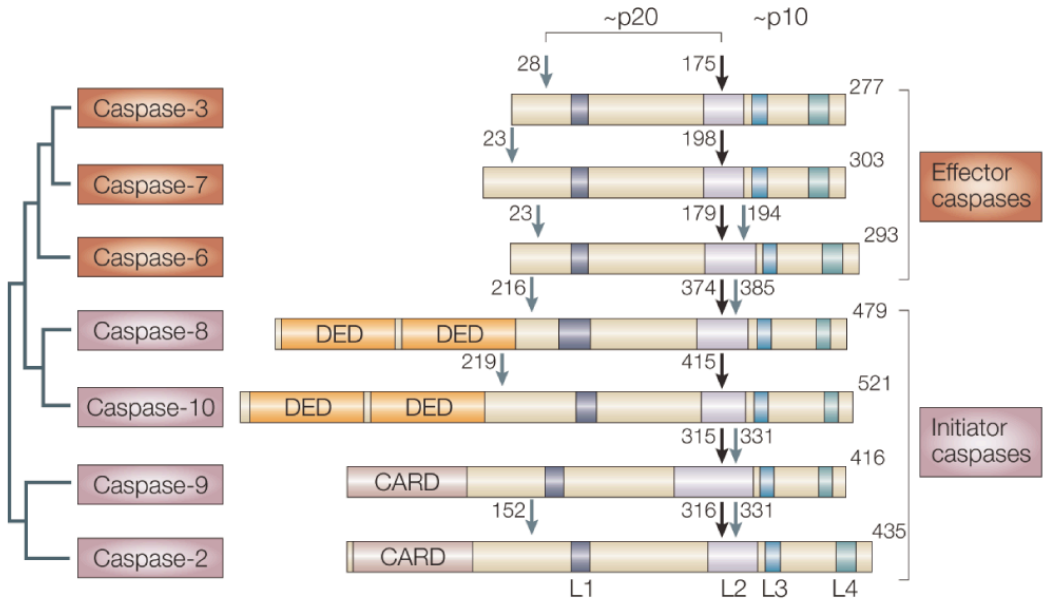

Figure 7. Apoptotic caspases in mammals.
The effector and initiator caspases are shown in red and purple, respectively. The position of the first intra-chain activation cleavage (between the large and small subunits, ~p20 and ~p10, respectively) is highlighted by a black arrow, whereas other sites of cleavage are represented by grey arrows. These other cleavage events are thought to modulate caspase activity and the regulation of caspases by inhibitor of apoptosis (IAP) proteins and by other proteins. Unlike other protease zymogens, removal of the N-terminal prodomain of a caspase is unnecessary for its catalytic activity. The prodomains in initiator caspases invariably contain homotypic interaction motifs, such as the caspase-recruitment domain (CARD) and the death-effector domain (DED). The four surface loops (L1–L4) that shape the catalytic groove are indicated. The catalytic residue Cys is shown as a red line at the beginning of L2. The p20 and p10 subunits together form a caspase monomer. The caspases and the location of functional segments are drawn to scale.
Adapted from *Riedl SJ and Shi Y, Nat. Rev. Mol. Cell Biol., 2004, vol. 5 pp. 897-907.*

1.3.1 Activation.

In contrast to the reversible nature of the kinase action, the result of protease activity is irreversible. Therefore, the activity of proteases has to be tightly controlled. In the case of caspases, they are synthesized in the form of inactive zymogens and they dependend on a complex machinery for their activation.

Initiator caspases lay at the top of the caspase activation cascade, and therefore there is no upstream protease to activate them. As the activation of the caspase cascade depends upon their activation, they need to be sensitive to activation signals, but they do not have to be activated irreversibly. This requisite is needed to avoid that their accidental activation triggers rapid cell death. In contrast to what was originally thought, apical or initator caspases are not activated by cleavage, but rather by dimerization [77]. This dimerization-

driven activation occurs in the context of large supramolecular complexes that act as sensors for death signals.

In the case of the extrinsic pathway, the binding of a death signal to a death receptor triggers the clustering and recruitment of adaptor proteins as well as procaspase-8. Almost ten years ago the Induced-Proximity Model for the activation of caspase-8 was proposed [78]. In this model, the formation of the death-inducing signalling complex (DISC) brings procaspase-8 molecules in close proximity so that they can cleave each other. This model has now evolved and in the current model, named proximity-induced dimerization, dimerization rather than cleavage, triggers caspase-8 activation [77].

In the case of the intrinsic pathway, the apoptosome plays the role of a receptor of intracellular death signals and as for the case of caspase-8 and the DISC, caspase-9 is activated by dimerization, mediated by the formation of the apoptosome [79]. This is confirmed by the fact that processed caspase-9 was found to be catalytically inactive [80]. In contrast, dimers were highly active [80].

The dimerization-induced activation of apical caspases contains in itself a safeguard mechanism. If the apoptotic stimulus is short (incomplete Cyt c release or a short death-receptor activation) initiator caspases will not be irreversibly committed to the activation of executioners caspases, and could in turn activate other physiological processes.

Executioner caspases are in turn activated through a proteolytic cascade set out by the initiator caspases [53], resulting in a cleavage that generates a large and small subunits [81]. Because their activation is irreversible, the activity of executioner caspases needs to be tightly regulated. This is achieved by a family of proteins called Inhibitor of Apoptosis Proteins (IAPs). First discovered in baculovirus [35], mammalian orthologs were subsequently found [82, 83]. IAPs are characterized by the presence of one to three copies of the Baculovirus IAP repeat (BIR) and a RING domain (a zinc binding motif). The best-

characterized IAP is X-linked IAP (XIAP) [84, 85], which is a very potent anti-apoptotic molecule due to its capacity to directly inhibit caspases. IAPs activity is not restricted to apoptosis regulation. Survivin, an IAP family member that possesses one BIR repeat and lacks the RING domain, is involved in cell cycle regulation [86].

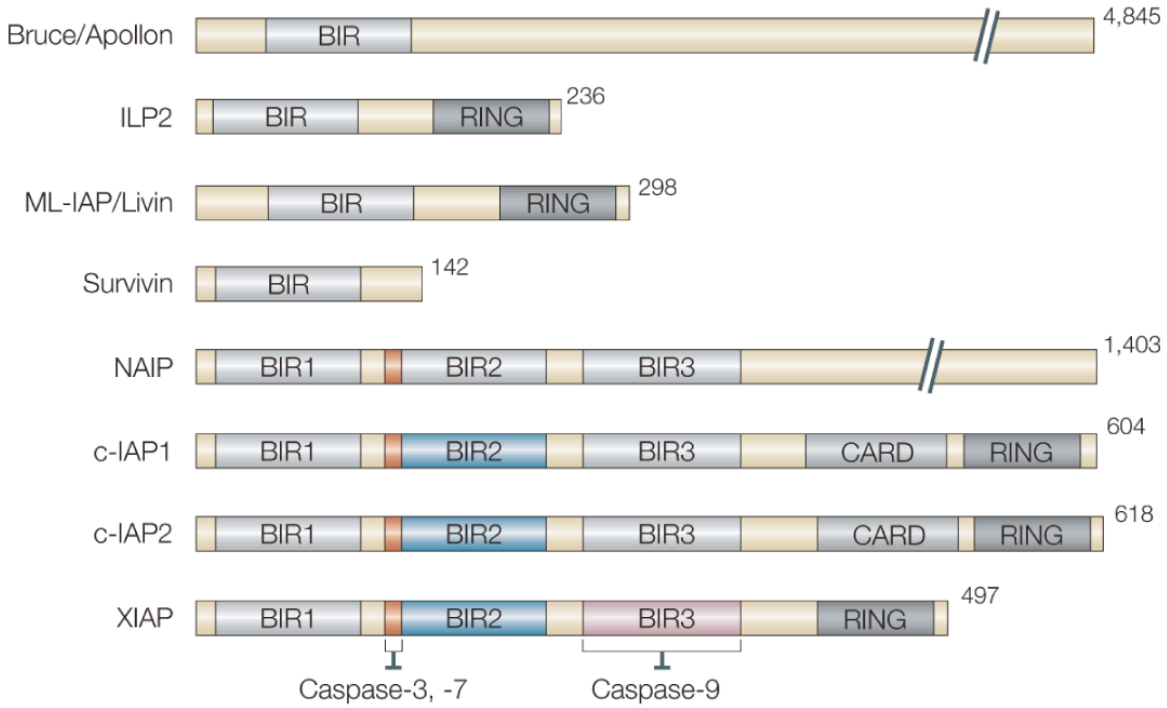

Figure 8. IAPs in mammals.
Proteins of the inhibitor of apoptosis (IAP) family include XIAP (X-linked IAP), c-IAP1, c-IAP2, ILP2 (IAP-like protein-2), ML-IAP (melanoma IAP)/Livin, NAIP (neuronal apoptosis-inhibitory protein) and survivin, and are also known as MIHA/ILP1, MIHB/HIAP2, MIHC/HIAP1, Ts-IAP, KIAP, BIRC1 and TIAP, respectively. A conserved linker peptide that precedes the BIR2 (baculoviral IAP repeat-2) domain of XIAP, c-IAP1 or c-IAP2 (shown in red) is responsible for inhibiting caspases-3 and -7 in mammals. On the basis of structural information, residues 126–143 (FLLNKDVGNIAKYDIRVK) of NAIP are predicted to carry out this function, as indicated in red. Only the BIR3 domain of XIAP can potently inhibit caspase-9. The biochemically characterized BIR domains that have known functions are highlighted in colour, whereas other domains in the various IAPs are shown in grey. CARD, caspase-recruitment domain.
Adapted from *Riedl SJ and Shi Y, Nat. Rev. Mol. Cell Biol., 2004, vol. 5 pp. 897-907.*

The effector caspases are responsible for cleaving most of the known apoptotic substrates, such as the DNA fragmentation factor 45 (DFF 45), poly- (ADP-ribose) polymerase (PARP), ACINUS (apoptotic chromatin condensation inducer in the nucleus) and lamin [87], all of which characterize nuclear apoptosis. Other caspase substrates have different locations within the cell and are involved in many cellular functions. Disruption of their functions by caspases ensures both inhibition of basic cell functions that could inhibit

apoptosis [81] and the formation of the apoptotic bodies. These last structures are recognised and eliminated by neighbour and/or immune cells [88].

1.3.2 Substrates.

Caspases do not degrade other proteins; they cleave targets at one of a few highly selective sites. Even though caspases cleave some structural proteins, they more frequently target signalling proteins and thus modulate specific downstream pathways, which in turn execute cell death. Therefore, caspases serve as signalling mediators that orchestrate a complex network of downstream execution pathways.

Caspase substrates can be divided into six major categories [81]:

I. Proteins directly involved in the regulation of apoptosis.

The most obvious example of the cleavage of a protein involved in apoptosis is the cleavage of executioner caspases by initiator caspases. Other examples of pro-apoptotic proteins activated by caspase cleavage are Bid [55, 89] and ICAD (inhibitor of caspase-activated DNAse) [90, 91] which plays a critical role in the internucleosomal DNA degradation characteristic of apoptosis [92]. Anti-apoptotic molecules such as Bcl-2, [93] Bcl-X_L [94] and XIAP [95] are inactivated by caspase cleavage.

II. Proteins mediating/regulating apoptosis signal transduction.

A number of anti-apoptotic protein kinases are rendered inactive by caspase cleavage. Akt, a known pro-survival factor, is cleaved following matrix detachment in epithelial cells [96, 97]. RIP kinase, the survival-signalling component associated to the DISC complex, is also cleaved by caspase 8 causing its inactivation [98, 99]. On the other hand, pro-apoptotic kinases are activated by caspase cleavage. Fas signalling results in caspase-3-mediated cleavage of PAK2 (p21-activated kinase 2), which contributes to the formation of apoptotic bodies [100]. Another kinase activated during genotoxic stress and Fas-induced apoptosis is MEKK1 [101, 102].

III. Structural and essential function proteins.

In addition to the activation of different apoptotic pathways, caspases contribute to the dismantling of the cell. For example, cleavage of gelsolin [103] and fodrin [104] leads to disruption of the actin filament network and contributes to cells rounding up and detaching from the matrix during apoptosis. Nuclear fragmentation critically depends on the disruption of the nuclear filamentous network through the cleavage of lamins A, B1 and C by caspases [105, 106].

IV. Proteins required for cellular repair.

Failure to repair or restore cellular functions in response to cellular distress is one of the main triggers of apoptosis. DNA-dependent protein kinase (DNA-PK), which play a critical role in the induction of DNA repair in response to double-strand breaks [107], is one of the upstream caspase targets during apoptosis [33, 108]. Another protein involved in DNA repair, poly(ADP-ribose) polymerase (PARP) (widely used experimentally as an apoptosis marker) is also cleaved during apoptosis [109].

V. Proteins regulating cell cycle

Induction of apoptosis appears to coincide with the activation of multiple cell cycle associated factor through cleavage and inactivation of their inhibitors (wee1, $p21^{CIP1}$ and $p27^{KIP1}$ [110, 111]).

VI. Proteins involved in human pathologies.

Caspases may be involved in the direct cleavage of disease-associated factors. Two of the most striking examples are Huntington disease and Alzheimer's disease. In Huntington disease, caspases may contribute to the generation of expanded polyQ fragment on huntingtin through cleavage in the cluster of DXXD sites [112, 113]. In Alzheimer's disease, caspase 3 has been found to cleave the cytosolic tail of the amyloid precursor protein (APP) [114].

As mentioned, the great majority of caspase substrates are involved in the promotion of apoptosis when cleaved. There are, however, exceptions to this rule. A small part of the caspase substrates acquires new anti-apoptotic properties when cleaved by caspases. For example, cleavage of PKCε activates the enzyme and this seems to generate an anti-apoptotic signal [115]. Triggering of the B-cell receptor induces the cleavage by caspases of Lyn and Fyn [116, 117] into fragments that inhibit apoptosis. The p54 Lyn fragment may favour cell survival by modulating c-myc levels [117]. The survival pathways activated after the cleavage of Fyn or PKCε have not been characterized. Moreover, the ability to regulate apoptosis in cells specifically lacking the capacity of cleaving Fyn, Lyn, or PKCε has not been evaluated yet. Low levels of caspase activity provoke the cleavage of RasGAP [118] and its N-terminal fragment induces the activation of the Ras/PI3K/Akt antiapoptotic pathway [119].

1.4 RasGAP

RasGAP is a cytosolic protein involved in the regulation of Ras and Rho signalling pathways [120-122] and necessary for normal cell mobility [123].

1.4.1 Ras.

Ras proteins have defined a group of 20-25 kDa guanine nucleotide-binding proteins that share structural homology, the superfamily of Ras-related proteins. The Ras proteins were the first oncogene to be described. First discovered as the transforming genes of the Harvey and Kirsten murine sarcoma viruses [124], subsequently they were found in the eukaryotic genome [125-127].

Mammalian cells encode three functional ras genes: H-Ras, K-Ras and N-Ras, which show a very similar structure and function. The protein product of each vertebrate Ras gene is approximately 21 kD in size, containing 188 amino acids.

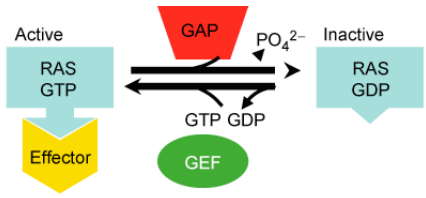

Figure 9. Ras activity regulation.
The activation state of Ras is controlled by the cycle of hydrolysis of bound GTP, which is catalyzed by GTPase activating proteins (GAPs), and the replacement of bound GDP with fresh GTP, which is catalyzed by guanine nucleotide exchange factors (GEFs) Adapted from John *Colicelli, Science STKE, 2004*.

Ras proteins act as molecular switches. According to the structures of small G proteins, they have two interconvertible forms: GDP-bound inactive and GTP-bound active forms [128-130], figure 9. Ras affinity for GDP is higher than for GTP and its intrinsic GTPase activity is extremely low. Without the assistance of "facilitator" proteins Ras would be constitutively locked in the inactive state [131]. Son of Sevenless (Sos) acts as a nucleotide exchange factor (GEF); upon binding to Ras, Sos facilitates the release of the tightly bound GDP and its replacement by GTP. On the other hand, GTPase activating proteins (GAPs) activate Ras GTPase activity by up to 10^5 folds [132, 133], by directly interacting with Ras [134]. Therefore, GAPs and GEFs act in concert to keep Ras activity in check.

Ras controls the activity of multiple effectors [135]. The protein kinase c-Raf was the first effector to be discovered [136] and is so far the most studied one. Ras binding to c-Raf leads to its activation and initiation of the MEK-ERK signalling pathway. Another well established Ras effectors are the catalytic subunit of PI3K [137] and the Ral guanine nucleotide dissociation stimulator (RalGDS) [138, 139].

1.4.2 RasGAP

p120RasGAP, a key regulator in the Ras signalling pathway [120-122], was the first GAP to be characterized at a molecular level [140, 141]. It was first described as a cytosolic protein fraction able to stimulate hydrolysis of Ras-bound GTP [141]. *Rasa*1, encodes for two different isoforms: p100 and p120 [132]. The expression of p100 is restricted to the primate

placenta. In mammals, p120 is expressed ubiquitously, although there is a great amount of variability between organs. Disruption of RasGAP gene (*Rasa*1) leads to embryonic lethality at day 10.5 due to aberrant cardiovascular development [142].

p120 RasGAP is active on Ha-Ras, Ki-Ras, N-Ras, and R-Ras, but not on Rho/Rac/Rab proteins [128, 140, 141]. To date at least seven different GAPs have been found in mammals: p120RasGAP, the neurofibromatosis type 1 protein NF1 [143], GAP1m, GAP^{1IP4BP}[144], IQGAP1 [145], SynGAP (a Ras GAP selectively expressed at excitatory synapses in the brain [146]) and CAPRI which is calcium dependent [147].

Figure 10. Schematic representation of RasGAP.
PPPP: proline-rich region; SH2: Src homology domain 2; SH3 Src homology domain 3; PH: pleckstrin homology domain; C2: calcium-dependent lipid binding domain and GAP: GTPase activation protein domain.

The C-terminal part of RasGAP contains the GTPase activating domain (GAP), responsible for GTP hydrolysis. This domain is highly conserved, both among the different forms of Ras GAPs and between species. Interestingly the N-terminal region contains several domains susceptible to be involved in interaction with other proteins (Figure 10):

- C2 domain: is involved in binding phospholipids in a calcium dependent manner or calcium independent manner
- PH domain: consist of approximately 120 amino acids that binds with high affinity to specific phosphoinositides such as phosphatidyl-inositol (PI)-4,5-bisphosphate, PI-3,4-P2 or PI-3,4,5-P3.
- SH2 (Src homology 2) domain: is a domain of approximately 100 amino acids that binds to specific phospho (pY)-containing peptide motifs.
- SH3 (Src homology 3) domain: it generally binds to Pro-rich peptides.
- Proline-rich modules interact with SH3 domains.

All these RasGAP functional domains specify different ways of interacting with numbers of signalling proteins [148]. A non exhaustive list of proteins that can associate with the SH3 domain flanked with two SH2 domains include a number of tyrosine kinase receptors (Platelet derived growth factor receptor [149] and Insulin growth factor receptor [150]), v-Src, p62Dok and p190RhoGAP [151-153].

1.4.2.1 RasGAP as a possible effector of Ras.

RasGAP is usually described as a negative regulator or Ras. In cells expressing an oncogenic form of Ras, RasGAP is no longer able to negatively regulate Ras. However, in these cells RasGAP has been described to act as a Ras effector, in functions related with cells proliferation, differentiation and apoptosis, independently of its GAP activity.

I. The opening of the muscarinic receptor-activated potassium channel was inhibited by the Ras-RasGAP complex. This inhibition was found to rely on RasGAP SH2-SH3 domains [129, 154, 155]).

II. The microinjection of an antibody directed at RasGAP SH3 domain in *Xenopus* oocytes blocked H-Ras-induced germinal vesicle breakdown and blocked the Ras-mediated activation of cdc2 kinase [156-158].

III. A RasGAP mutant, lacking the Ras binding domain, inhibited the activity of oncogenic Ras, when targeted to the plasma membrane, without affecting the action of normal Ras [159].

IV. RasGAP modulate cell adhesion and cytoskeleton [160] through its interaction with p190RhoGAP in a Ras-independent manner [161]. Accordingly, overexpression of p120GAP impairs the chemotactic response of fibroblasts to PDGF and lysophosphatidic acid [162].

V. RasGAP interacts, in a Ras independent manner, with G3BP, a protein showing similarity to RNA binding proteins and which has been proposed to affect both the stability and translation efficiency of mRNAs [163].

1.4.2.2 RasGAP is a caspase substrate.

RasGAP is a caspase substrate [122, 164] that bears two distinct caspase-3 consensus cleavage sites that are sequentially targeted by the caspases as their activity increases [118]. The first consensus site, located at position 455, is cleaved at caspase activity that are hardly detectable and more importantly that do not induce apoptosis. The cleavage at position 157 only occurs at higher caspase activity and requires that the first cleavage had already taken place [118], suggesting that the first cleavage induces structural modifications that allow the second cleavage to take place.

The first caspase cleavage generates two fragments. The C-terminal fragment consists of the GAP, C2 and PH domains while the N-terminal domain contains the SH2-SH3-SH2 tandem and the proline rich domain. Surprisingly, when overexpressed, RasGAP N-terminal fragment induces a potent anti-apoptotic signal, mediated via the Ras/Phosphatidylinositol 3-Kinase/Akt pathway [119]. This protective pathway occurs independently of NFκB activity, since fragment N blocks the activation of the NFκB pathway [119]. Activation of this pathway seems to be crucial for cell survival in low-stress conditions [10]. At higher caspase activity, RasGAP N-terminal fragment is further processed by caspases at position 157 generating two smaller fragments named N1 and N2. This cleavage abrogates fragment N mediated anti-apoptotic signalling, allowing the apoptotic pathway to proceed. Interestingly, fragment N2 when overexpressed in cancer cells potentiate the pro-apoptotic effect of genotoxins in a p53-dependent manner [118, 165].

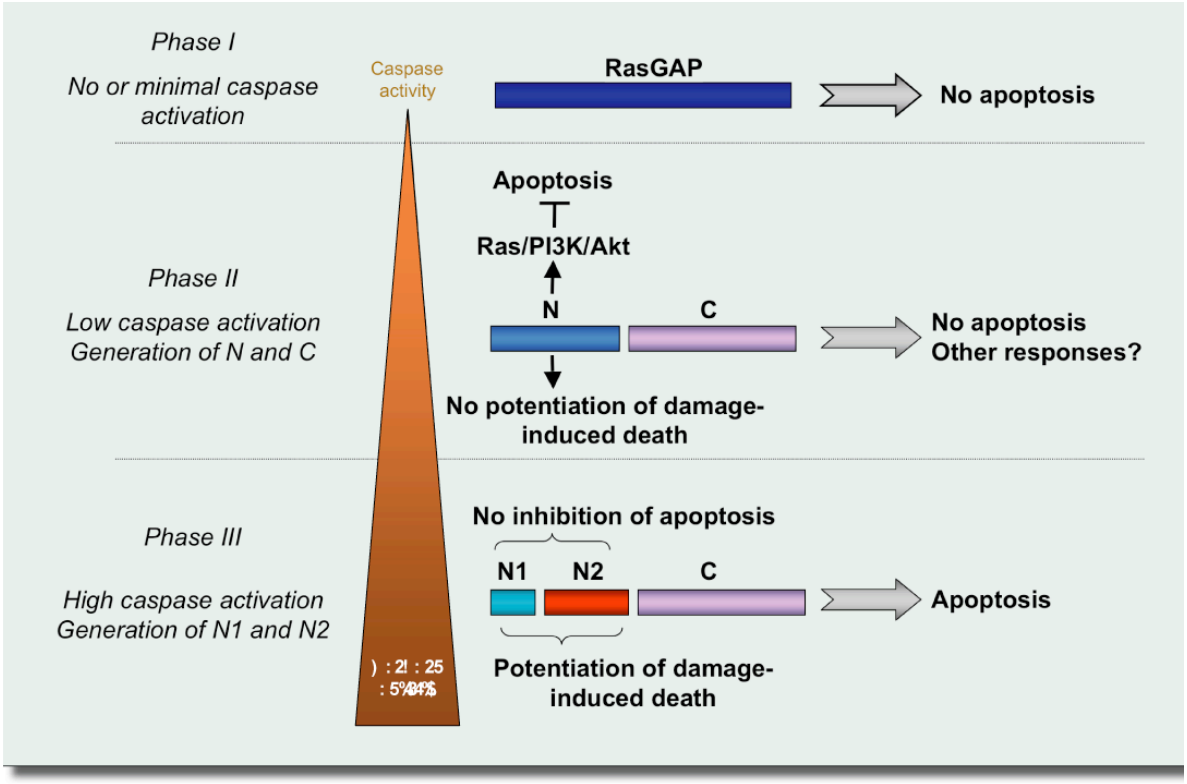

Figure 11. Model of the role of RasGAP cleavage fragments in the regulation of apoptosis

1.5 Aim of the work.

We have previously shown that when RasGAP is cleaved it induces a potent antiapoptotic signal and particularly that cells unable to generate fragment N are extremely sensitive to low stress conditions [10].

The aim of this work was to understand the physiological role played by the cleavage of RasGAP by the caspases. Therefore, the following projects were developed.

1. Characterization of how fragment-N mediates Ras/PI3K/akt pathway activation.
2. Generation and characterization of knock-in mice expressing a mutant form of RasGAP that cannot be cleaved by caspases (RasGAP (D455A)).
3. Generation and characterization of transgenic mice expressing fragment-N in the ß-cells of the pancreas, to study its protective effect in the context of diabetes.

1.6 References.

1. Vogt, C., *Untersuchungen über die Entwicklungsgeschichte der Geburtshelferkroete (Alytes obstetricans)*. . Jent and Gassmann, Solothurn, 1842.
2. Glucksman, A., *Cell death in normal vertebrate ontogeny*. Biological reviews of the Cambridge philosophical society, 1951. **26**: p. 59-86.
3. Clarke, P. and S. Clarke, *Nineteenth century research on naturally occurring cell death and related phenomena*. Anat Embryol, 1996. **193**(2): p. 81-99.
4. Lockshin, R., *Programmed cell death. Activation of lysis by a mechanism involving the synthesis of protein*. J Insect Physiol, 1969. **15**(9): p. 1505-16.
5. Kerr, J., A. Wyllie, and A. Currie, *Apoptosis: a basic biological phenomenon with wide-ranging implications in tissue kinetics*. Br J Cancer, 1972. **26**(4): p. 239-57.
6. Horvitz, H., *Worms, life, and death (Nobel lecture)*. Chembiochem, 2003. **4**(8): p. 697-711.
7. Kroemer, G., et al., *Classification of cell death: recommendations of the Nomenclature Committee on Cell Death*. Cell Death Differ., 2005. **12 Suppl 2**: p. 1463-7.
8. Melino, G., R. Knight, and P. Nicotera, *How many ways to die? How many different models of cell death?* Cell Death Differ., 2005. **12 Suppl 2**: p. 1457-62.
9. Frisch, S. and E. Ruoslahti, *Integrins and anoikis*. Curr Opin Cell Biol, 1997. **9**(5): p. 701-6.
10. Yang, J., et al., *Partial cleavage of RasGAP by caspases is required for cell survival in mild stress conditions*. Mol. Cell. Biol., 2004. **24**(23): p. 10425-36.
11. Blank, M. and Y. Shiloh, *Programs for cell death: apoptosis is only one way to go*. Cell Cycle, 2007. **6**(6): p. 686-95.
12. Degenhardt, K., et al., *Autophagy promotes tumor cell survival and restricts necrosis, inflammation, and tumorigenesis*. Cancer Cell, 2006. **10**(1): p. 51-64.
13. Ricci, M. and W. Zong, *Chemotherapeutic approaches for targeting cell death pathways*. Oncologist, 2006. **11**(4): p. 342-57.
14. Sun, X., et al., *Selective induction of necrotic cell death in cancer cells by beta-lapachone through activation of DNA damage response pathway*. Cell Cycle, 2006. **5**(17): p. 2029-35.
15. Okada, H. and T. Mak, *Pathways of apoptotic and non-apoptotic death in tumour cells*. Nat. Rev. Cancer, 2004. **4**(8): p. 592-603.
16. Thompson, C., *Apoptosis in the pathogenesis and treatment of disease*. Science, 1995. **267**(5203): p. 1456-62.
17. Vaux, D. and S. Korsmeyer, *Cell death in development*. Cell, 1999. **96**(2): p. 245-54.
18. Meier, P., A. Finch, and G. Evan, *Apoptosis in development*. Nature, 2000. **407**(6805): p. 796-801.
19. Zuzarte-Luís, V. and J. Hurlé, *Programmed cell death in the developing limb*. Int. J. Dev. Biol., 2002. **46**(7): p. 871-6.
20. Gañan, Y., et al., *Role of TGF beta s and BMPs as signals controlling the position of the digits and the areas of interdigital cell death in the developing chick limb autopod*. Development, 1996. **122**(8): p. 2349-57.
21. Zou, H. and L. Niswander, *Requirement for BMP signaling in interdigital apoptosis and scale formation*. Science, 1996. **272**(5262): p. 738-41.
22. Hutchins, J. and S. Barger, *Why neurons die: cell death in the nervous system*. Anat Rec, 1998. **253**(3): p. 79-90.

23. Kerr, J., B. Harmon, and J. Searle, *An electron-microscope study of cell deletion in the anuran tadpole tail during spontaneous metamorphosis with special reference to apoptosis of striated muscle fibers*. J. Cell. Sci., 1974. **14**(3): p. 571-85.
24. Rathmell, J. and C. Thompson, *Pathways of apoptosis in lymphocyte development, homeostasis, and disease*. Cell, 2002. **109 Suppl**: p. S97-107.
25. Reed, J., *Dysregulation of apoptosis in cancer*. J Clin Oncol, 1999. **17**(9): p. 2941-53.
26. Reed, J., *Mechanisms of apoptosis avoidance in cancer*. Current opinion in oncology, 1999. **11**(1): p. 68-75.
27. Ionov, Y., et al., *Mutational inactivation of the proapoptotic gene BAX confers selective advantage during tumor clonal evolution*. Proc. Natl. Acad. Sci. U.S.A., 2000. **97**(20): p. 10872-7.
28. Lane, D., *Cancer. p53, guardian of the genome*. Nature, 1992. **358**(6381): p. 15-6.
29. Wallace-Brodeur, R. and S. Lowe, *Clinical implications of p53 mutations*. Cell. Mol. Life Sci., 1999. **55**(1): p. 64-75.
30. Altieri, D., *Validating survivin as a cancer therapeutic target*. Nat. Rev. Cancer, 2003. **3**(1): p. 46-54.
31. Tamm, I., et al., *Expression and prognostic significance of IAP-family genes in human cancers and myeloid leukemias*. Clin Cancer Res, 2000. **6**(5): p. 1796-803.
32. Taylor, P., et al., *A hierarchical role for classical pathway complement proteins in the clearance of apoptotic cells in vivo*. J. Exp. Med., 2000. **192**(3): p. 359-66.
33. Casciola-Rosen, L., G. Anhalt, and A. Rosen, *DNA-dependent protein kinase is one of a subset of autoantigens specifically cleaved early during apoptosis*. J. Exp. Med., 1995. **182**(6): p. 1625-34.
34. Herrmann, M., et al., *Impaired phagocytosis of apoptotic cell material by monocyte-derived macrophages from patients with systemic lupus erythematosus*. Arthritis Rheum, 1998. **41**(7): p. 1241-50.
35. Crook, N., R. Clem, and L. Miller, *An apoptosis-inhibiting baculovirus gene with a zinc finger-like motif*. J. Virol., 1993. **67**(4): p. 2168-74.
36. Thome, M., et al., *Viral FLICE-inhibitory proteins (FLIPs) prevent apoptosis induced by death receptors*. Nature, 1997. **386**(6624): p. 517-21.
37. Tschopp, J., M. Irmler, and M. Thome, *Inhibition of fas death signals by FLIPs*. Curr Opin Immunol, 1998. **10**(5): p. 552-8.
38. Siegel, R., et al., *SPOTS: signaling protein oligomeric transduction structures are early mediators of death receptor-induced apoptosis at the plasma membrane*. J. Cell Biol., 2004. **167**(4): p. 735-44.
39. Laurent-Crawford, A., et al., *The cytopathic effect of HIV is associated with apoptosis*. Virology, 1991. **185**(2): p. 829-39.
40. Meyaard, L., et al., *Programmed death of T cells in HIV-1 infection*. Science, 1992. **257**(5067): p. 217-9.
41. Laurent-Crawford, A., et al., *Membrane-expressed HIV envelope glycoprotein heterodimer is a powerful inducer of cell death in uninfected CD4+ target cells*. Res Virol, 1995. **146**(1): p. 5-17.
42. Cao, J., et al., *Molecular determinants of acute single-cell lysis by human immunodeficiency virus type 1*. J. Virol., 1996. **70**(3): p. 1340-54.
43. Isacson, O., *On neuronal health*. Trends Neurosci, 1993. **16**(8): p. 306-8.
44. Lee, S. and S. Pervaiz, *Apoptosis in the pathophysiology of diabetes mellitus*. Int J Biochem Cell Biol, 2007. **39**(3): p. 497-504.

45. Efanova, I., et al., *Glucose and tolbutamide induce apoptosis in pancreatic beta-cells. A process dependent on intracellular Ca2+ concentration*. J. Biol. Chem., 1998. **273**(50): p. 33501-7.
46. Biarnés, M., et al., *Beta-cell death and mass in syngeneically transplanted islets exposed to short- and long-term hyperglycemia*. Diabetes, 2002. **51**(1): p. 66-72.
47. Haber, E., et al., *New insights into fatty acid modulation of pancreatic beta-cell function*. Int Rev Cytol, 2006. **248**: p. 1-41.
48. Delaney, C., et al., *Cytokines induce deoxyribonucleic acid strand breaks and apoptosis in human pancreatic islet cells*. Endocrinology, 1997. **138**(6): p. 2610-4.
49. Ashkenazi, A., *Targeting death and decoy receptors of the tumour-necrosis factor superfamily*. Nat. Rev. Cancer, 2002. **2**(6): p. 420-30.
50. Naismith, J. and S. Sprang, *Modularity in the TNF-receptor family*. Trends Biochem Sci, 1998. **23**(2): p. 74-9.
51. Irmler, M., et al., *Inhibition of death receptor signals by cellular FLIP*. Nature, 1997. **388**(6638): p. 190-5.
52. Thome, M. and J. Tschopp, *Regulation of lymphocyte proliferation and death by FLIP*. Nat. Rev. Immunol., 2002. **1**(1): p. 50-8.
53. Shi, Y., *Caspase activation: revisiting the induced proximity model*. Cell, 2004. **117**(7): p. 855-8.
54. Scaffidi, C., et al., *Two CD95 (APO-1/Fas) signaling pathways*. EMBO J., 1998. **17**(6): p. 1675-87.
55. Luo, X., et al., *Bid, a Bcl2 interacting protein, mediates cytochrome c release from mitochondria in response to activation of cell surface death receptors*. Cell, 1998. **94**(4): p. 481-90.
56. Verhagen, A., et al., *Identification of DIABLO, a mammalian protein that promotes apoptosis by binding to and antagonizing IAP proteins*. Cell, 2000. **102**(1): p. 43-53.
57. Suzuki, Y., et al., *A serine protease, HtrA2, is released from the mitochondria and interacts with XIAP, inducing cell death*. Mol. Cell, 2001. **8**(3): p. 613-21.
58. Kroemer, G. and S. Martin, *Caspase-independent cell death*. Nat. Med., 2005. **11**(7): p. 725-30.
59. Tsujimoto, Y., et al., *The t(14;18) chromosome translocations involved in B-cell neoplasms result from mistakes in VDJ joining*. Science, 1985. **229**(4720): p. 1390-3.
60. Cleary, M. and J. Sklar, *Nucleotide sequence of a t(14;18) chromosomal breakpoint in follicular lymphoma and demonstration of a breakpoint-cluster region near a transcriptionally active locus on chromosome 18*. Proc Natl Acad Sci USA, 1985. **82**(21): p. 7439-43.
61. Oltvai, Z., C. Milliman, and S. Korsmeyer, *Bcl-2 heterodimerizes in vivo with a conserved homolog, Bax, that accelerates programmed cell death*. Cell, 1993. **74**(4): p. 609-19.
62. Adams, J. and S. Cory, *The Bcl-2 protein family: arbiters of cell survival*. Science, 1998. **281**(5381): p. 1322-6.
63. Kelekar, A. and C. Thompson, *Bcl-2-family proteins: the role of the BH3 domain in apoptosis*. Trends Cell Biol., 1998. **8**(8): p. 324-30.
64. Reed, J., *Bcl-2 family proteins*. Oncogene, 1998. **17**(25): p. 3225-36.
65. Letai, A., et al., *Distinct BH3 domains either sensitize or activate mitochondrial apoptosis, serving as prototype cancer therapeutics*. Cancer Cell, 2002. **2**(3): p. 183-92.
66. Krajewski, S., et al., *Investigation of the subcellular distribution of the bcl-2 oncoprotein: residence in the nuclear envelope, endoplasmic reticulum, and outer mitochondrial membranes*. Cancer Res., 1993. **53**(19): p. 4701-14.

67. de Jong, D., et al., *Subcellular localization of the bcl-2 protein in malignant and normal lymphoid cells*. Cancer Res., 1994. **54**(1): p. 256-60.
68. Zhu, W., et al., *Bcl-2 mutants with restricted subcellular location reveal spatially distinct pathways for apoptosis in different cell types*. EMBO J., 1996. **15**(16): p. 4130-41.
69. Wei, M., et al., *Proapoptotic BAX and BAK: a requisite gateway to mitochondrial dysfunction and death*. Science, 2001. **292**(5517): p. 727-30.
70. Kuwana, T., et al., *Bid, Bax, and lipids cooperate to form supramolecular openings in the outer mitochondrial membrane*. Cell, 2002. **111**(3): p. 331-42.
71. Alnemri, E., et al., *Human ICE/CED-3 protease nomenclature*. Cell, 1996. **87**(2): p. 171.
72. Yuan, J., et al., *The C. elegans cell death gene ced-3 encodes a protein similar to mammalian interleukin-1 beta-converting enzyme*. Cell, 1993. **75**(4): p. 641-52.
73. Kumar, S. and J. Doumanis, *The fly caspases*. Cell Death Differ., 2000. **7**(11): p. 1039-44.
74. Madeo, F., et al., *A caspase-related protease regulates apoptosis in yeast*. Mol. Cell, 2002. **9**(4): p. 911-7.
75. Koenig, U., L. Eckhart, and E. Tschachler, *Evidence that caspase-13 is not a human but a bovine gene*. Biochem. Biophys. Res. Commun., 2001. **285**(5): p. 1150-4.
76. Nadiri, A., M. Wolinski, and M. Saleh, *The inflammatory caspases: key players in the host response to pathogenic invasion and sepsis*. J. Immunol., 2006. **177**(7): p. 4239-45.
77. Boatright, K., et al., *A unified model for apical caspase activation*. Mol. Cell, 2003. **11**(2): p. 529-41.
78. Salvesen, G. and V. Dixit, *Caspase activation: the induced-proximity model*. Proc. Natl. Acad. Sci. U.S.A., 1999. **96**(20): p. 10964-7.
79. Pop, C., et al., *The apoptosome activates caspase-9 by dimerization*. Mol. Cell, 2006. **22**(2): p. 269-75.
80. Renatus, M., et al., *Dimer formation drives the activation of the cell death protease caspase 9*. Proc. Natl. Acad. Sci. U.S.A., 2001. **98**(25): p. 14250-5.
81. Degterev, A., M. Boyce, and J. Yuan, *A decade of caspases*. Oncogene, 2003. **22**(53): p. 8543-67.
82. Duckett, C., et al., *A conserved family of cellular genes related to the baculovirus iap gene and encoding apoptosis inhibitors*. EMBO J., 1996. **15**(11): p. 2685-94.
83. Roy, N., et al., *The gene for neuronal apoptosis inhibitory protein is partially deleted in individuals with spinal muscular atrophy*. Cell, 1995. **80**(1): p. 167-78.
84. Holcik, M. and R. Korneluk, *XIAP, the guardian angel*. Nat. Rev. Mol. Cell Biol., 2001. **2**(7): p. 550-6.
85. Holcik, M., H. Gibson, and R. Korneluk, *XIAP: apoptotic brake and promising therapeutic target*. Apoptosis, 2001. **6**(4): p. 253-61.
86. Suzuki, A., et al., *Survivin initiates cell cycle entry by the competitive interaction with Cdk4/p16(INK4a) and Cdk2/cyclin E complex activation*. Oncogene, 2000. **19**(29): p. 3225-34.
87. Fischer, U., R. Jänicke, and K. Schulze-Osthoff, *Many cuts to ruin: a comprehensive update of caspase substrates*. Cell Death Differ., 2003. **10**(1): p. 76-100.
88. Chimini, G., *Apoptosis: repulsive encounters*. Nature, 2002. **418**(6894): p. 139-41.
89. Li, H., et al., *Cleavage of BID by caspase 8 mediates the mitochondrial damage in the Fas pathway of apoptosis*. Cell, 1998. **94**(4): p. 491-501.
90. Liu, X., et al., *DFF, a heterodimeric protein that functions downstream of caspase-3 to trigger DNA fragmentation during apoptosis*. Cell, 1997. **89**(2): p. 175-84.

91. Enari, M., et al., *A caspase-activated DNase that degrades DNA during apoptosis, and its inhibitor ICAD*. Nature, 1998. **391**(6662): p. 43-50.
92. Sakahira, H., et al., *Apoptotic nuclear morphological change without DNA fragmentation*. Curr. Biol., 1999. **9**(10): p. 543-6.
93. Kirsch, D., et al., *Caspase-3-dependent cleavage of Bcl-2 promotes release of cytochrome c*. J. Biol. Chem., 1999. **274**(30): p. 21155-61.
94. Clem, R., et al., *Modulation of cell death by Bcl-XL through caspase interaction*. Proc Natl Acad Sci USA, 1998. **95**(2): p. 554-9.
95. Deveraux, Q., et al., *Cleavage of human inhibitor of apoptosis protein XIAP results in fragments with distinct specificities for caspases*. EMBO J., 1999. **18**(19): p. 5242-51.
96. Bachelder, R., et al., *The cleavage of Akt/protein kinase B by death receptor signaling is an important event in detachment-induced apoptosis*. J. Biol. Chem., 2001. **276**(37): p. 34702-7.
97. Bachelder, R., et al., *p53 inhibits alpha 6 beta 4 integrin survival signaling by promoting the caspase 3-dependent cleavage of AKT/PKB*. J. Cell Biol., 1999. **147**(5): p. 1063-72.
98. Martinon, F., et al., *Activation of a pro-apoptotic amplification loop through inhibition of NF-kappaB-dependent survival signals by caspase-mediated inactivation of RIP*. FEBS Lett., 2000. **468**(2-3): p. 134-6.
99. Lin, Y., et al., *Cleavage of the death domain kinase RIP by caspase-8 prompts TNF-induced apoptosis*. Genes Dev., 1999. **13**(19): p. 2514-26.
100. Rudel, T. and G. Bokoch, *Membrane and morphological changes in apoptotic cells regulated by caspase-mediated activation of PAK2*. Science, 1997. **276**(5318): p. 1571-4.
101. Widmann, C., et al., *MEK kinase 1, a substrate for DEVD-directed caspases, is involved in genotoxin-induced apoptosis*. Mol. Cell. Biol., 1998. **18**(4): p. 2416-29.
102. Deak, J., et al., *Fas-induced proteolytic activation and intracellular redistribution of the stress-signaling kinase MEKK1*. Proc Natl Acad Sci USA, 1998. **95**(10): p. 5595-600.
103. Kothakota, S., et al., *Caspase-3-generated fragment of gelsolin: effector of morphological change in apoptosis*. Science, 1997. **278**(5336): p. 294-8.
104. Jänicke, R., et al., *Caspase-3 is required for alpha-fodrin cleavage but dispensable for cleavage of other death substrates in apoptosis*. J. Biol. Chem., 1998. **273**(25): p. 15540-5.
105. Rao, L., D. Perez, and E. White, *Lamin proteolysis facilitates nuclear events during apoptosis*. J. Cell Biol., 1996. **135**(6 Pt 1): p. 1441-55.
106. Lazebnik, Y., et al., *Studies of the lamin proteinase reveal multiple parallel biochemical pathways during apoptotic execution*. Proc Natl Acad Sci USA, 1995. **92**(20): p. 9042-6.
107. Lees-Miller, S., *The DNA-dependent protein kinase, DNA-PK: 10 years and no ends in sight*. Biochem Cell Biol, 1996. **74**(4): p. 503-12.
108. Song, Z., X. Yao, and M. Wu, *Direct interaction between survivin and Smac/DIABLO is essential for the anti-apoptotic activity of survivin during taxol-induced apoptosis*. J. Biol. Chem., 2003. **278**(25): p. 23130-40.
109. Kaufmann, S., et al., *Specific proteolytic cleavage of poly(ADP-ribose) polymerase: an early marker of chemotherapy-induced apoptosis*. Cancer Res., 1993. **53**(17): p. 3976-85.

110. Zhou, B., et al., *Caspase-dependent activation of cyclin-dependent kinases during Fas-induced apoptosis in Jurkat cells*. Proc Natl Acad Sci USA, 1998. **95**(12): p. 6785-90.
111. Levkau, B., et al., *Cleavage of p21Cip1/Waf1 and p27Kip1 mediates apoptosis in endothelial cells through activation of Cdk2: role of a caspase cascade*. Mol. Cell, 1998. **1**(4): p. 553-63.
112. Wellington, C., et al., *Caspase cleavage of mutant huntingtin precedes neurodegeneration in Huntington's disease*. J Neurosci, 2002. **22**(18): p. 7862-72.
113. Goldberg, Y., et al., *Cleavage of huntingtin by apopain, a proapoptotic cysteine protease, is modulated by the polyglutamine tract*. Nat. Genet., 1996. **13**(4): p. 442-9.
114. Gervais, F., et al., *Involvement of caspases in proteolytic cleavage of Alzheimer's amyloid-beta precursor protein and amyloidogenic A beta peptide formation*. Cell, 1999. **97**(3): p. 395-406.
115. Basu, A., et al., *Proteolytic activation of protein kinase C-epsilon by caspase-mediated processing and transduction of antiapoptotic signals*. J. Biol. Chem., 2002. **277**(44): p. 41850-6.
116. Ricci, J., et al., *An absolute requirement for Fyn in T cell receptor-induced caspase activation and apoptosis*. FASEB J, 2001. **15**(10): p. 1777-9.
117. Luciano, F., et al., *The p54 cleaved form of the tyrosine kinase Lyn generated by caspases during BCR-induced cell death in B lymphoma acts as a negative regulator of apoptosis*. FASEB J., 2003. **17**(6): p. 711-3.
118. Yang, J. and C. Widmann, *Antiapoptotic signaling generated by caspase-induced cleavage of RasGAP*. Mol. Cell. Biol., 2001. **21**(16): p. 5346-58.
119. Yang, J. and C. Widmann, *The RasGAP N-terminal fragment generated by caspase cleavage protects cells in a Ras/PI3K/Akt-dependent manner that does not rely on NFkappa B activation*. J. Biol. Chem., 2002. **277**(17): p. 14641-6.
120. Campbell, S., et al., *Increasing complexity of Ras signaling*. Oncogene, 1998. **17**(11 Reviews): p. 1395-413.
121. Leblanc, V., B. Tocque, and I. Delumeau, *Ras-GAP controls Rho-mediated cytoskeletal reorganization through its SH3 domain*. Mol. Cell. Biol., 1998. **18**(9): p. 5567-78.
122. Wen, L., et al., *Proteolytic cleavage of ras GTPase-activating protein during apoptosis*. Cell Death Differ., 1998. **5**(9): p. 729-34.
123. Kulkarni, S., et al., *Role of p120 Ras-GAP in directed cell movement*. J. Cell Biol., 2000. **149**(2): p. 457-70.
124. Shih, T., et al., *Identification of a sarcoma virus-coded phosphoprotein in nonproducer cells tranformed by Kirsten or Harvey murine sarcoma virus*. Virology, 1979. **96**(1): p. 64-79.
125. Tabin, C., et al., *Mechanism of activation of a human oncogene*. Nature, 1982. **300**(5888): p. 143-9.
126. Perucho, M., et al., *Human-tumor-derived cell lines contain common and different transforming genes*. Cell, 1981. **27**(3 Pt 2): p. 467-76.
127. Krontiris, T. and G. Cooper, *Transforming activity of human tumor DNAs*. Proc. Natl. Acad. Sci. U.S.A., 1981. **78**(2): p. 1181-4.
128. Bourne, H., D. Sanders, and F. McCormick, *The GTPase superfamily: a conserved switch for diverse cell functions*. Nature, 1990. **348**(6297): p. 125-32.
129. Hall, A., *The cellular functions of small GTP-binding proteins*. Science, 1990. **249**(4969): p. 635-40.
130. Takai, Y., et al., *Small GTP-binding proteins*. Int Rev Cytol, 1992. **133**: p. 187-230.

131. Vetter, I. and A. Wittinghofer, *The guanine nucleotide-binding switch in three dimensions*. Science, 2001. **294**(5545): p. 1299-304.
132. Trahey, M., et al., *Molecular cloning of two types of GAP complementary DNA from human placenta*. Science, 1988. **242**(4886): p. 1697-700.
133. Gideon, P., et al., *Mutational and kinetic analyses of the GTPase-activating protein (GAP)-p21 interaction: the C-terminal domain of GAP is not sufficient for full activity*. Mol. Cell. Biol., 1992. **12**(5): p. 2050-6.
134. Ahmadian, M., et al., *Confirmation of the arginine-finger hypothesis for the GAP-stimulated GTP-hydrolysis reaction of Ras*. Nat Struct Biol, 1997. **4**(9): p. 686-9.
135. Marshall, C., *Ras effectors*. Curr Opin Cell Biol, 1996. **8**(2): p. 197-204.
136. Van Aelst, L., et al., *Complex formation between RAS and RAF and other protein kinases*. Proc Natl Acad Sci USA, 1993. **90**(13): p. 6213-7.
137. Rodriguez-Viciana, P., et al., *Phosphatidylinositol-3-OH kinase as a direct target of Ras*. Nature, 1994. **370**(6490): p. 527-32.
138. Kikuchi, A., et al., *ralGDS family members interact with the effector loop of ras p21*. Mol. Cell. Biol., 1994. **14**(11): p. 7483-91.
139. Vetter, I., et al., *Structural and biochemical analysis of Ras-effector signaling via RalGDS*. FEBS Lett., 1999. **451**(2): p. 175-80.
140. Gibbs, J., et al., *Intrinsic GTPase activity distinguishes normal and oncogenic ras p21 molecules*. Proc. Natl. Acad. Sci. U.S.A., 1984. **81**(18): p. 5704-8.
141. Trahey, M. and F. McCormick, *A cytoplasmic protein stimulates normal N-ras p21 GTPase, but does not affect oncogenic mutants*. Science, 1987. **238**(4826): p. 542-5.
142. Henkemeyer, M., et al., *Vascular system defects and neuronal apoptosis in mice lacking ras GTPase-activating protein*. Nature, 1995. **377**(6551): p. 695-701.
143. Ballester, R., et al., *The NF1 locus encodes a protein functionally related to mammalian GAP and yeast IRA proteins*. Cell, 1990. **63**(4): p. 851-9.
144. Maekawa, M., et al., *A novel mammalian Ras GTPase-activating protein which has phospholipid-binding and Btk homology regions*. Mol. Cell. Biol., 1994. **14**(10): p. 6879-85.
145. Weissbach, L., et al., *Identification of a human rasGAP-related protein containing calmodulin-binding motifs*. J. Biol. Chem., 1994. **269**(32): p. 20517-21.
146. Kim, J., et al., *SynGAP: a synaptic RasGAP that associates with the PSD-95/SAP90 protein family*. Neuron, 1998. **20**(4): p. 683-91.
147. Lockyer, P., S. Kupzig, and P. Cullen, *CAPRI regulates Ca(2+)-dependent inactivation of the Ras-MAPK pathway*. Curr. Biol., 2001. **11**(12): p. 981-6.
148. Moran, M., et al., *Src homology region 2 domains direct protein-protein interactions in signal transduction*. Proc. Natl. Acad. Sci. U.S.A., 1990. **87**(21): p. 8622-6.
149. Kazlauskas, A., et al., *Binding of GAP to activated PDGF receptors*. Science, 1990. **247**(4950): p. 1578-81.
150. Seely, B., et al., *Localization of the insulin-like growth factor I receptor binding sites for the SH2 domain proteins p85, Syp, and GTPase activating protein*. J. Biol. Chem., 1995. **270**(32): p. 19151-7.
151. Molloy, C., et al., *PDGF induction of tyrosine phosphorylation of GTPase activating protein*. Nature, 1989. **342**(6250): p. 711-4.
152. Gibbs, J., et al., *Modulation of guanine nucleotides bound to Ras in NIH3T3 cells by oncogenes, growth factors, and the GTPase activating protein (GAP)*. J. Biol. Chem., 1990. **265**(33): p. 20437-42.
153. Ellis, C., et al., *Phosphorylation of GAP and GAP-associated proteins by transforming and mitogenic tyrosine kinases*. Nature, 1990. **343**(6256): p. 377-81.

154. Yatani, A., et al., *ras p21 and GAP inhibit coupling of muscarinic receptors to atrial K+ channels*. Cell, 1990. **61**(5): p. 769-76.
155. Martin, G., et al., *GAP domains responsible for ras p21-dependent inhibition of muscarinic atrial K+ channel currents*. Science, 1992. **255**(5041): p. 192-4.
156. Gibbs, J., et al., *Xenopus oocyte germinal-vesicle breakdown induced by [Val12]Ras is inhibited by a cytosol-localized Ras mutant*. Proc Natl Acad Sci USA, 1989. **86**(17): p. 6630-4.
157. Duchesne, M., et al., *Identification of the SH3 domain of GAP as an essential sequence for Ras-GAP-mediated signaling*. Science, 1993. **259**(5094): p. 525-8.
158. Pomerance, M., et al., *The Ras-GTPase-activating protein SH3 domain is required for Cdc2 activation and mos induction by oncogenic Ras in Xenopus oocytes independently of mitogen-activated protein kinase activation*. Mol. Cell. Biol., 1996. **16**(6): p. 3179-86.
159. Clark, G., et al., *Differential antagonism of Ras biological activity by catalytic and Src homology domains of Ras GTPase activation protein*. Proc. Natl. Acad. Sci. U.S.A., 1993. **90**(11): p. 4887-91.
160. McGlade, J., et al., *The N-terminal region of GAP regulates cytoskeletal structure and cell adhesion*. EMBO J., 1993. **12**(8): p. 3073-81.
161. Pronk, G., et al., *Complex formation between the p21ras GTPase-activating protein and phosphoproteins p62 and p190 is independent of p21ras signalling*. Oncogene, 1993. **8**(10): p. 2773-80.
162. Kundra, V., et al., *The chemotactic response to PDGF-BB: evidence of a role for Ras*. J. Cell Biol., 1995. **130**(3): p. 725-31.
163. Parker, F., et al., *A Ras-GTPase-activating protein SH3-domain-binding protein*. Mol. Cell. Biol., 1996. **16**(6): p. 2561-9.
164. Widmann, C., S. Gibson, and G. Johnson, *Caspase-dependent cleavage of signaling proteins during apoptosis. A turn-off mechanism for anti-apoptotic signals*. J. Biol. Chem., 1998. **273**(12): p. 7141-7.
165. Michod, D. and C. Widmann, *TAT-RasGAP317-326 requires p53 and PUMA to sensitize tumor cells to genotoxins*. Mol Cancer Res, 2007. **5**(5): p. 497-507.

Chapter 2 - Results 1

2 RASGAP IS INVOLVED IN THE ANTIAPOPTOTIC RESPONSE OF ITS CLEAVAGE FRAGMENTS.

2.1 Introduction.

Apoptosis is a vital phenomenon that participates in the elimination of infected, damaged or unnecessary cells. The elimination of those cells is essential for normal development and homeostasis in multicellular organism. Every cell is programmed to undergo apoptosis in response to the appropriate stimulus (e.g. growth factor withdrawal, DNA damage, oxidative stress and stimulation of death receptors). Cells undergoing apoptosis exhibit characteristics morphological and biochemical transformations including nuclear condensation, cell blebbing, DNA cleavage, abrogation of anti-apoptotic pathways, formation of apoptotic cell bodies and expression of apoptotic markers at the cell surface [1].

The ultimate responsible for the dismantling of cell undergoing apoptosis is a specific subset of cysteine-dependent proteases that cut after aspartic residues, named caspases [2]. Caspases exert their apoptotic function by cleaving many different kinds of proteins like structural proteins (e.g. fodrin [3]), other caspases (e.g. caspases 7/9), tumour suppressors (e.g. Retinoblastoma [4]), nucleases (e.g. ICAD [5]) and pro-apoptotic proteins (e.g. Bid [6]).

Until recently, the activation of caspases was considered a point of no return; once cells had activated their caspases they were irremediably committed to die [2]. Accordingly, most caspase substrates when cleaved become pro-apoptotic, like Bid or become pro-apoptotic by losing their anti-apoptotic effects [7].

This view has been contested with the recent discovery that apoptotic caspases have additional functions besides being the executioners of cell death. For example, caspase-3 has

been involved in lymphocyte proliferation [8] and muscle differentiation [9]. How cells deal with low levels of caspase activity without fully activating the cell death pathway? Part of the answer is now known: a small part of the caspases substrates acquires new anti-apoptotic properties when cleaved by caspases; this is the case for the protein kinases Fyn [10] and Lyn [11], although the biochemical mechanism has not being described yet.

The p120 Ras GTPase activating protein (RasGAP) a key regulator in the Ras signalling pathway [12-14] is a atypical caspase substrate [15]. RasGAP possesses 2 distinct caspase cleavage sites, located at aminoacids 157 and 455 [15]. At low caspase activity RasGAP is cleaved at its 455 site, and the N-terminal generated fragment induces an anti-apoptotic signal that is mediated via the activation of the Ras-PI3K-Akt pathway [16]. When caspase activity increases the N-terminal fragment is further cleaved at its 157 site abrogating its anti-apoptotic activity [15].

RasGAP in addition to its GTPase activating domain contains, in the N-terminal part, one SH3 domain flanked by two SH2 domains, a plekstrin homology domain (PH), a calcium dependent lipid binding domain (C2) and a proline rich domain. All these domains specify different ways for RasGAP to interact with the plasma membrane and other proteins. Confirming this, RasGAP has been reported to interact with many different proteins. Interestingly, RasGAP in addition of its role as a negative regulator of Ras, has been found to be a possible effector of Ras [17]. Accordingly, the role of RasGAP in the survival pathway mediated by its cleavage fragment was investigated.

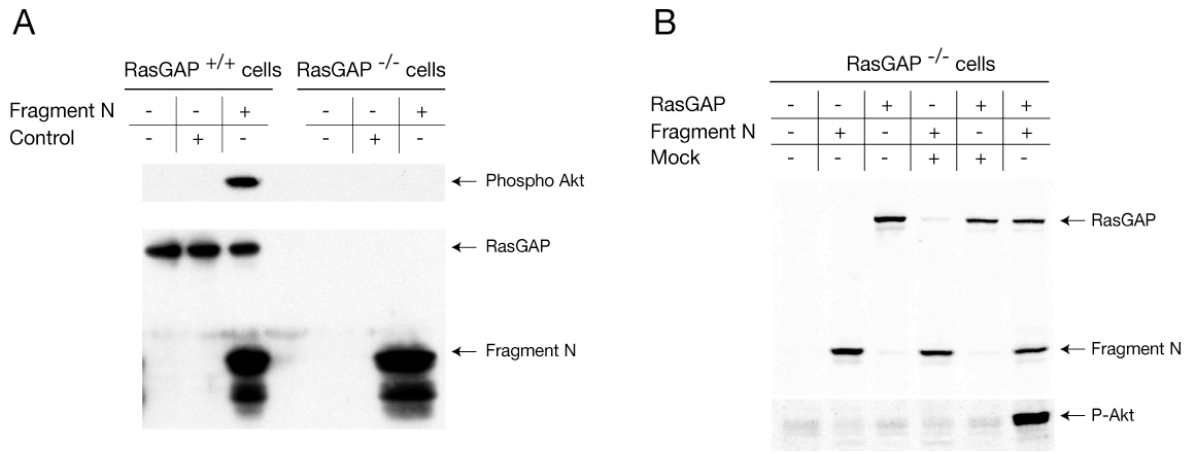

Figure 1. Fragment N-mediated Akt activation requires GAP activity of full-length RasGAP.
A. Mouse embryonic fibroblasts (MEFs) expressing or lacking RasGAP were-left untreated (C) or infected with empty lentiviruses (E) or lentiviruses encoding fragment N (N). Forty-eight hours after infection, the cells were starved for an additional 48 h period and Akt activation was measured by Western blot using a specific anti-phospho-Akt (Ser-473) antibody. The presence of fragment N and full-length RasGAP was visualized by reprobing the membrane with an anti-RasGAP antibody.
B. Mouse embryonic fibroblasts (MEFs) lacking RasGAP were infected with empty lentiviruses or lentiviruses encoding full-length RasGAP and fragment N. Akt activation and RasGAP expression was determined as in A.

2.2 Results

2.2.1 RasGAP is involved in the anti-apoptotic pathway activated by its cleavage fragments.

The detailed mechanism by which fragment N activates Ras and Akt is currently unknown. To assess the role played by full-length RasGAP in the activation of this pathway, mouse embryonic fibroblast (MEFs) derived from mice expressing the wild-type form of RasGAP (RasGAP+/+ MEFs) or RasGAP knock-out (RasGAP-/- MEFs) were infected with lentiviruses coding for fragment N or empty lentiviruses as a control. The activation of Akt was then assessed. As it can be seen in Figure 1A, Akt is activated by fragment N only in cells expressing full-length RasGAP. To determine if the lack of Akt stimulation by fragment N in RasGAP knock-out cells was specifically due to the absence of RasGAP, a rescue experiment was performed. RasGAP-/- MEFs were infected with an empty virus or a lentivirus encoding an HA-tagged form of RasGAP. Additionally, the cells were co-infected or not with a lentivirus expressing fragment N (Figure 1B). Figure 1 B shows that only in the

presence of RasGAP were RasGAP-/- MEFs able to support fragment N-induced Akt activation. Infection with lentiviruses (especially when two different viruses were used) led to some processing of the ectopically expressed RasGAP protein into fragment N (see lanes 3 and 5 in Figure 1B), which is an indication that viral infection exerts a stress on the cells [2]. However, when the cells were infected with either RasGAP- or fragment N-encoding lentiviruses together with an empty virus, no activation of Akt was detected (Figure 1B, lanes 4 and 5). This indicates that the very low levels of fragment N that were generated from the expressed RasGAP protein were not sufficient to activate Akt.

2.2.2 RasGAP cleavage is not the trigger for Akt activation.

The results described above indicate that full-length RasGAP is required for fragment N-induced Akt stimulation. As RasGAP can be cleaved into various fragments by caspases [3], it could be envisioned that RasGAP fragments rather than the full-length protein were required for fragment N to activate Akt. Mutation of the cleavage recognition site at position 455 completely prevents RasGAP from being processed by caspases [2, 3]. When RasGAP -/- MEFs were infected with the uncleavable form of RasGAP (RasGAP D455A), fragment N was still able to induce Akt phosphorylation (Figure 2A). This indicates that processing of RasGAP is not required to allow fragment N-induced Akt stimulation.

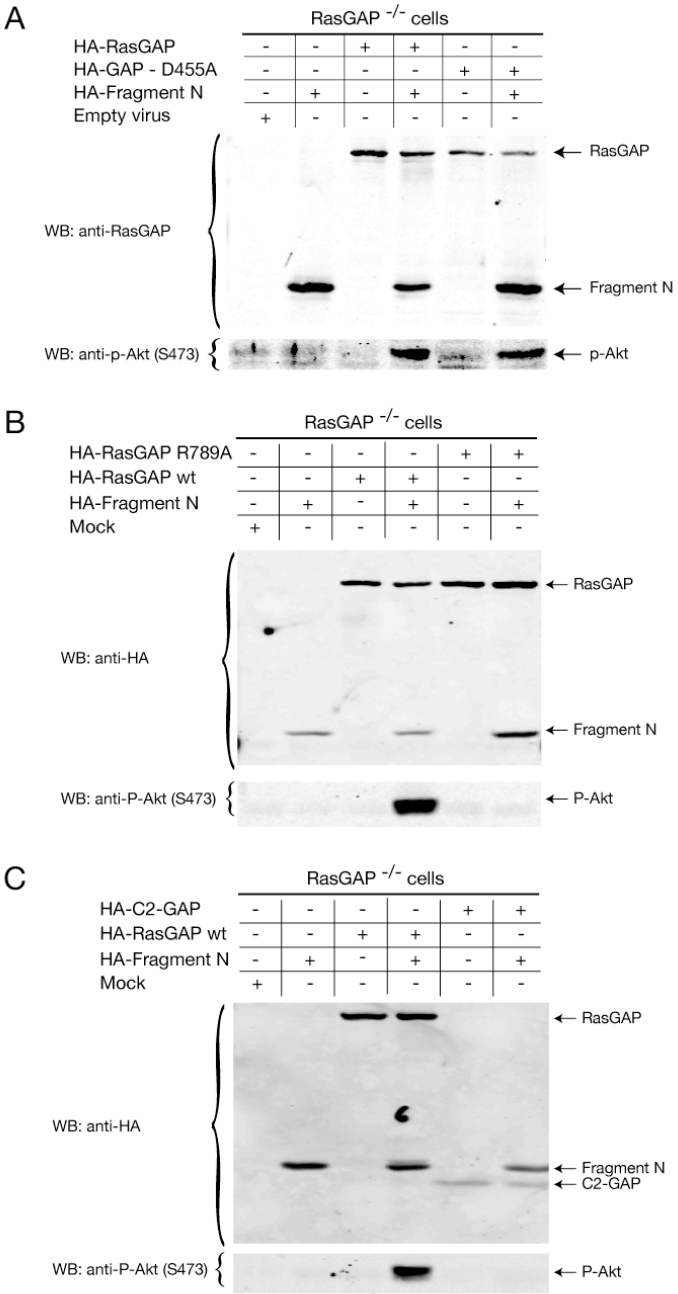

Figure 2. Fragment N-mediated Akt activation requires GAP activity of full-length RasGAP.
A. Mouse embryonic fibroblasts (MEFs) lacking RasGAP expression, were infected with empty lentiviruses (mock) or lentiviruses encoding fragment N, full-length RasGAP and RasGAP uncleavable mutant D455A. Forty-eight hours after infection, the cells were starved for an additional 24h period and Akt activation was measured by Western blot using a specific anti-phospho-Akt (Ser-473) antibody. The presence of fragment N and both wt and mutant RasGAP was visualized using an anti-HA antibody
B. Mouse embryonic fibroblasts (MEFs) lacking RasGAP expression, were infected with empty lentiviruses (mock) or lentiviruses encoding fragment N, full-length RasGAP and the GAP deficient RasGAP mutant R789A. Akt activation and RasGAP expression was determined as in A..
C. MEFs lacking RasGAP were infected with empty lentiviruses (mock) or lentiviruses encoding full-length RasGAP, C2-GAP truncated form of RasGAP and fragment N. Akt activation and RasGAP expression was determined as in A.

2.2.3 The GTPase-activating domain of RasGAP is required but not sufficient to allow fragment N-induced Akt activation.

RasGAP bears multiple domains, including SH and PH domains and a GTPase-activating domain. To assess if the function of the latter was important to allow fragment N-induced Akt stimulation, a mutant form of RasGAP in which arginine 789 is mutated into an alanine residue was generated ($RasGAP^{R789A}$). Arginine 789 of RasGAP favors Ras-mediated GTP hydrolysis and its mutation is expected to hamper the GTPase-activating function of RasGAP [18]. $RasGAP^{-/-}$ MEFs infected with a lentivirus encoding $RasGAP^{R789A}$ did not support fragment N-induced Akt phosphorylation (Figure 2A). This suggests that the GAP activity of RasGAP is required for fragment N to activate Akt. We next assessed if the GAP activity was sufficient for fragment N-mediated Akt stimulation. Initially, we wanted to test a construct bearing only the GAP domain of RasGAP. However, this construct was very poorly expressed in cells. We therefore generated a slightly longer construct consisting of the C2 domain and the GAP domain of RasGAP (C2-GAP). When $RasGAP^{-/-}$ MEFs were infected with lentiviruses encoding C2-GAP and fragment N, no Akt phosphorylation was detected (Figure 2C). These results indicate that the GAP activity of full-length RasGAP is required but not sufficient for fragment N-mediated Akt activation.

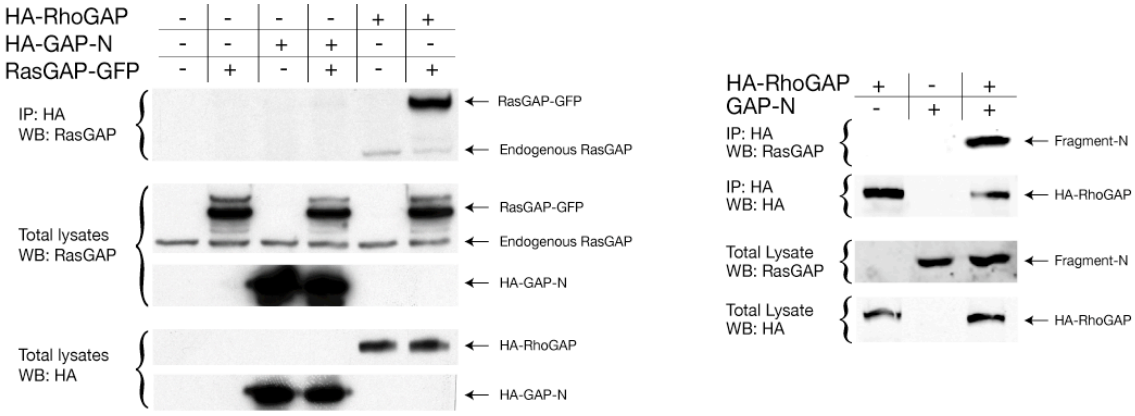

Figure 3. Fragment N does not interact with RasGAP
293T cells (2x106) were plated in a 10 cm petri dish and transfected with plasmids encoding the indicated constructs. Twenty-four hours after the transfection, the cells were lysed in RIPA buffer (50 mM Tris/HCl pH 7.4, 150 mM NaCl, 0.25 % Na-Deoxycholate, 1 % NP40, 1 mM EGTA, 1 mM NaF, 0.5 mM Na3VO4 and protease inhibitor). One milligram of total cellular protein was precleared with protein G sepharose for 15' at 4°C. The precleared lysate was then incubated with an anti-HA antibody for 2 hr at 4°C. After two hours, protein G sepharose beads were added and incubated for a further hour in identical conditions. The beads were then washed 3 times and the proteins released using 60 µl of 2x sample buffer at 95°C. The samples were loaded on a 10 % polyacrilamide gel, blotted onto nitrocelulose membrane and analyzed by Western blot, as indicated.

2.2.4 Fragment N does not interact with RasGAP.

Recent data on the structure of the SH3 domain of RasGAP (amino acids 281–341) suggests that this domain can form dimers [19]. This raises the possibility that RasGAP and fragment N, which both bear the SH3 domain, could form homo- or hetero-dimers. Immuno-precipitation experiment were performed to assess if RasGAP can interact with fragment N. HEK 293T cells were transfected with an HA-tagged forms of fragment N together with a GFP-tagged version of RasGAP. An HA-tagged form of RhoGAP was used as positive control due to its known ability to bind RasGAP [20]. Figure 4A shows that, in conditions where interaction between RasGAP-GFP and RhoGAP can readily be detected, no binding of RasGAP to its fragment N was observed. This was not due to an intrinsic inability of fragment N to interact with proteins because fragment N could interact with RhoGAP and be co-immuno-precipitated (Figure 3B). These results suggest that fragment N does not bind to its parental molecule.

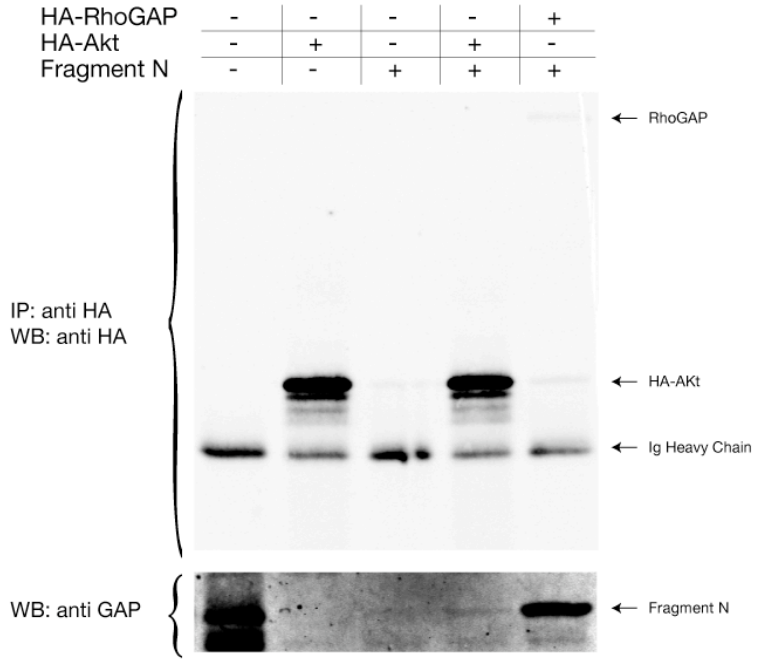

Figure 4. Fragment N does not Interact with Akt.
293T cells (2x106) were plated in a 10 cm petri dish and transfected with plasmids encoding the indicated constructs. Twenty-four hours after the transfection, immunoprecipitaion was performed as indicated.

2.2.5 Fragment N does not interact with Akt.

Earlier results have indicated that fragment N leads to Akt activation in a Ras-dependent manner [16]. However, there has been a claim that fragment N directly binds Akt, leading to a Ras-independent activation of the kinase [21]. We therefore assessed whether we could detect an interaction between fragment N and Akt. As seen in figure 4, whilst the immuno-precipitation of RhoGAP brings down fragment N, immuno-precipitation of Akt did not, despite larger immuno-precipitated amounts of Akt compared to RhoGAP. It appears therefore unlikely that the way fragment N activates Akt can be attributed to a direct interactions of the two proteins.

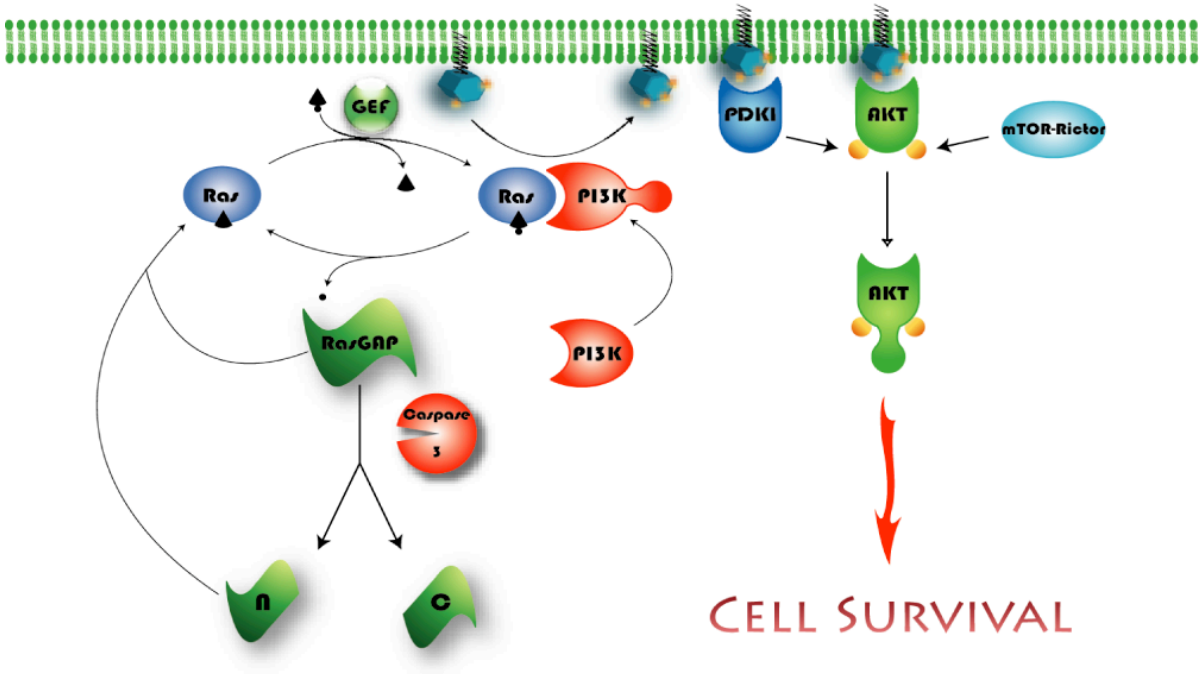

Figure 5. Fragment N-mediated Akt activation requires GAP activity of full-length RasGAP.

2.3 Discussion.

In addition to modulate Ras activity and to be a potential effector of Ras [22], RasGAP plays a role in the regulation of apoptosis [23]. The first cleavage of RasGAP by caspases allows the cells to maintain a low level of caspase activity while avoiding the cells to engage themselves in apoptosis [23]. The anti-apoptotic signaling generated by RasGAP cleavage is mediated by the N-terminal fragment (fragment N) that activates the Ras-PI3K-Akt pathway [16]. Cells unable to cleave RasGAP are very sensitive to different stresses [23] demonstrating the important function of RasGAP cleavage in cell survival.

RasGAP has been shown to be required for some Ras-mediated cellular responses [24-27]. The N-terminal part of RasGAP has in fact been shown to activate Ras and, subsequently, PI3K and Akt [16]. However, how fragment N stimulates the Ras-PI3K-Akt pathway is not understood. Here we show that fragment N cannot act independently of its parental molecule RasGAP to activate the pathway leading to Akt stimulation. This suggests that besides its

well known inhibitory action on Ras via its GAP domain, RasGAP in concert with its fragment N participate in the activation of the Ras-PI3K-Akt pathway. However, we could not detect any physical interaction between RasGAP and fragment N, which suggests that the mechanisms by which RasGAP and its fragment regulate Ras pathways are complex and probably involve other molecules.

2.4 Materials and Methods.

2.4.1 Cell culture and transfection.

The RasGAP +/+ mouse embryonic fibroblasts (MEFs; clone 12.78), the RasGAP -/- MEFs (clone 12.64) [23], and HEK 293T cells were maintained in DMEM containing 10% newborn calf serum (Invitrogen, cat. no. 26010-074) at 37°C and 5% CO_2. Transfections were performed using the calcium phosphate DNA precipitation method [28], and DNA amounts were normalized using pcDNA3 vector.

2.4.2 Plasmids.

The plasmid bearing the uncleavable form of fragment N (N-D157A.lti) used for the production of fragment N-encoding lentivirus has been described previously [23]. Plasmid HA-GAP.dn3 encodes the full-length human RasGAP protein bearing an HA tag (MGYPYDVPDYAS) at the amino-terminal end [15]. Plasmid HA-D455A.dn3 encodes a RasGAP mutant that cannot be cleaved at position 455 [15]. HA-GAPN.dn3 encodes the HA-tagged (at the N terminus) version of RasGAP fragments from positions 1 to 455 [15]..

Plasmid HA-RasGAP (no 3' UTR).lti, used for the production of lentiviruses encoding full-length RasGAP without the 3' UTR was described previously [29]. HA-RhoGAP.dn3 is a generous gift from Jeffrey Settleman. HA-RasGAP (R789A).dn3 was generated by PCR mutagenesis [30] using the following primers: ATGAAGCCACTACCCTATTTGCAGCCACAACACTTGCAAGCAC,

TACCTAGCATGAACAGATTGAGGGGCAAACAACAGATG,

TACCTAGCATGAACAGATTG and CTCATGCAAGGGAAGGGCAA. HA-C2-GAP.dn3 was generated by PCR amplification of plasmid HA-RasGAP (no 3' UTR).dn3 with primers sense

GGGGATCCGCCACCATGGGCTACCCGTACGACGTGCCGGACTACGCTTCTACAT

CCAATAAACGCCTTCGT and antisense GGGACCCTGGTTCAATACCT; a 369 bps BamHI/BlpI PCR fragment was ligated to a 6460 bps BamHI/BlpI from HA-RasGAP (no 3' UTR).dn3, to generate the HA-C2-GAP.dn3 plasmid. All of the constructs containing PCR inserts have been sequenced to verify that no PCR errors occurred.

2.4.3 Chemicals

Hexadimethrine bromide (Sigma, Polybrene, cat. no. 52495)

Alexa Fluor 680-conjugated anti-rabbit antibody (Molecular Probes, Eugene, OR; cat. no. A21109) or an IRDye 800-conjugated anti-mouse antibody (Rockland, Gilbertsville, PA; cat. no. 610-132-121)

2.4.4 Western Blot

Cells were lysed in monoQ-c buffer (70 mM ß-glycerophosphate, 0.5% Triton X-100, 2 mM $MgCl_2$, 1 mM EGTA, 100 mM Na_3VO_4, 1 mM dithiothreitol, 20 mg of aprotinin per ml) Western blotting was performed as described previously [31] using a homemade ECL reagent [15] or the infrared imaging system (LICOR Biosciences, Bad Homburg, Germany [29].

2.4.5 Lentiviral Infection

Recombinant lentivirus was produced as described previously [32]. Briefly, 293T cells were cotransfected using the calcium phosphate DNA precipitation method [28] with 10 µg of the lentiviral vector containing the cDNA of interest (e.g., N-D157A.lti), 2.5 µg of the envelope protein-coding plasmid (pMD.G), and 7.5 µg of the packaging construct (pCMVΔR8.91).

Two days after the transfection, the virus-containing medium was harvested. To determine how much of the virus preparation was needed to infect 100% of the MEFs, subconfluent wild-type MEFs seeded in six-well plates were cultured overnight with various volumes of fragment N or RasGAP encoding recombinant virus. After removal of the virus solution, the cells were maintained for two more days before fixation and immunocytochemical staining with antibodies directed at the protein expressed by the lentivirus. The lowest volumes of the lentiviral preparations required to infect 100% of the cells were chosen for further experiments.

Infection of the cells was performed as follows. Hexadimethrine bromide was added to cells cultured in six-well plates to a final concentration of 5 µg/ml, followed by the addition of the lentiviruses. The plates were then centrifuged 45 min at 800 *x*g and placed 24 h at 37°C in a 5% CO_2 humidified atmosphere. The medium was then replaced with fresh medium, and the cells were further cultured for an additional 48-h period before being used in specific experiments.

2.4.6 Immunoprecipitation.

HEK 293T cells ($2x10^6$) were plated in a 10 cm petri dish and transfected with plasmids encoding the appropriate constructs. Twenty-four hours after the transfection, the cells were lysed in RIPA buffer (50 mM Tris/HCl pH 7.4, 150 mM NaCl, 0.25 % Na-Deoxycholate, 1 % NP40, 1 mM EGTA, 1 mM NaF, 0.5 mM Na_3VO_4 and protease inhibitor). One milligram of total cellular protein was precleared with protein G sepharose for 15' at 4°C. The precleared lysate was then incubated with an anti-HA antibody for 2 hr at 4°C. After two hours, protein G sepharose beads were added and incubated for a further hour in identical conditions. The beads were then washed 3 times and the proteins released using 60 µl of 2x sample buffer at 95°C. The samples were loaded on a 10 % polyacrilamide gel, blotted onto nitrocelulose membrane and analyzed by Western blot.

2.5 References.

1. Ziegler, U. and P. Groscurth, *Morphological features of cell death.* News Physiol Sci, 2004. **19**: p. 124-8.
2. Thornberry, N. and Y. Lazebnik, *Caspases: enemies within.* Science, 1998. **281**(5381): p. 1312-6.
3. Cryns, V., et al., *Specific cleavage of alpha-fodrin during Fas- and tumor necrosis factor-induced apoptosis is mediated by an interleukin-1beta-converting enzyme/Ced-3 protease distinct from the poly(ADP-ribose) polymerase protease.* J. Biol. Chem., 1996. **271**(49): p. 31277-82.
4. Jänicke, R., et al., *Specific cleavage of the retinoblastoma protein by an ICE-like protease in apoptosis.* EMBO J., 1996. **15**(24): p. 6969-78.
5. Liu, X., et al., *DFF, a heterodimeric protein that functions downstream of caspase-3 to trigger DNA fragmentation during apoptosis.* Cell, 1997. **89**(2): p. 175-84.
6. Li, H., et al., *Cleavage of BID by caspase 8 mediates the mitochondrial damage in the Fas pathway of apoptosis.* Cell, 1998. **94**(4): p. 491-501.
7. Widmann, C., S. Gibson, and G. Johnson, *Caspase-dependent cleavage of signaling proteins during apoptosis. A turn-off mechanism for anti-apoptotic signals.* J. Biol. Chem., 1998. **273**(12): p. 7141-7.
8. Tang, J., H. Kawadler, and X. Yang, *Lymphocyte life and death: the caspase-8 connection.* Cancer Biol Ther, 2005. **4**(7): p. 700-2.
9. Fernando, P., et al., *Caspase 3 activity is required for skeletal muscle differentiation.* Proc. Natl. Acad. Sci. U.S.A., 2002. **99**(17): p. 11025-30.
10. Ricci, J., et al., *An absolute requirement for Fyn in T cell receptor-induced caspase activation and apoptosis.* FASEB J, 2001. **15**(10): p. 1777-9.
11. Luciano, F., et al., *The p54 cleaved form of the tyrosine kinase Lyn generated by caspases during BCR-induced cell death in B lymphoma acts as a negative regulator of apoptosis.* FASEB J., 2003. **17**(6): p. 711-3.
12. Campbell, S., et al., *Increasing complexity of Ras signaling.* Oncogene, 1998. **17**(11 Reviews): p. 1395-413.
13. Leblanc, V., B. Tocque, and I. Delumeau, *Ras-GAP controls Rho-mediated cytoskeletal reorganization through its SH3 domain.* Mol. Cell. Biol., 1998. **18**(9): p. 5567-78.
14. Wen, L., et al., *Proteolytic cleavage of ras GTPase-activating protein during apoptosis.* Cell Death Differ., 1998. **5**(9): p. 729-34.
15. Yang, J. and C. Widmann, *Antiapoptotic signaling generated by caspase-induced cleavage of RasGAP.* Mol. Cell. Biol., 2001. **21**(16): p. 5346-58.
16. Yang, J. and C. Widmann, *The RasGAP N-terminal fragment generated by caspase cleavage protects cells in a Ras/PI3K/Akt-dependent manner that does not rely on NFkappa B activation.* J. Biol. Chem., 2002. **277**(17): p. 14641-6.
17. Tocque, B., et al., *Ras-GTPase activating protein (GAP): a putative effector for Ras.* Cell. Signal., 1997. **9**(2): p. 153-8.
18. Resat, H., et al., *The arginine finger of RasGAP helps Gln-61 align the nucleophilic water in GAP-stimulated hydrolysis of GTP.* Proc. Natl. Acad. Sci. U.S.A., 2001. **98**(11): p. 6033-8.
19. Ross, B., et al., *High resolution crystal structures of the p120 RasGAP SH3 domain.* Biochem. Biophys. Res. Commun., 2006. **353**(2): p. 463-8.
20. Hu, K. and J. Settleman, *Tandem SH2 binding sites mediate the RasGAP-RhoGAP interaction: a conformational mechanism for SH3 domain regulation.* EMBO J., 1997. **16**(3): p. 473-83.

21. Yue, Y., et al., *Ras GTPase-activating protein binds to Akt and is required for its activation.* J. Biol. Chem., 2004. **279**(13): p. 12883-9.
22. Tocqué, B., et al., *Ras-GTPase activating protein (GAP): a putative effector for Ras.* Cell. Signal., 1997. **9**(2): p. 153-8.
23. Yang, J., et al., *Partial cleavage of RasGAP by caspases is required for cell survival in mild stress conditions.* Mol. Cell. Biol., 2004. **24**(23): p. 10425-36.
24. Duchesne, M., et al., *Identification of the SH3 domain of GAP as an essential sequence for Ras-GAP-mediated signaling.* Science, 1993. **259**(5094): p. 525-8.
25. Schweighoffer, F., et al., *Implication of GAP in Ras-dependent transactivation of a polyoma enhancer sequence.* Science, 1992. **256**(5058): p. 825-7.
26. Martin, G., et al., *GAP domains responsible for ras p21-dependent inhibition of muscarinic atrial K+ channel currents.* Science, 1992. **255**(5041): p. 192-4.
27. Yatani, A., et al., *ras p21 and GAP inhibit coupling of muscarinic receptors to atrial K+ channels.* Cell, 1990. **61**(5): p. 769-76.
28. Jordan, M., A. Schallhorn, and F. Wurm, *Transfecting mammalian cells: optimization of critical parameters affecting calcium-phosphate precipitate formation.* Nucleic Acids Res, 1996. **24**(4): p. 596-601.
29. Yang, J., et al., *Impaired Akt activity down-modulation, caspase-3 activation, and apoptosis in cells expressing a caspase-resistant mutant of RasGAP at position 157.* Mol. Biol. Cell, 2005. **16**(8): p. 3511-20.
30. Nelson, R. and G. Long, *A general method of site-specific mutagenesis using a modification of the Thermus aquaticus polymerase chain reaction.* Anal Biochem, 1989. **180**(1): p. 147-51.
31. Widmann, C., W. Dolci, and B. Thorens, *Agonist-induced internalization and recycling of the glucagon-like peptide-1 receptor in transfected fibroblasts and in insulinomas.* Biochem. J., 1995. **310 (Pt 1)**: p. 203-14.
32. Dull, T., et al., *A third-generation lentivirus vector with a conditional packaging system.* J. Virol., 1998. **72**(11): p. 8463-71.

Chapter 3 – Results 2

3 IMPORTANCE OF RASGAP CLEAVAGE IN MOUSE PHYSIOLOGY.

3.1 Introduction

Caspases are known as the executioners of apoptotic cell death [1]. Once cell are subjected to an apoptotic stimulus, upstream or initiator caspases (e.g. caspase 8 and 9) are activated, and in turn cleave and activate downstream or executioner caspases (e.g. caspase 3 and 7) [2]. Once activated, executioner caspases cleave a plethora of proteins resulting in the stimulation of pro-apoptotic pathways and the inactivation of pro-survival pathways, eventually leading to the physical dismantling of the cell [3, 4].

It was earlier assumed that caspase activation would inexorably lead to apoptotic cell death [1]. Even though this remains true in most situations, there is increasing evidence linking caspase activation and physiological functions other than apoptosis. For example, caspase 3 is required for skeletal muscle [5] and neural stem cell development [6]. Moreover, caspase 8 is required for lymphocyte activation and homeostasis [7, 8].

The involvement of caspases in non-lethal responses implies that the pro-death functions of the caspases are kept in check in these particular cases. Cells have developed several anti-apoptotic mechanisms to ensure cell survival involving proteins of the Bcl2 family and members of the inhibitor of apoptosis (IAP) family [9-11]. There is however a major difference between these two types of proteins. While the anti-apoptotic Bcl2 family members prevent the activation of caspases, the IAPs can, directly or indirectly, inhibit caspase activity [12].

As mentioned above, the great majority of caspase substrates, when cleaved, participate in the apoptotic process. There are however some exceptions. Cleavage of PKCε activates the

enzyme and this in turn mediates the activation of antiapoptotic signals [13]. Activation of B-cell receptor triggers the cleavage of the kinases Fyn and Lyn generating fragments that inhibit apoptosis [14, 15]. In addition, we have shown that RasGAP, a regulator of Ras and Rho signalling pathways, when cleaved by caspases generates a potent anti-apoptotic response [16].

RasGAP possesses two conserved caspase-3 cleavage sites [16]. At low levels of caspase activity, RasGAP is first cleaved at position 455. The N-terminal fragment (fragment N) generated by the cleavage activates a potent anti-apoptotic-signalling pathway mediated by the Ras/PI3K/Akt pathway [17], which is crucial for cell survival in low stress conditions [18]. However, at higher caspase activity, fragment N is further cleaved at position 157 and this abrogates its anti-apoptotic activity [19]. This has led us to postulate that RasGAP acts as a sensor of caspase activity to control a death/survival switch [20]. At low levels of caspase activity (i.e. levels that would be required for the non-apoptotic functions of caspases), RasGAP is cleaved once into fragment N to protect cells from fully activating their executioner caspases. When caspase activity increases, fragment N is further cleaved and inactivated, allowing the full caspase activation and apoptosis induction.

In the present work, we present the characterization of the first animal model, in which a caspase substrate involved in anti-apoptotic signalling, has been rendered caspase resistant.

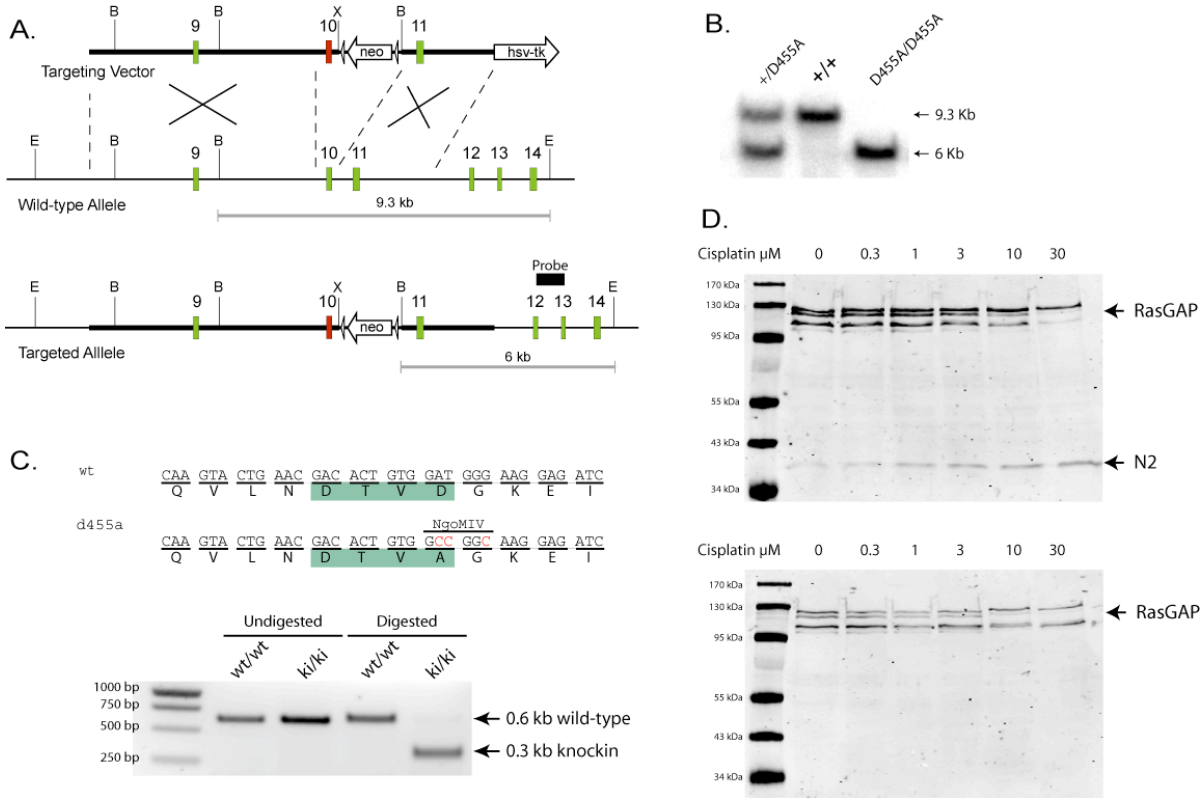

Figure 1. Generation of RasGAP D455A knock-in mice.
A. The targeting vector consists of mouse RasGAP exon 9, 10 and 11. Exon 10 (red box) bears the RasGAP D455A mutation. E, X and B stand for *Eco*RV, *Xho*I and *Bam*HI. The grey bars located below the alleles represent the length of the *Bam*HI/*Eco*RV fragments recognized by the probe (indicated by the black bar) when performing for Southern blot genotyping.
B. Tail-purified genomic DNA was digested with *Eco*RV and *Bam*HI and tested by Southern blot, using the probe shown in panel A.
C. Detection of the D455A allele by PCR. The D455A allele bears a new *Ngo*MIV restriction site encompassing the aspartate to alanine mutation (in red) within the first caspase recognition site in RasGAP (in green). Genomic DNA was subjected to PCR amplification using primers flanking exon 10. The amplified fragments, after having been digested or not with *Ngo*MIV, were separated in a 1.5 % agarose gel. Presence of the D455A mutation results in cleavage of the ~600 bp PCR fragment into two ~300 bp fragments.
D. Wild-type and RasGAP $^{D455A/D455A}$ macrophages were treated with increasing concentrations of cisplatin for 24 hours. The cells were then lysed, subjected to SDS-PAGE, and blotted with an anti-RasGAP polyclonal antibody.

3.2 Results

3.2.1 Generation of a knock-in mouse expressing a caspase insensitive mutant of RasGAP.

The introduction of a mutation into the RasGAP genomic sequence was made by homologous recombination. The targeting strategy consisted in replacing RasGAP exon 10 by a mutant form carrying the mutation (Figure 1A). The targeting vector (described in material and methods) contained a mutant version of exon 10 in which the D455A mutation was introduced together with a silent mutation to introduce a restriction site (Figure 1C). The

presence of the targeted allele was visualized by southern blot (Figure 1B) or by PCR followed by *Ngo*MIV digestion (Figure 1C). Additionally, the presence of the mutation in mice homozygous for the mutated allele (RasGAP$^{D455A/D455A}$ mice) was assessed by Western blot of protein extracts of macrophages from wild-type mice of from RasGAP$^{D455A/D455A}$ mice treated with increasing concentrations of cisplatin. Even though fragment N could not be detected in macrophages, fragment N2, which can only be generated from fragment N [16], was only detected in wild-type macrophages (Figure 1D).

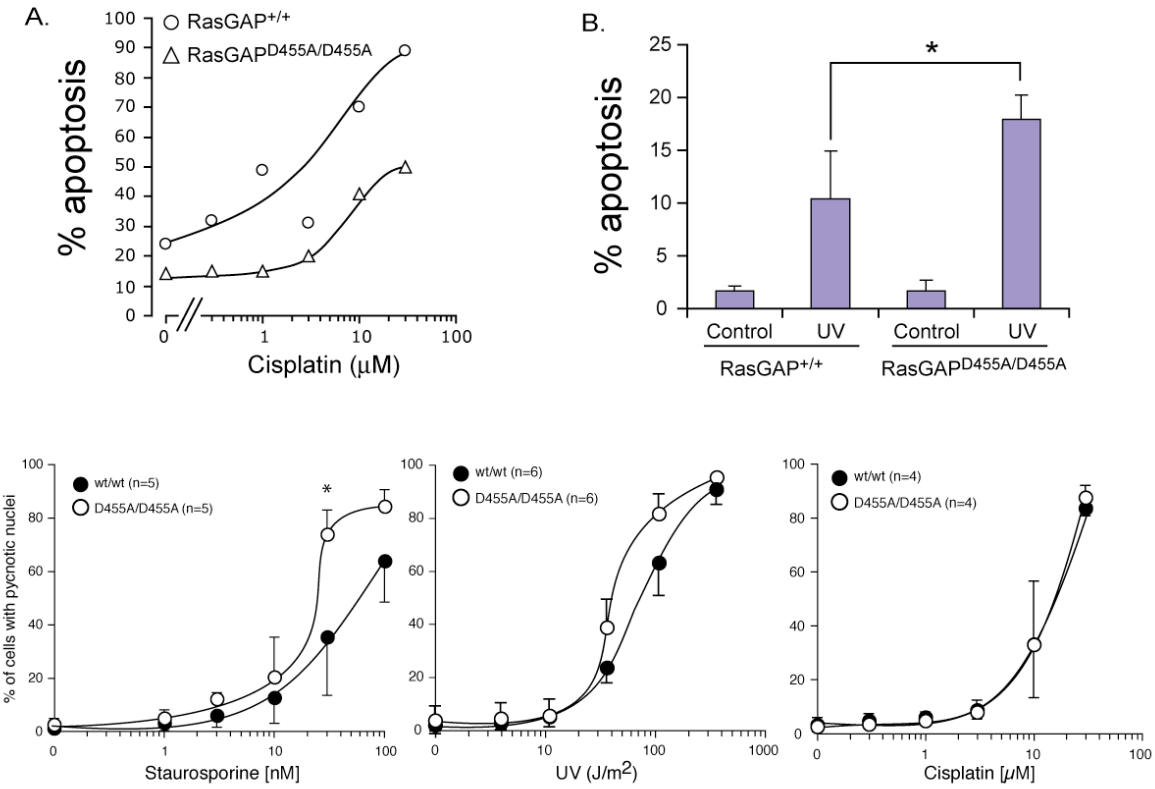

Figure 2. RasGAP$^{D455A/D455A}$ derived cells respond differently to stress induced apoptosis.
A. Wild-type and RasGAP$^{D455A/D455A}$ MEFs were treated with increasing concentrations of cisplatin for 24 hs and the percentage of cells with pycnotic nuclei was determined.
B. Wild-type and RasGAP$^{D455A/D455A}$ macrophages were treated with 2.5 J/m2 of UV light and 24 hs later the percentage of cells with pyknotic nuclei was determined.
C. Wild-type and RasGAP$^{D455A/D455A}$ macrophages were treated with increasing amouts of cisplatin, staurosporine and UV light. 24 hs later the percentage of cells with pyknotic nuclei was determined. * $p<0.05$.

The mutated and wild-type alleles segregated following the expected Mendelian ratios among the offsprings obtained after breeding RasGAP$^{+/D455A}$ mice (Table 1). Furthermore, fertility and longevity were not affected in the knock-in mice. In addition, histology of six month-old RasGAP$^{D455A/D455A}$ mice was apparently identical to wild-type littermates

(supplementary Figures S1-4). This indicates that preventing RasGAP cleavage does not affect development and homeostasis of the mice.

3.2.2 Apoptosis sensitivity.

We have previously demonstrated that cell lines lacking the capacity to generate fragment N were more sensitive to stress-induced apoptosis compared to their wild-type counterparts [18]. As expected, MEFs derived from RasGAP$^{D455A/D455A}$ mice treated with increasing concentrations of cisplatin showed increased levels of apoptosis when compared to the wild-type-derived counterparts (Figure 2A). Surprisingly when primary macrophages where treated with cisplatin they did no exhibit a different in apoptotic levels. When treated with UV macrophages showed balanced results. RasGAP$^{D455A/D455A}$ macrophages apoptosis levels where consistently higher that their wt counterparts, but the differences were not always significant. When treated with staurosporine RasGAP$^{D455A/D455A}$ macrophages were clearly more sensitive when compared to wt macrophages.

If different cells types showed increased sensitivity towards apoptosis we hypothesized that if treated chronically with an apoptotic stimulus, RasGAP$^{D455A/D455A}$ mice should decrease survival rate than the wt mice. The results obtained (data not shown) were contradictory, indicating that probably the absence of fragment N was not detrimental for mice survival, probably due to the presence of redundant mechanisms that could cope with the cisplatin-induced stress.

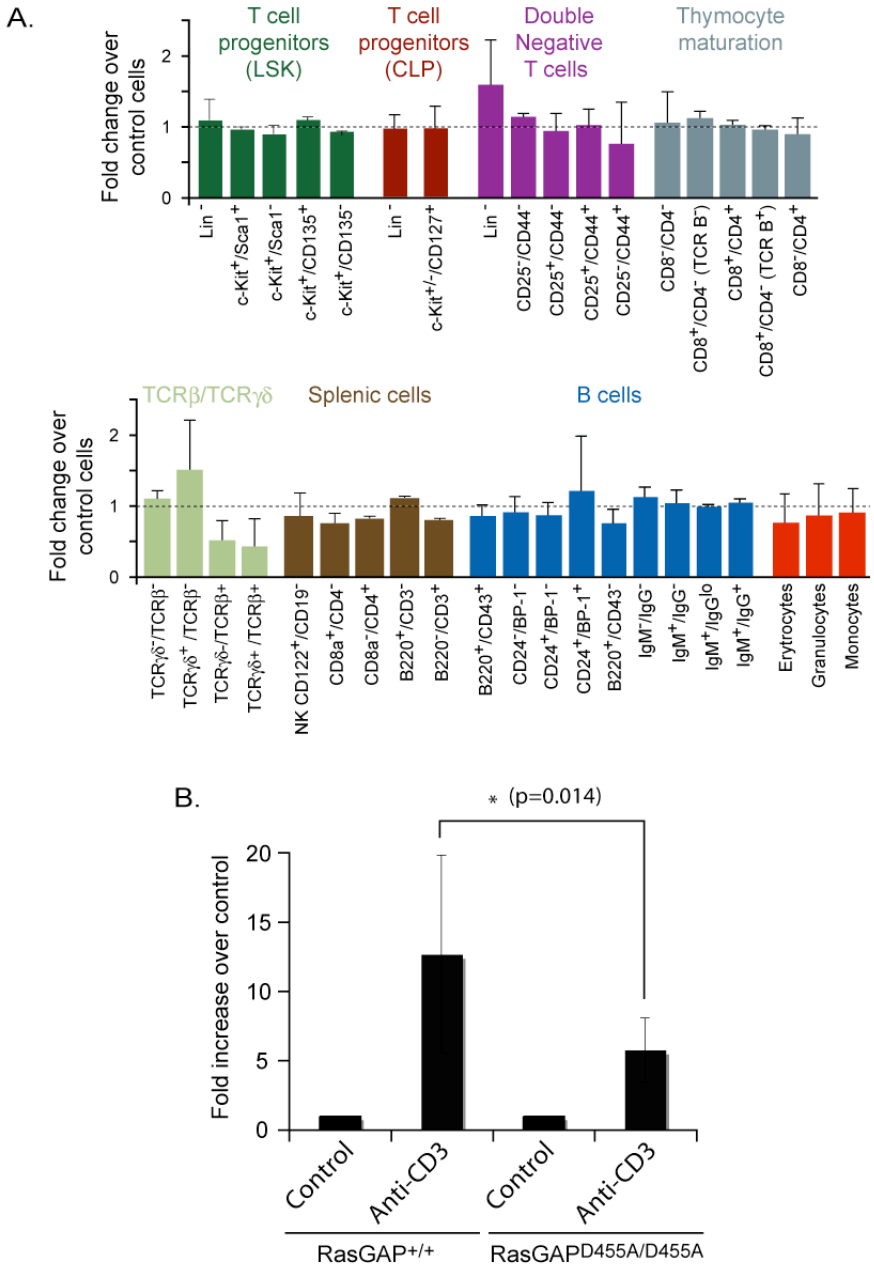

Figure 3. Role of RasGAP in haematopoietic cells.
A.The graph represents the fold change of RasGAP$^{D455A/D455A}$ over wild-type cell population. The different populations were determined by flow cytometry. The results correspond to the mean plus minus SD of two or three independent experiments.
B.Wild-type and RasGAP$^{D455A/D455A}$ splenocytes were isolated from the indicated mice and incubated 3 days in PBS of anti-CD3 antibody coated wells in a 96-well plate. Cell numbers were then measured using a MTT assay. The results correspond to the mean plus or minus SD of three independent experiments perfomed in triplicate.

3.2.3 RasGAP and the immune system.

Caspases have been involved in the development and homeostasis of the haematopoietic system. In order to determine if the immune system development was affected, different haematopietic precursor and their development was followed in the bone marrow, spleen and

thymus. As shown in figure 3A, none of these lineages seems to be affected, and the remaining differences can be attributed to inter-individual differences.

Caspase activity has also been involved in T-cell proliferation. To establish whether RasGAP cleavage play a role, T-cell activation induced proliferation was assessed. As shown in figure 3B, splenocytes derived from RasGAP$^{D455A/D455A}$ mice, showed a decreased proliferative rate, as measured by MTT. The MTT assay being by no means specific these results should be confirmed using other more specific methods to establish if the increased proliferation is due to T-cell proliferation and not to the proliferation of another cell type present in the splenocyte population. Furthermore, the decreased proliferation measured by MTT could be due to both, increased proliferation of wt cell or increased apoptosis in the RasGAP$^{D455A/D455A}$ cells. All these parameters should be assessed in order to establish the veracity of these findings.

Mendelian ratios	*Expected*	*Found*
RasGAP$^{wt/wt}$	25	26
RasGAP$^{D455A/wt}$	50	47
RasGAP$^{D455A/D455A}$	25	27

Table 1. Mendelian ratios obtained from RasGAP$^{D455A/wt}$ breeding.

3.2.4 Role of RasGAP in the regulation of chronic stress in cardiomyocites.

To study the effect of RasGAP cleavage in a model of chronic stress, RasGAP$^{D455A/D455A}$ and RasGAP$^{wt/wt}$ were left untreated of subjected to transaortic constriction (TAC) to induce a pressure overload in the heart. The increase in pressure in turn induces cardiac hypertrophy. After performing the TACs, heart evolution was followed by ecography and a series of parameters (showed in figure 4) were measured. Mice were measured at 2, 4 and 6 weeks post TAC. Figure 4 show the results obtained at 6 weeks post TAC. Even though no

difference showed to be significative, some parameters showed a clear tendency with p values very close to the threshold of significance. These parameters show a tendency for a higher level of hypertrophy in RasGAP$^{D455A/D455A}$ mice, with an increased HW/BW ratio and an increased left ventricular mass, figure 4.

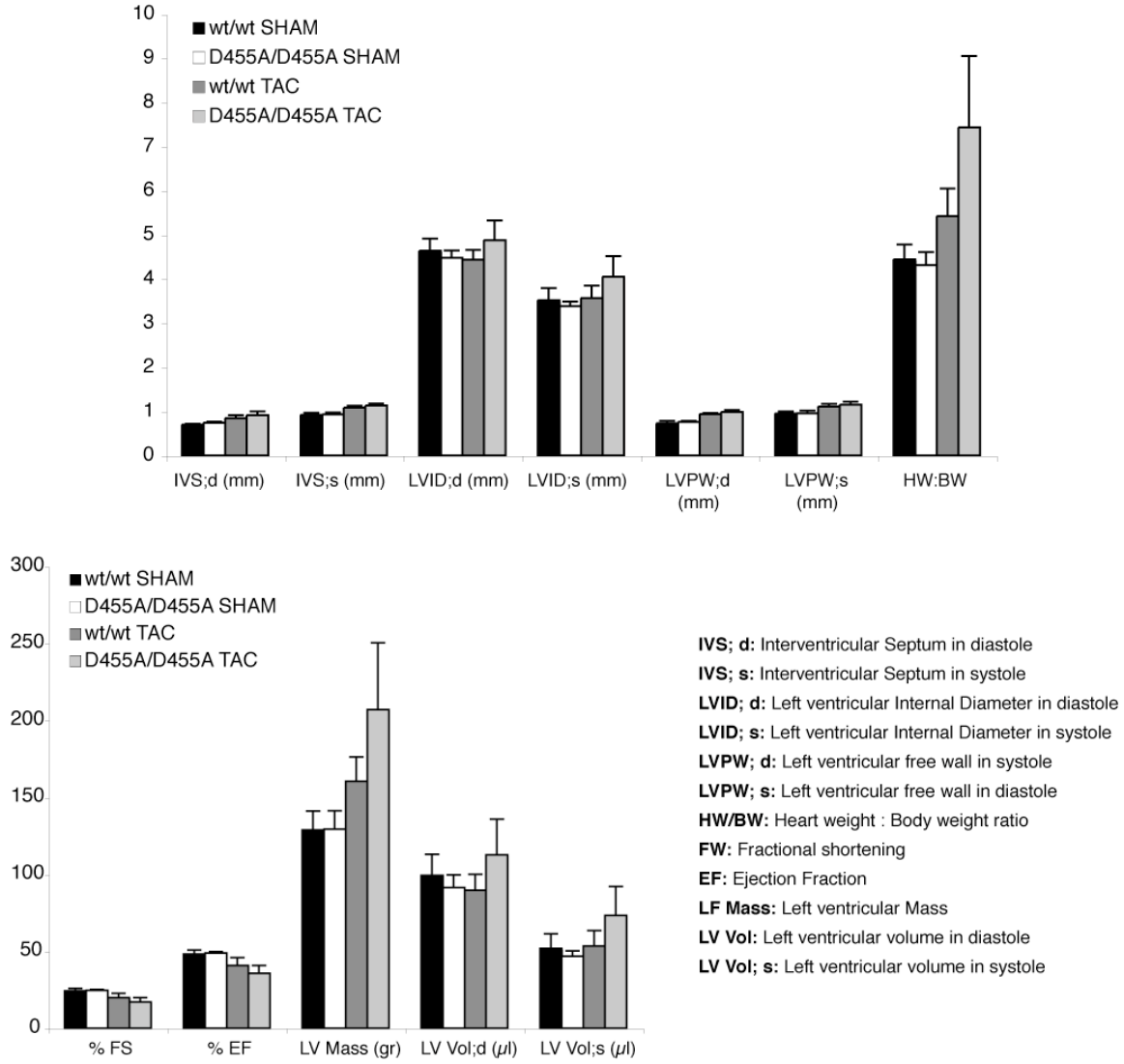

Figure 4. RasGAP$^{D455A/D455A}$ mice have increased heart hypertrophy following TAC.
Wild-type and **RasGAP$^{D455A/D455A}$** were left untreated of subjected to transaortic constriction (TAC). The graph represents different parameters measured by ecography. The units used are indicated together with the description, on the X axis.

3.3 Discussion

The results obtained so far demonstrate that RasGAP cleavage is not indispensable for normal development and homeostasis in mice. As shown in Figure 1, the RasGAP D455A mutation was successfully introduced into the genome of the mice. The southern blot shows

that the recombination was successful and Figure 1C clearly shows that the mutation is effectively present in the genome of mice bearing the targeted allele. At the protein level, the presence of the mutation is clear in the absence of fragment N2 in macrophages derived from $RasGAP^{D455A/D455A}$ mice. Even though only fragment-N2 is visible in macrophages derived from $RasGAP^{wt/wt}$, as fragment-N2 is generated by the cleavage of RasGAP at both caspase-cleavage sites (see Figure 11 in chapter 1), the presence of fragment N2 is an indirect probe of impossibility of fragment-N generation.

We have previously shown that cells expressing a caspase-insensitive RasGAP mutant were rendered more sensitive to low stress conditions, caused by the impossibility of cells to cleave RasGAP and induce the associated cell survival pathway [18]. Different cells isolated from $RasGAP^{D455A/D455A}$ showed an increase sensibility to stress-induced apoptosis. Remarkably, macrophages showed no significative difference when treated with increasing doses of UV light or cisplatin. This may be explained by the macrophages physiology. The assessment of increased sensibility to stress-induced apoptosis should be performed in a greater number of primary cell lines.

Preliminary experiments using γ irradiation and intraperitoneal injection of sublethal doses of cisplatin did not show any significative difference. These results indicate that RasGAP is not necessary for organism to survive after a sublethal stress. This is probably due to the presence of redundant survival mechanisms.

Caspases are involved in the development and maintenance of the immune system [21, 22] RasGAP cleavage does not appear to play a role in the development of the different haematopoietic cell lines (Figure 2A), since no significative difference was observed between $RasGAP^{D455A/D455A}$ and $RasGAP^{wt/wt}$ mice, and the variations could be attributed to inter-individual differences.

However, RasGAP$^{D455A/D455A}$ derived splenocytes showed an increased proliferative rate (measured by MTT assay) when stimulated with and anti-CD3 antibody. Nevertheless, these results should be confirmed. Further experiments, should aim at identify the nature of the proliferating population (since splenocytes are a mixed cell population) and clarify whether the increased proliferative rate is due to increased proliferation of increased apoptosis in the less proliferating cells.

Transaortic constriction (TAC) leads to hemodynamic overloading that in turn induces cardiac hypertrophy. Preliminary experiments in which TAC was performed in RasGAP$^{D455A/D455A}$ and RasGAP$^{wt/wt}$ mice showed that an increased hypertrophy in the RasGAP$^{D455A/D455A}$ mice that was confirmed by an increased Heart Weight (mg)/Body Weight (gr) ratio. Even though biochemical and histological characterizations remain to be done, we can hypothesize that increased apoptosis in KI hearts would induce proliferation as a compensatory mechanism, leading to an increased hypertrophy.

Even if a part of the results is still preliminary we can conclude that RasGAP cleavage it is not involved in the develoment and homestoasis of unchallenged mice. When mice were challenged the responses varied with the different stimuli, suggesting the existence of redundant protective mechanism. These result also imply that RasGAP cleavage might be an important survival factor in response to specific stress-inducers.

3.4 Materials and Methods

3.4.1 Generation of the RasGAP D455A knock-in mice.

The strategy used to create the targeting vector is presented in the supplementary Figure 1. The genomic clones containing the sequences required to construct the D455A targeting vector were obtained by screening the RPCI - 22 (129S6/SvEvTac) Mouse BAC Library (Bacpac Resources Children's Hospital Oakland) [23] with a probe corresponding to

nucleotides 7137306-7136366 of the *Mus musculus* chromosome 13, strain C57BL/6J (accession n° NT_039589.2). Three clones were identified as carrying the required sequence (RP22 - 250D10, RP22 - 268I2 and RP22 - 257P13).

Each clone was digested with *Swa*I in order to release a ~10 kb fragment containing parts of the genomic sequence (RasGAP exons 9-10-11) necessary to construct the targeting vector. The 10 kb bands were subcloned in the *Eco*RV restriction site of pBluescript II SK + (Stratagene). A plasmid containing RasGAP exons 9-10-11 was identified by PCR and called RasGAP exons 9-10-11.blu. From this plasmid, a blunt-ended 6.5 kb *Bst*XI fragment [nucleotides 7139579-7145879 from the *Mus musculus* chromosome 13 genomic contig (accession n° NT_039589.2)] was subcloned in the *Eco*RV restriction site of pBluescript II SK + to generate the 5' homology arm composed of parts of introns 8 and 9 and exon 9 (the resulting plasmid was called RasGAP exon 9.blu). A 2.6 kb *Hind*III fragment from RasGAP exons 9-10-11.blu (nucleotides 7138985-7136418 from the chromosome 13 genomic contig) was subcloned in the *Hind*III restriction site of pcDNA3 to generate the 3' homology arm composed of parts of introns 10 and 11 and exon 11 (the resulting plasmid was called RasGAP exon 11.dn3).

A 590 pb fragment (called the Vital Region [VR] as it encodes amino acid 455 of RasGAP) containing exon 10 and connecting the 5' and 3' homology arms was PCR amplified from the BAC clones described above using the Pwo polymerase (Roche Applied Science, catalogue number 04 340 868 001), sub-cloned into the *Sma*I and *Not*I sites pBluescript II SK+, and sequenced twice to confirm that no PCR-generated errors occurred (the resulting plasmid was called Lox 66 - RasGAP Exon 10.blu).

The mutation of the caspase cleavage site in exon 10 was done using the megaprimer PCR mutagenesis method [24] using the following primers:

1) sense primer for the first PCR: AA GTA CTG AAC GAC ACT GTG G**C**C GG**C** AAG GAG ATC TAT AAC ACA AT (sequence 641-685 from the *Mus musculus* RasGAP mRNA [gi 21703899] carrying an A to C mutation (underlined) that destroys the first RasGAP caspase cleavage site by substituting an aspartate (D) residue for an alanine (A) [16] and two additional silent mutations (bold) that, together with the D to A mutation, create a new restriction site recognized by the *Nae*I and *Ngo*MIV endonucleases.

2) anti-sense primer for the first PCR: TACCTAGCATGAACAGATTG (a random sequence not found in the plasmid) GCGGCCGC (NotI) GTTCTAAAACCCTGGTTATA (3' terminal sequence of the Vital Region; sequence 42026-42007 of *Mus musculus* BAC clone RP23-222G16 [gi 29367036]).

3) sense primer for the second PCR: CGTA CCCGGG (SmaI) AGTAGGTGGGTTCAGGAGCAG (sequence 42007-42026 of *Mus musculus* BAC clone RP23-222G16 [gi 29367036]).

4) anti-sense primer for the second PCR: TACCTAGCATGAACAGATTG (the same random sequence found in primer 2).

The mutated PCR product was digested with *Sma*I and *Not*I and subcloned into the *Sma*I/*Not*I sites of pBluescript II SK + [generating plasmid RasGAP exon 10 (D455A).blu].

The LoxP Targeting Vector (LTV) [kindly provided by Dr. Olivier Staub] was used as a backbone to construct the targeting vector. The LTV vector consists of a Neo cassette (PGK-Neo) flanked with two LoxP sites and a Herpes Simplex Virus - Timidine Kinase gene (HSV-TK).

RasGAP Exon 11.dn3 was digested with *Hind*III and the resulting 2.6 kb fragment was ligated into the *Hind*III site of LTV (generating plasmid LTV - Lox-Neo-Lox - RasGAP Exon 11). The 0.6 kb *Sma*I/*Not*I fragment of RasGAP Exon 10 (D455A).blu was ligated into

the *Sma*I/*Not*I sites of RasGAP Exon 9.blu, creating plasmid RasGAP Exons 9-10 (D455A).blu.

Finally, the *Sal*I/*Not*I 7 kb fragment of RasGAP Exons 9-10 (D455A).blu was inserted into the *Sal*I/*Not*I sites of LTV - Lox-Neo-Lox - RasGAP Exon 11 plasmid to obtain the final D455A Targeting Vector [plasmid RasGAP Exons 9-10 (D455A)-Lox-Neo-Lox-RasGAP Exon 11].

The targeting vector electroporation, clone selection and injection into D57/BL6 blastocystes was performed at the Transgenic Animal Facility of the Lausanne University.

3.4.2 Chemicals and antibodies

The anti-phospho-(serine 473)-Akt rabbit polyclonal IgG antibody was from Cell Signaling Technology (catalogue number 9271). The anti-RasGAP antibody directed at the Src homology domains of RasGAP was from Alexis (catalogue number ALX-210-860). Glucose was from Merck (catalogue number 1.08342). Cisplatin, staurosporine, 5(6)-carboxyfluorescein diacetate N-succinimidyl ester (CFSE), propidium iodide and Concanavalin A from *C. ensiformis* were from Sigma (catalogue number, P4394, S4400, 21888, P4170 and C0412, respectively). Annexin V-FITC and the 70 µm nylon mesh Cell strainer were from BD Biosciences (catalogue number 556419 and 352350, respectively).

3.4.3 Bone marrow-derived macrophages.

Mice were killed by cervical dislocation and soaked with 70% ethanol. A mid-back incision was performed to remove the skin from the lower part of the body. Feet were cut and hind legs were removed and placed in a Petri dish containing sterile medium. Excess muscle was removed for the legs, the knee joint was dislocated and the bone tips cut off. Total bone marrow cells were obtained by flushing the femur and tibia with 4 ml of RPMI-1640, 10% heat-inactivated fetal calf serum (FCS) and penicillin (100 units/ml) / streptomycin (100 µg/ml) (Invitrogen, catalogue number 61870, 10270 and 15140, respectively) using a 27-

gauge needle. Cell suspensions were passed up and down six times through an 18-gauge needle in the same medium to disperse cell clumps. Finally, the cells were centrifuged 3 minutes at 190 x g and residual erythrocytes were eliminated by hypotonic lysis following resuspension of the cell pellet in 1 ml of ACK-lysing reagent (0.15 M NH_4Cl, 1.0 mM $KHCO_3$, 0.1 mM EDTA) for 5 minutes. The reaction was stopped by the addition of 10 ml fresh medium and the cells were counted using Trypan blue.

To induce differentiation approximately 10^7 bone marrow cells were seeded in 15 cm bacteriological plates in Iscove's Modified Dulbecco's Medium (IMDM) (Invitrogen, catalogue number 31980), 10 % FCS, 50 μM β-mercaptoethanol supplemented with 30 % (v/v) of L929 cell conditioned medium (containing M-CSF) [25] (see below) and kept in culture for 1 week. When differentiated, the cells were washed with PBS and harvested by adding 10 ml of Versene (0.2 g/L EDTA•4 Na^+ in phosphate-buffered saline) (Invitrogen catalogue number 15040) and incubation at 4°C for 30 min.

3.4.4 L929 conditioned medium

L929 conditioned medium was obtained by plating L929 cells in 150-cm^2 tissue culture flasks (BDbiosciences, catalogue number 355000) at an initial density of 3×10^4 cells per ml in 100 ml of RPMI-1640, 10% heat-inactivated fetal calf serum and penicillin/streptomycin. After 7 days in culture, the culture supernatant was filtered, aliquoted in 50-ml tubes, and stored at -20°C.

3.4.5 Mouse splenocytes.

Mice were killed by cervical dislocation and soaked with 70% ethanol. The peritoneal cavity was opened, the spleen isolated and placed in a 15 ml falcon tube, filled with RPMI 1640, 10% FCS and penicillin/streptomycin. In a sterile tissue culture hood, the spleen was placed into the cell strainer and, using the plunger end of a syringe, mashed through the cell strainer into a Petri dish. Finally, the cells were centrifuged 3 minutes at 190 x g and residual

erythrocytes were eliminated by hypotonic lysis (see above).

3.4.6 Western Blot Analysis.

Cells were lysed in monoQ-c buffer [16]. The primary antibodies were revealed with a 1/5000 dilution of an Alexa Fluor 680-conjugated anti-rabbit antibody (Molecular Probes, Eugene, OR; cat. no. A21109) or an IRDye 800-conjugated anti-mouse antibody (Rockland, Gilbertsville, PA; cat. no. 610-132-121) and subsequently visualized with the Odyssey infrared imaging system (LICOR Biosciences, Bad Homburg, Germany).

3.4.7 Southern Blot.

DNA was purified from 2 to 5 mm mice tail biopsies. Briefly, tails were digested overnight at 56° C in 750 µl digestion buffer (100 mM NaCl; 10 mM Tris-HCl pH 8; 25 mM EDTA pH 8; 0.5 % SDS; 0.1 mg/ml proteinase K). The following day, samples were mixed 5 minutes at maximum speed in an Eppendorf Thermomixer Comfort mixer. Two hundred µl of a saturated solution of NaCl was added, the samples were mixed for 5 minutes at maximum speed in an Eppendorf Thermomixer Comfort mixer and centrifuged at maximum speed for 5 minutes in a benchtop Eppendorf centrifuge. The intermediate phase (~750 ml) was recovered and 500 µl of isopropanol was added. Samples were mixed and centrifuged as mentioned above. Finally the DNA pellet was washed with cold 70% ethanol and resuspended in 90 µl of Tris-EDTA buffer (10 mM Tris; 1 mM EDTA; pH 8.0).

DNA (30 µl) was digested with XhoI and BamHI overnight and separated on a 0.8 % agarose gel. The gel was then washed sequentially in 0.25 M HCl, for 10 minutes, 0.4 M NaOH for 30 minutes, in neutralizing solution (1.5 M NaCl; 0.5 M Tris-HCl pH 7.2; 1 mM EDTA pH 8) for 20 minutes and 5 minutes in 20x SSC (3 M Sodium Chloride; 0.3 M Sodium Citrate, pH 7.0).

The gel was transferred by capillarity overnight in 20x SSC to an Amersham Hybond™-N+ membrane (GE Healthcare; catalogue number RPN303B). The following day, the membrane

was briefly washed in 2x SSC, air-dried and UV-fixed with 120 mJ (UV Stratalinker 2400; Stratagene). The membrane was then probed overnight in hybridization solution (0.5 M Sodium Phosphate pH 7.2; 7% SDS, 1mM EDTA and 1% BSA) with a probe corresponding to nucleotides 7134443-7133563 of the *Mus musculus* chromosome 13 genomic contig, strain C57BL/6J (accession n° NT_039589.2). The probe was labelled by random priming (Random Primed DNA Labelling Kit, catalogue number 1 004 760; Roche Applied Science). The probe recognizes a 9.3 band corresponding to the wild-type allele and a 6 kb band corresponding to the targeted allele. Finally, the membrane was washed twice in washing solution (40 mM Sodium Phosphate pH 7.2; 1% SDS; 5 mM EDTA and 0.5 % BSA) and visualized using a BioRad® Personal Molecular Imager FX™ System.

3.4.8 Apoptosis Measurements

Apoptosis was determined by scoring the number of cells displaying pyknotic nuclei (a pyknotic nucleus is condensed and reduced in size and usually displays increased staining capacity). Nuclei of live cells were labelled with Hoechst 33342 (10 µg/ml final concentration) for 5 min, and the cells (at least 400 per condition) were then analyzed using an inverted Zeiss Axiovert 25 microscope equipped with fluorescence (HBO/AC) and transmitted light optics and a 40x objective (Zeiss 440865; LD Achroplan 40x/0.60 Korr Ph2; /0-2).

3.4.9 PCR.

The presence of the D455A mutation was detected by PCR of genomic DNA isolated from tail biopsies (see Southern Blot for details) followed by an *Ngo*MIV restriction digestion of the PCR product. Briefly, sense AGTAGGTGGGTTCAGGAGCAG and antisense GTTCTAAAACCCTGGTTATA primers were used to amplify a band of 0.6 kb. Touchdown PCR was performed as follows: one 5 minute-incubation at 94° C; 10 cycles using the following conditions: 30 seconds at 94° C, 30 seconds at 65° C for the first cycle

or at a temperature decremented by 1°C in each subsequent cycle, and 45 seconds at 72° C; 25 cycles using the following conditions: 30 seconds at 94° C, 30 seconds at 55° C; 45 seconds at 72° C; a final elongation of 7 minutes at 72° C. The reactions were performed using *Taq* DNA Polymerase (Roche Applied Science, catalogue number 11647679001). At the end of the reaction, 20 µl of a mix containing *Ngo*MIV (Promega, catalogue number R7171) were added and samples digested overnight at 37° C. The PCR products were analyzed on 1.5 % agarose gel containing ethidium bromide. The presence of the mutation was assessed by the appearance of a 0.3 kb band corresponding to digestion of the mutated PCR product by *Ngo*MIV.

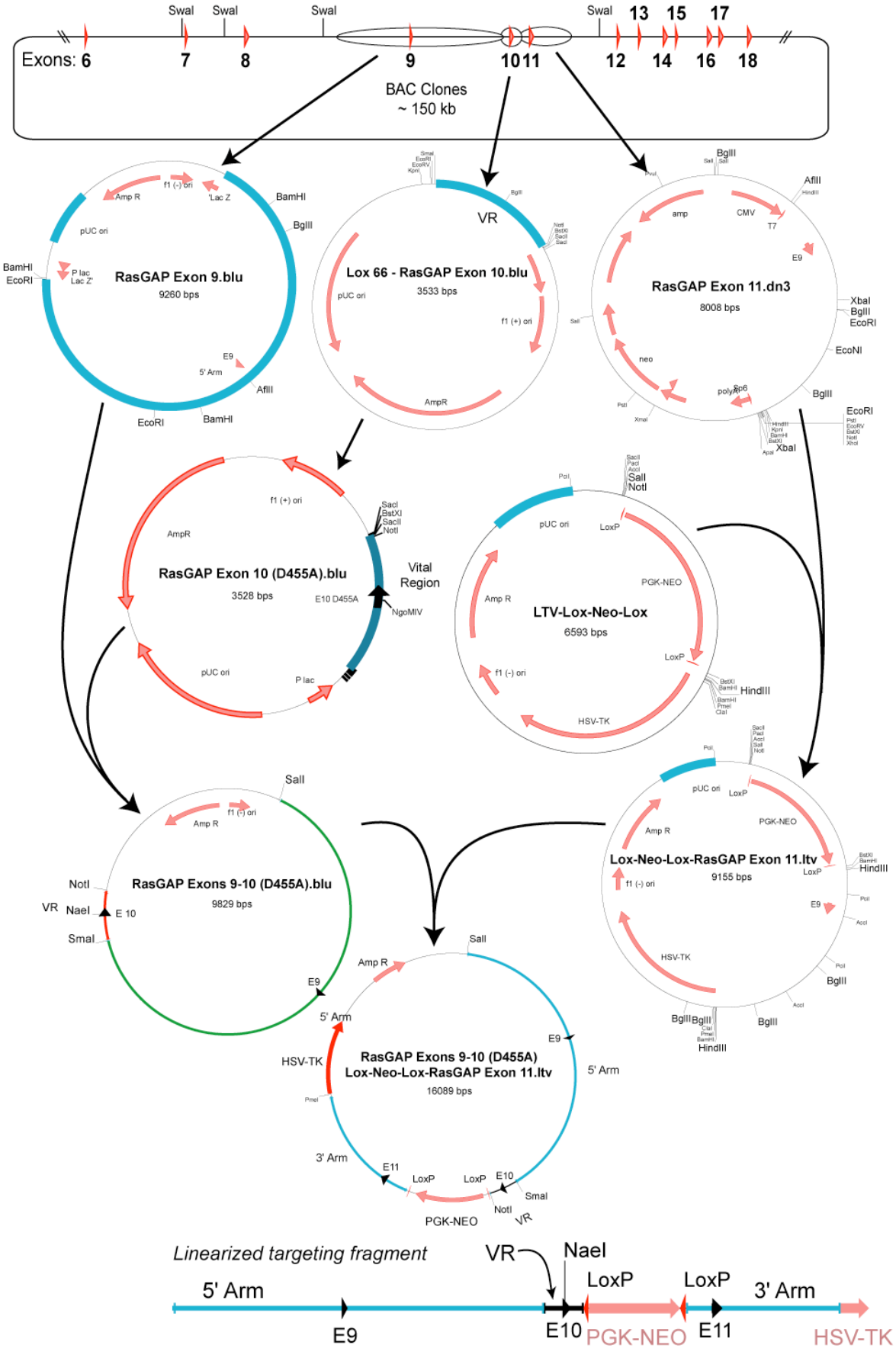

Figure S1. Schematic representation of the generation of the RasGAP^{D455A} targeting vector

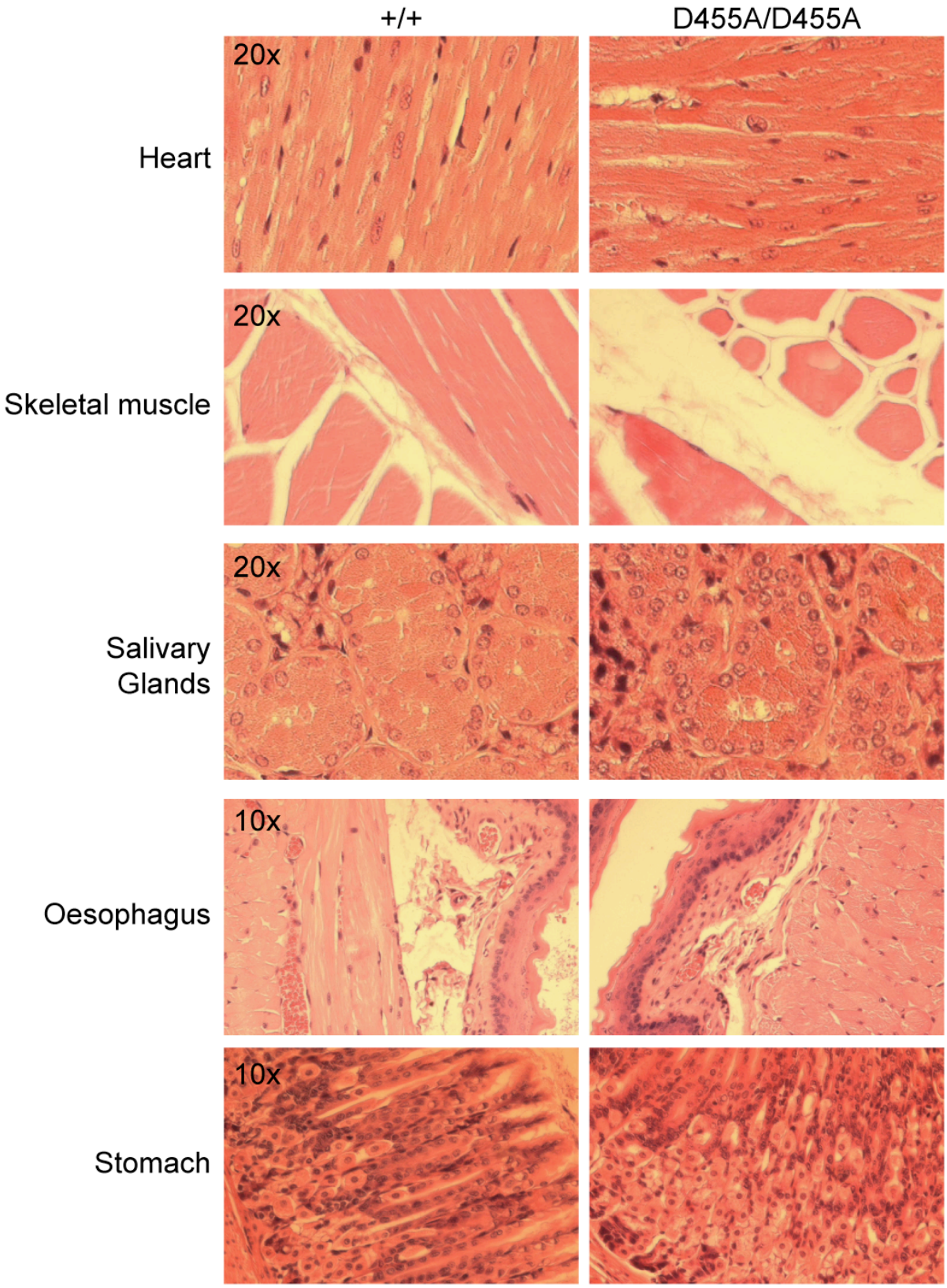

Figure S2.1. Histological analysis of different organs

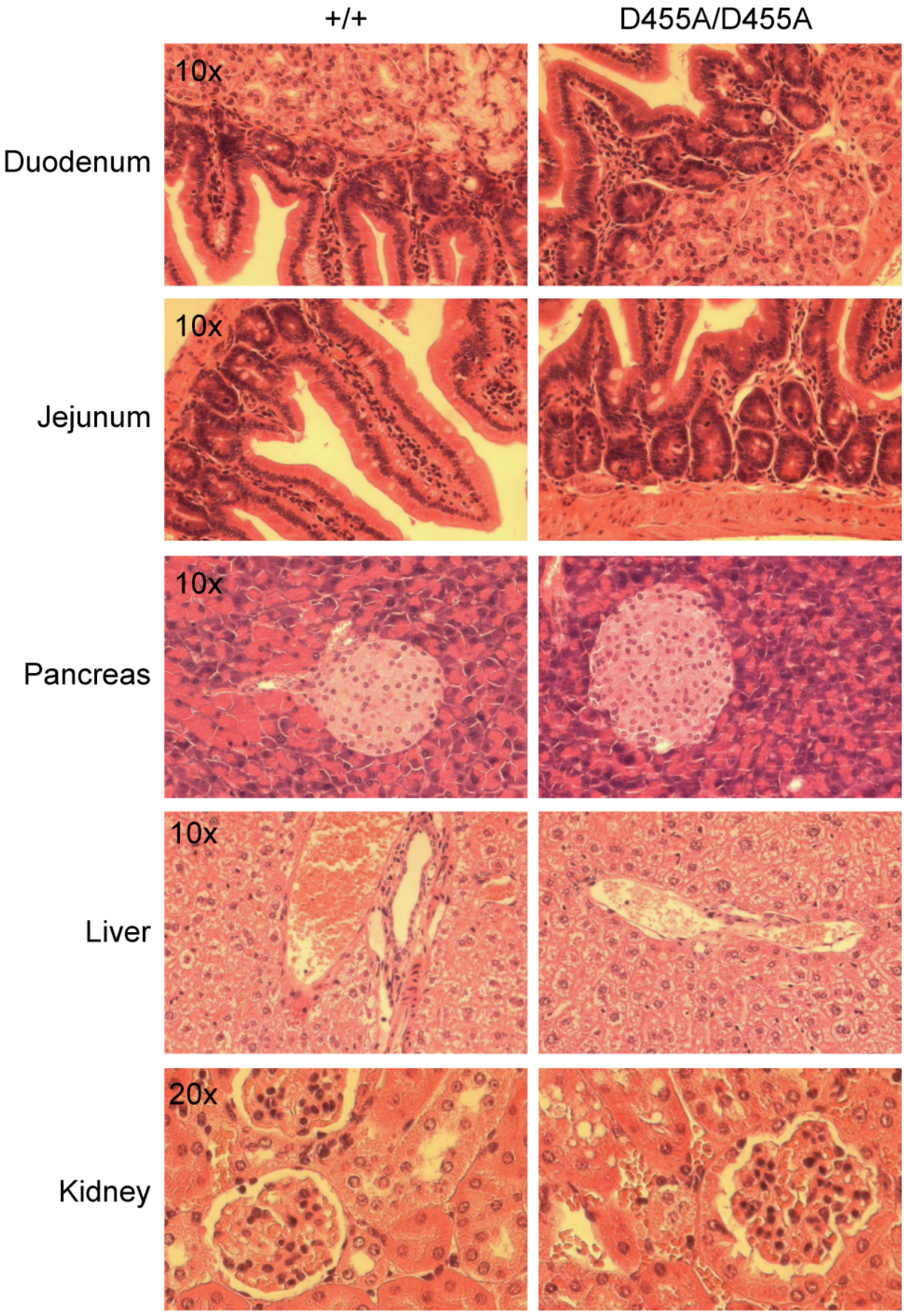

Figure S2.2. Histological analysis of different organs

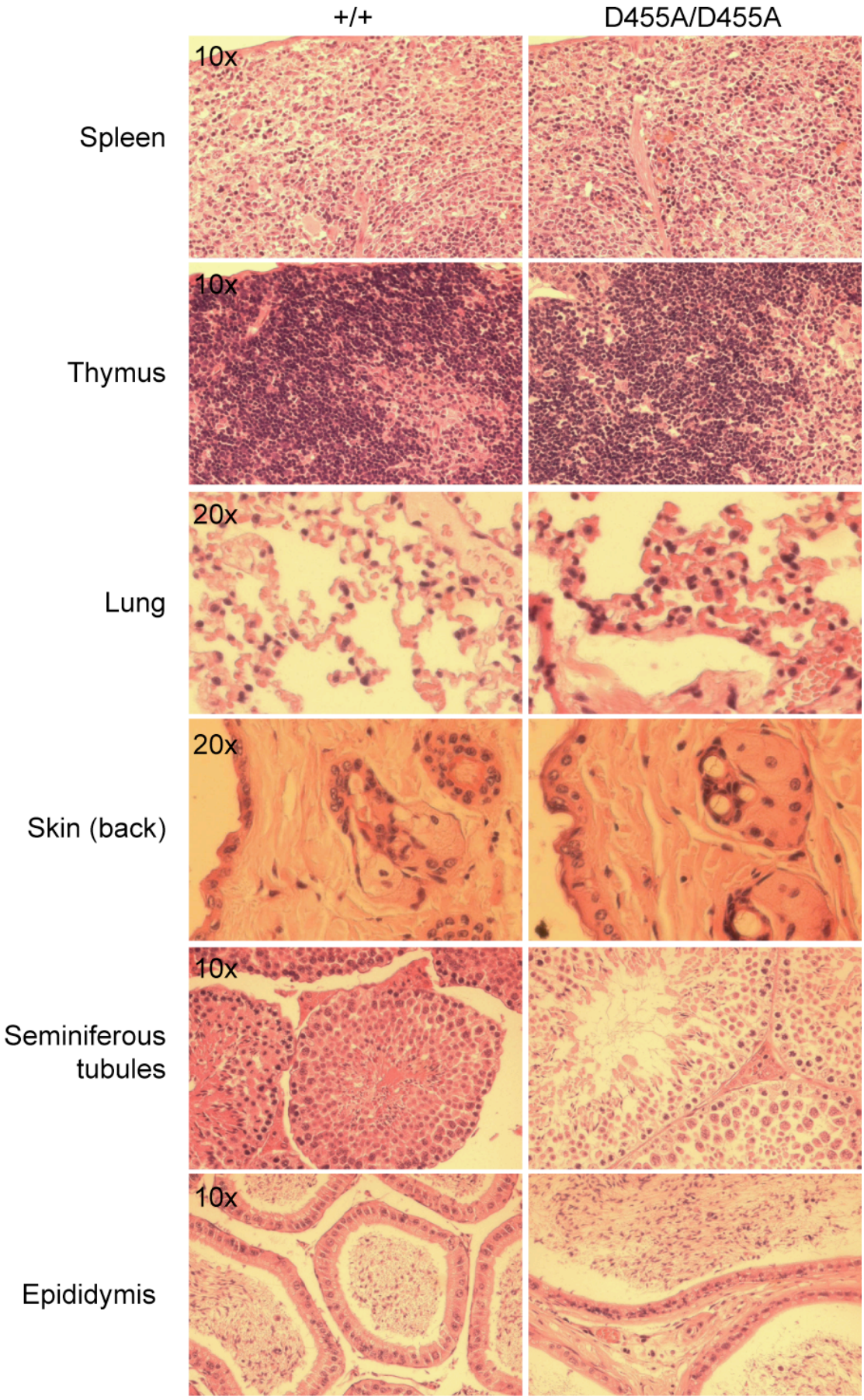

Figure S2.3. Histological analysis of different organs

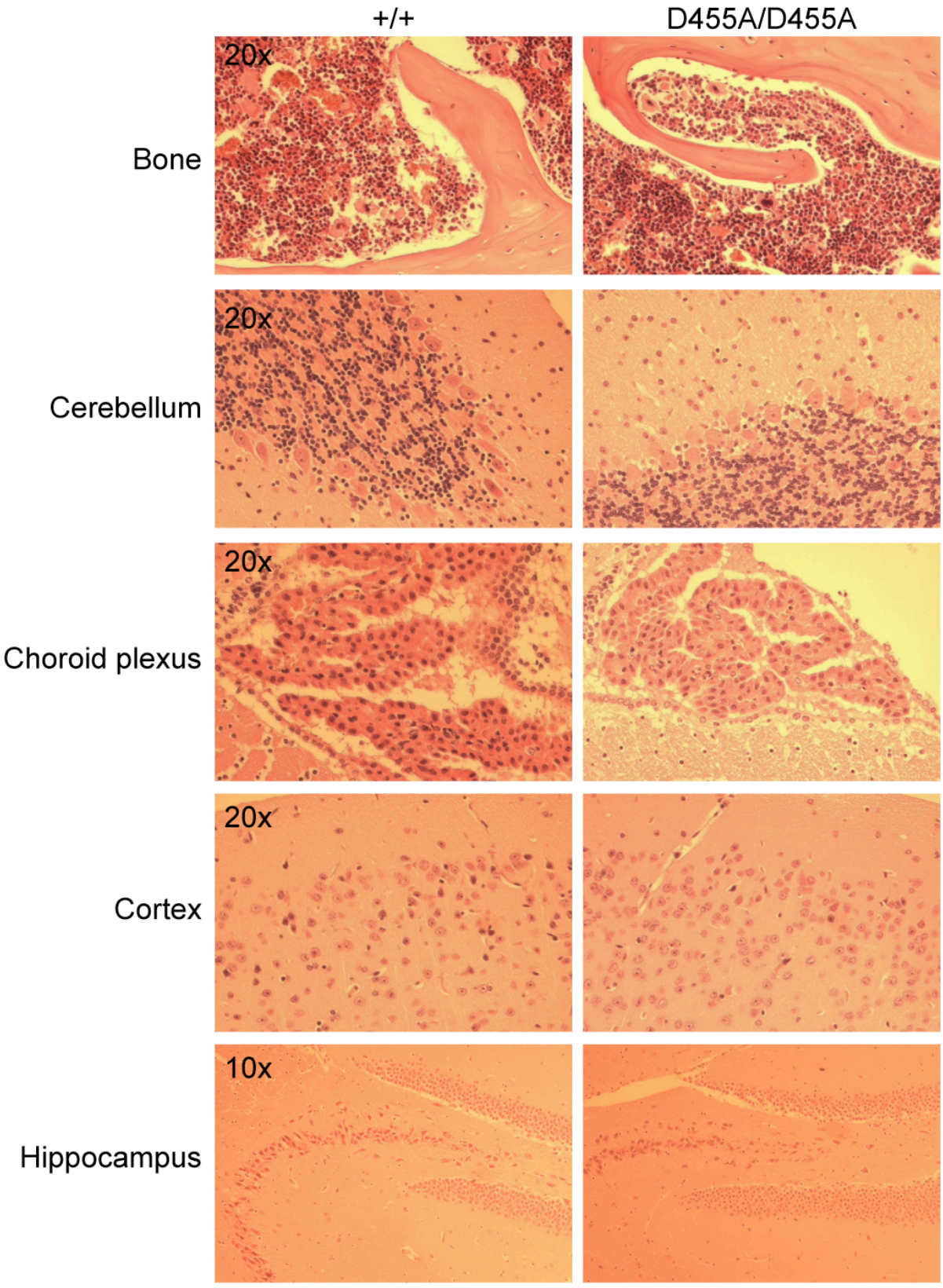

Figure S2.4. Histological analysis of different organs

3.5 References

1. Thornberry, N. and Y. Lazebnik, *Caspases: enemies within.* Science, 1998. **281**(5381): p. 1312-6.
2. Budihardjo, I., et al., *Biochemical pathways of caspase activation during apoptosis.* Annu. Rev. Cell Dev. Biol., 1999. **15**: p. 269-90.
3. Stroh, C. and K. Schulze-Osthoff, *Death by a thousand cuts: an ever increasing list of caspase substrates.* Cell Death Differ., 1998. **5**(12): p. 997-1000.
4. Fischer, U., R. Jänicke, and K. Schulze-Osthoff, *Many cuts to ruin: a comprehensive update of caspase substrates.* Cell Death Differ., 2003. **10**(1): p. 76-100.
5. Fernando, P., et al., *Caspase 3 activity is required for skeletal muscle differentiation.* Proc. Natl. Acad. Sci. U.S.A., 2002. **99**(17): p. 11025-30.
6. Fernando, P., S. Brunette, and L. Megeney, *Neural stem cell differentiation is dependent upon endogenous caspase 3 activity.* FASEB J., 2005. **19**(12): p. 1671-3.
7. Kennedy, N., et al., *Caspase activation is required for T cell proliferation.* J. Exp. Med., 1999. **190**(12): p. 1891-6.
8. Salmena, L., et al., *Essential role for caspase 8 in T-cell homeostasis and T-cell-mediated immunity.* Genes Dev., 2003. **17**(7): p. 883-95.
9. Goping, I., et al., *Granzyme B-induced apoptosis requires both direct caspase activation and relief of caspase inhibition.* Immunity, 2003. **18**(3): p. 355-65.
10. Kataoka, T., et al., *The caspase-8 inhibitor FLIP promotes activation of NF-kappaB and Erk signaling pathways.* Curr. Biol., 2000. **10**(11): p. 640-8.
11. Reed, J., *Bcl-2 family proteins.* Oncogene, 1998. **17**(25): p. 3225-36.
12. Callus, B. and D. Vaux, *Caspase inhibitors: viral, cellular and chemical.* Cell Death Differ., 2007. **14**(1): p. 73-8.
13. Basu, A., et al., *Proteolytic activation of protein kinase C-epsilon by caspase-mediated processing and transduction of antiapoptotic signals.* J. Biol. Chem., 2002. **277**(44): p. 41850-6.
14. Ricci, J., et al., *An absolute requirement for Fyn in T cell receptor-induced caspase activation and apoptosis.* FASEB J, 2001. **15**(10): p. 1777-9.
15. Luciano, F., et al., *The p54 cleaved form of the tyrosine kinase Lyn generated by caspases during BCR-induced cell death in B lymphoma acts as a negative regulator of apoptosis.* FASEB J., 2003. **17**(6): p. 711-3.
16. Yang, J. and C. Widmann, *Antiapoptotic signaling generated by caspase-induced cleavage of RasGAP.* Mol. Cell. Biol., 2001. **21**(16): p. 5346-58.
17. Yang, J. and C. Widmann, *The RasGAP N-terminal fragment generated by caspase cleavage protects cells in a Ras/PI3K/Akt-dependent manner that does not rely on NFkappa B activation.* J. Biol. Chem., 2002. **277**(17): p. 14641-6.
18. Yang, J., et al., *Partial cleavage of RasGAP by caspases is required for cell survival in mild stress conditions.* Mol. Cell. Biol., 2004. **24**(23): p. 10425-36.
19. Yang, J., et al., *Impaired Akt activity down-modulation, caspase-3 activation, and apoptosis in cells expressing a caspase-resistant mutant of RasGAP at position 157.* Mol. Biol. Cell, 2005. **16**(8): p. 3511-20.
20. Yang, J., et al., *Surviving the kiss of death.* Biochem. Pharmacol., 2004. **68**(6): p. 1027-31.
21. Opferman, J. and S. Korsmeyer, *Apoptosis in the development and maintenance of the immune system.* Nat. Immunol., 2003. **4**(5): p. 410-5.
22. Siegel, R., *Caspases at the crossroads of immune-cell life and death.* Nat. Rev. Immunol., 2006. **6**(4): p. 308-17.

23. Osoegawa, K., et al., *Bacterial artificial chromosome libraries for mouse sequencing and functional analysis.* Genome Res., 2000. **10**(1): p. 116-28.
24. Nelson, R. and G. Long, *A general method of site-specific mutagenesis using a modification of the Thermus aquaticus polymerase chain reaction.* Anal Biochem, 1989. **180**(1): p. 147-51.
25. Austin, P., E. McCulloch, and J. Till, *Characterization of the factor in L-cell conditioned medium capable of stimulating colony formation by mouse marrow cells in culture.* J Cell Physiol, 1971. **77**(2): p. 121-34.

Chapter 4 – Results 3

4 EXPRESSION OF THE N-TERMINAL FRAGMENT OF RASGAP IN PANCREATIC BETA CELLS INCREASES THEIR RESISTANCE TO STRESSES AND PROTECTS MICE FROM DIABETES

4.1 Introduction

Elimination of pancreatic β cells by apoptosis is a culminating event leading to type 1 [1] and possibly type 2 diabetes [2, 3]. The development of tools favoring β cell survival in patients is therefore of critical importance to delay or prevent the development of the disease. Moreover, compounds that increase β cell survival would be extremely useful in islet transplantation procedures, such as the Edmonton Protocol, to increase the yield of islet cells production from diseased donors and to ameliorate the rate of successful engraftment of the pancreatic islets in the host.

Apoptosis is induced when a family of proteases called the caspases is activated [4, 5]. These enzymes cleave a subset of cellular proteins, inducing the characteristic biochemical and morphological features of apoptosis. Pancreatic islet cells undergo apoptosis in response to many stimuli [6], including anoxia [7], nutrient deprivation [8], hyperglycemia [9] and inflammatory cytokines [10]. Counteracting the pro-apoptotic effects of caspases would therefore be advantageous to render islet cells more resistant to a series of noxious stimuli.

A very potent anti-apoptotic mediator is the Akt kinase [11]. Akt is able to stimulate the NFκB pathway [12-14] and in some cells types, Akt-induced NFκB activation is required for cell survival [13]. In β cells though, NFκB, depending on how it is activated, can be detrimental [15-19]. Therefore in contrast to many cell types, expression of active Akt in β cells can lead to apoptosis. This has indeed been confirmed *in vivo* in mice expressing an Akt1 transgene under the control of the insulin promoter [20]. In this model, the presence of Akt1 in β cells increased the apoptotic rate by at least 10 times compared to control β cells.

Despite inducing an increase in the basal apoptotic rate, Akt1 inhibited streptozotocin-induced β cell apoptosis. Why Akt1 can either favour (e.g. in basal conditions) or inhibit β cell death (upon streptozotocin injection) is unclear. But, as Akt1 expression in β cells induces a two- to three-fold increase in insulin blood levels [20] and since insulin protects β cell against cell death [21, 22], the resistance of β cells towards streptozotocin in Akt1 transgenic mice could be an indirect consequence of augmented insulin blood concentrations.

Akt, besides its ability to regulate cell death, also has the potential to modulate cell proliferation and cell growth [11]. For example, the specific expression of Akt1 in β cells in mice increased the number of islets in the pancreas and the size of the β cells, leading to increased β cell mass [20]. However, the number of β cells per islet was diminished [20].

Expression of an active form of Akt1 in β cells therefore generates two opposing forces: an increase in basal apoptosis and a stimulation of proliferation/growth. The potential beneficial effects of Akt1 activity in β cells are therefore mitigated by the increased susceptibility to cell death that is most likely mediated by the concomitant activation of NFκB. Thus, unless Akt is prevented from stimulating NFκB, it remains unclear whether expression of an active form of Akt1 is advantageous for the long-term survival and functionality of β cells.

RasGAP, a regulator of Ras and Rho, is a caspase-3 substrate bearing two cleavage sites. RasGAP is cleaved in a stepwise manner as caspase activity increases in cells. At low caspase-3 activity, RasGAP is cleaved only once, generating an N-terminal fragment, called fragment N, that induces a potent anti-apoptotic response [14, 23]. At higher caspase activity, fragment N is further processed into two additional fragments, called fragments N1 and N2, that no longer protect cells but rather promote apoptosis [23, 24]. Fragment N induces cell survival by activating the Ras-PI3K-Akt pathway [14]. Importantly, not only does fragment N not require NFκB activity for its anti-apoptotic properties, it inhibits the

ability of Akt to activate NFκB [14]. This indicates that different ways of activating Akt (i.e. via expression of an active mutant of Akt or via expression of fragment N) does not lead to the same cellular responses. We have recently demonstrated that expression of fragment N in β cells *in vitro* leads to the stimulation of Akt-dependent protective signals while blocking the ability of Akt to activate the pro-apoptotic NFκB pathway [25]. To determine whether fragment N would display its protective functions in an *in vivo* setting, a transgenic mouse was generated that expresses fragment N under the control of the rat insulin promoter to restrict its expression in pancreatic β cells. This mouse model displayed an increased resistance to experimentally induced diabetes and its β cells were less susceptible to apoptosis induced by a variety of death stimuli. Fragment N and the pathway it regulates represent therefore a potential target for the development of anti-diabetic tools.

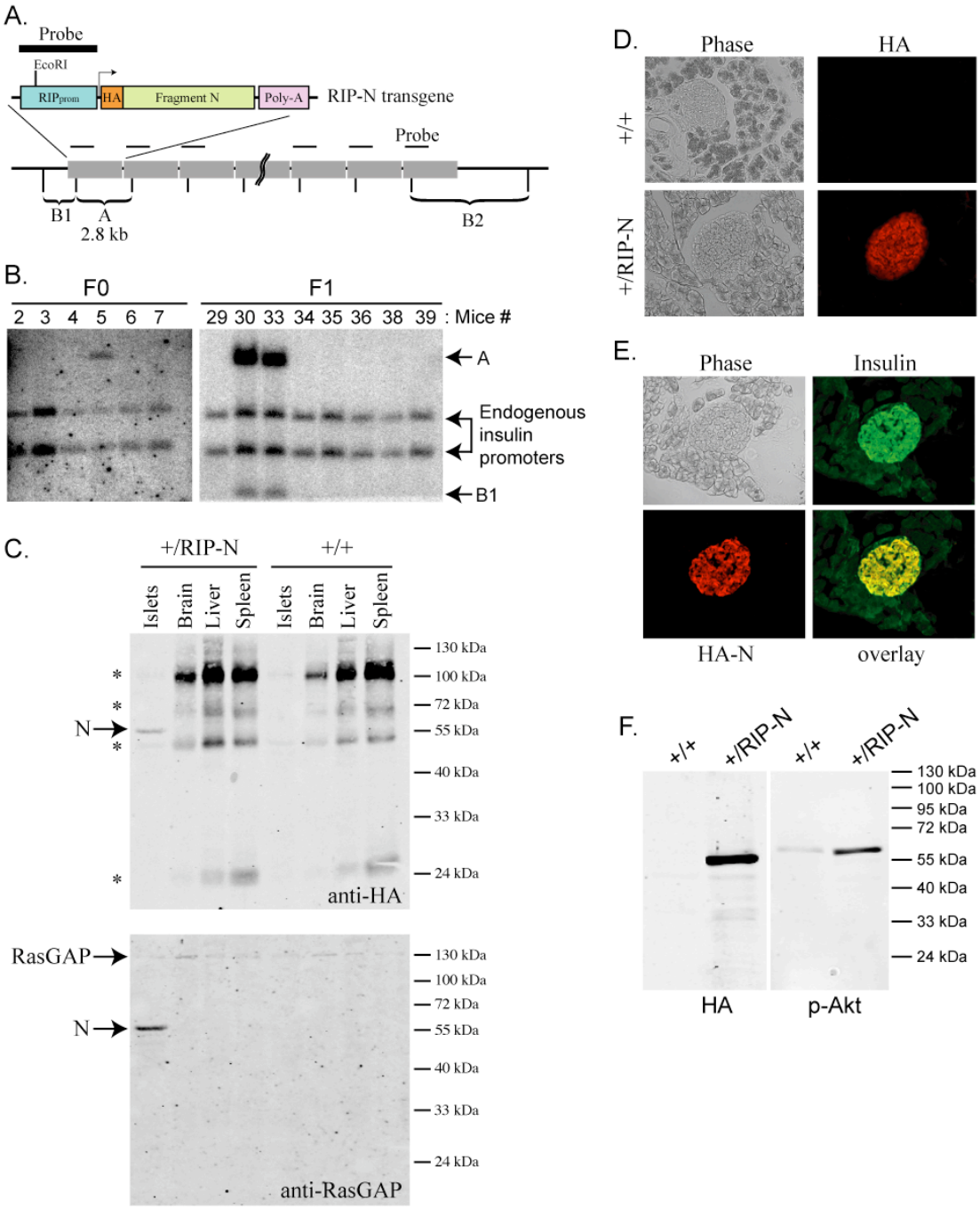

Figure 1: Transgenic mice express fragment N in pancreatic ß-cells.
A. Schematic representation of the RIP-N transgene together with the strategy for its detection by Southern blot. A HA-tagged form of fragment N (amino acids 1 to 455 of RasGAP) followed by an SV40 derived poly-A sequence was placed under the control of the rat insulin promoter (RIP). Band A corresponds to the transgene-specific *Eco*RI Southern blot fragment. B1 and B2 are examples of *Eco*RI Southern blot fragments derived from random insertions of the transgene into the host's genome.
B. Identification of RIP-N transgenic mice. The progeny of the injected pseudo-pregnant mice were genotyped by Southern blot (see Material and Methods for details). Band A (2.8 kb) is specific for the transgene. Founder #1 (mouse #5) was able to transmit the transgene to the F1 generation.
C. Tissue expression of fragment N. Lysates from the indicated tissues were analysed for the presence of fragment-N by Western blot using anti-HA and anti-RasGAP antibodies.
D. Expression of fragment-N in the pancreas. The presence of fragment N was assessed by immunofluorescense analysis of paraformaldehyde-fixed cryosections using an antibody recognizing the HA tag born by fragment N.
E. Colocalization of insulin and fragment N. The specific location of fragment-N in pancreatic ß-cells was determined by immunofluorescence of paraformaldehyde-fixed cryo-sections from RIP-N mice using anti-insulin and anti-HA antibodies.
F. Lysates from islets isolated form the indicated mice were analysed by Western blot for the presence of fragment N using an HA-specific antibody and for the activation of Akt using a phospho-specific anti-Akt antibody.

4.2 Results

4.2.1 Generation of a transgenic mouse, expressing fragment N in pancreatic β cells.

A transgenic vector was constructed (see Materials and Methods) to encode an HA-tagged form of fragment N bearing the D455A mutation (preventing it from being cleaved by caspases) under the control of the rat insulin promoter (RIP) and regulatory sequences of the simian virus 40 (SV40) gene (Figure 1A). The construct was injected into FVB/N oocytes and transgene-positive mice where identified by Southern blotting (Figure 1B). In total 4 founder mice were obtained. The data presented here were all generated from founder #1 (labelled mouse 5 in Figure 1B). By comparison with the endogenous insulin promoters, it was estimated that founder #1 bore 12-15 copies of the transgene in its genome (Figure 1B).

To determine the expression pattern of fragment N in the transgenic line, lysates from pancreatic islets, liver, brain, and spleen were analyzed by Western blotting using antibodies specific for the HA tag or for the N-terminal part of RasGAP. Figure 1C, shows that fragment N was, as expected, only expressed in islet cells. Immuno-fluorescence analysis revealed that fragment N was restricted to the endocrine part of the pancreas (Figure 1D) and that the vast majority of fragment N-expressing cells corresponded to β cells (i.e. insulin-containing cells) (Figure 1E). As expected, the presence of fragment N in islet cells led to a strong Akt activation (Figure 1F).

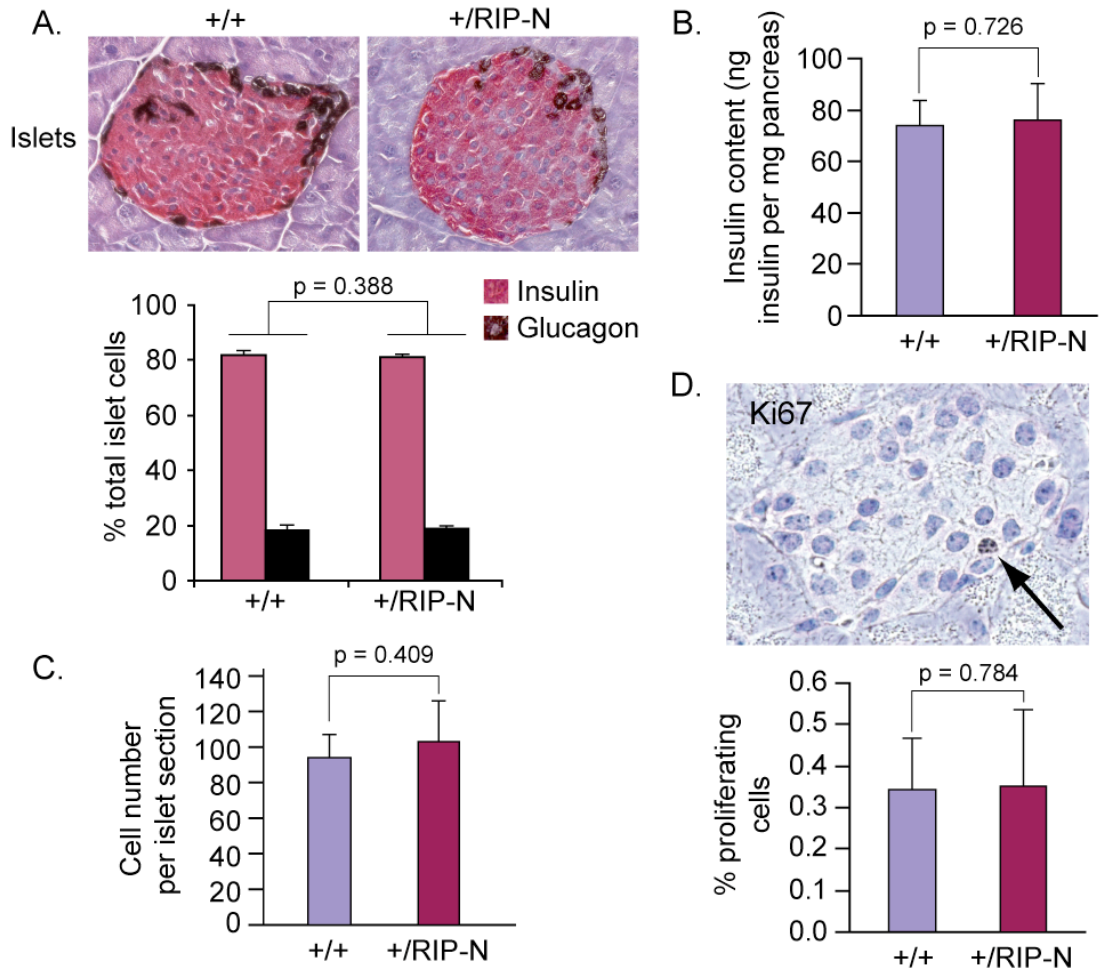

Figure 2: Fragment N expression does not affect islet morphology and cellularity.
A. The proportion of pancreatic α- and β-cells was determined by immuno-histochemistry of paraffin-embedded pancreas section with antibodies directed against glucagon (dark brown staining) and insulin (purple-red staining). The bar graph depicts the proportion of α- and β-cells in islets (mean ± SD) derived from the analysis of at least 25 islets from two different wild-type and RIP-N mice.
B. Freshly isolated pancreases where homogenized and extracted with acid ethanol. Insulin concentration in the supernatant was determined by enzyme-linked immuno-sorbent assay. The results correspond to the mean ± SD of 9 (wild-type) and 6 (RIP-N) pancreases.
C. Number of cells per islet section was counted on HE stained paraffin embedded pancreas sections. The results correspond to the mean ± SD derived from 25 histological slices obtained from three different wild-type and RIP-N mice.
D. The percentage of proliferating cells was determined by scoring KI67-positive cells on paraffin embedded pancreas sections. The bar graph depicts the percentage of proliferating cells in islets (mean ± SD) derived from the analysis of at least 20 histological slices obtained from three different wild-type and RIP-N mice.

4.2.2 Fragment N expression does not affect islet morphology and cellularity.

Expression of fragment N in insulinomas and islet cells leads to Akt activation (Figure 1F and [25]). Since Akt signalling has the potential to stimulate cell survival and proliferation [28] and since transgenic mice expressing a constitutively active form of Akt (*myr*-Akt) show an increase in both β-cell size and total islet mass [20], the presence of fragment in

islets might affect the morphology and cellularity of the endocrine pancreas. However, neither the proportion of α and β cells (Figure 2A), nor the insulin content of the pancreas (Figure 2B) were affected by the presence of fragment N. Moreover, the size of the islets did not appear to be different in RIP-N transgenic mice compared to control mice (Figure 2C). Finally, the percentage of cells positive for the nuclear protein Ki67 that is preferentially expressed in dividing cells was similar in both types of mice (Figure 2D). These results indicate that fragment N does not favour β cell proliferation in an *in vivo* setting and that it does not affect the normal development of the endocrine pancreas.

4.2.3 Islets from RIP-N transgenic mice display increased resistant to stress-induced apoptosis.

In wild-type mice, the basal apoptotic rate in islets is undetectable [20] to extremely low (0.06%). In contrast, islets from transgenic mice expressing a constitutively active form of Akt show a marked increase in β cell apoptosis. Islets isolated from RIP-N mice were more resistant than those isolated from control mice when subjected to a variety of stress stimuli, including inflammatory cytokines, hypoxia, the free fatty acid palmitate, and high glucose concentrations (Figure 3A-C). These results demonstrate that fragment N efficiently protects pancreatic β cells against various conditions and stimuli, including some that are associated with the development of type 1 and type 2 diabetes (e.g. inflammatory cytokines and free fatty acids).

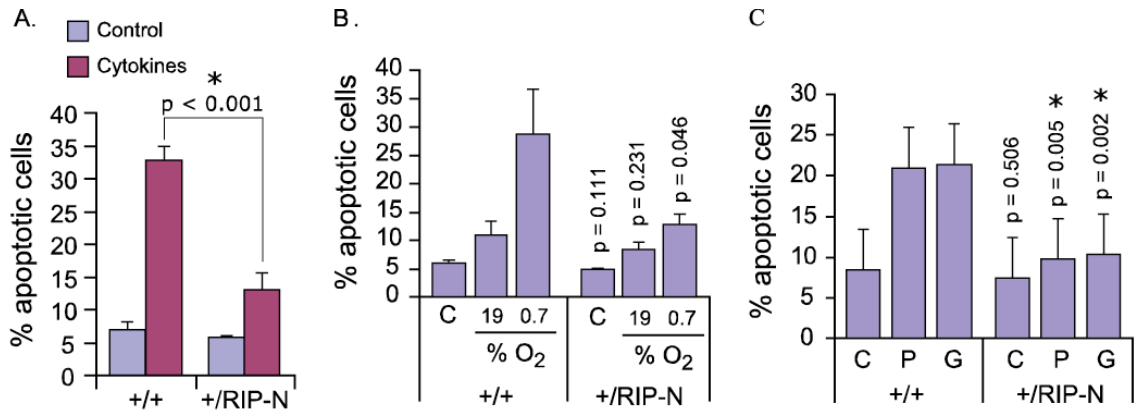

Figure 3: RIP-N islet cells are more resistant to basal and stress-induced apoptosis.
A. Freshly isolated islets were dissociated and incubated or not with inflammatory cytokines (1,000 units/ml TNFα, 1,000 units/ml interleukin-1β and 50 units/ml interferon-γ) for an additional 24 hour-period. Apoptotic cells were then scored. The results correspond to the mean ± SD of 3 independent experiments.
B. Islets were isolated and cultured in vitro for 24 hours (see material and methods). Some islets were kept in normal culture conditions (C), while others were incubated 90 minutes in normoxic conditions (19% O2, 5% CO2) in a sealed chamber. After this normoxic equilibration period, half of the islets were kept at normal oxygen pressure (19% O2) and half subjected to hypoxia (0.7% O2) during 240 minutes. The islets were then dissociated and apoptosis scored. The results correspond to the mean ± SD of 3 independent experiments.
C. Freshly isolated islet where left untreated (C) of treated during 72 hours with 33 mM glucose (G) or 1 mM palmitate (P). The islet where then dissociated and apoptosis scored. The results correspond to the mean ± SD of 3 independent experiments.

4.2.4 Fragment N does not adversely affect β cell functions *in vivo*.

Transgenic mice expressing a non-degradable form of IκBα under the control of *Pdx1* promoter, which drives its expression in the β cells of the pancreas, display impaired glucose-induced insulin secretion [29]. Fragment-N by blocking NFκB activity [14, 24] could potentially similarly affect insulin secretion. However, fragment N expression in β cells did not modify glycaemia under non-fasted (Figure 4A) or fasted (Figure 4B, first points in the graphs) conditions. Moreover, the ability of the transgenic mice to metabolize glucose, assessed by intraperitoneal glucose tolerance tests, was not negatively affected by the presence of the transgene in β cells (Figure 4B). There was even a tendency in RIP-N females to respond better to hyperglycaemia (Figure 4B, left panel). These results indicate that fragment N does not compromise the ability of β cells to secrete insulin in response to augmented glucose blood levels.

A.

♀		♂	
+/+	RIP-N/+	+/+	RIP-N/+
7.3±0.8	**7.4±0.9**	**8.4±1.1**	**8.1±0.3**
n=18	*n=24*	*n=3*	*n=5*

B.

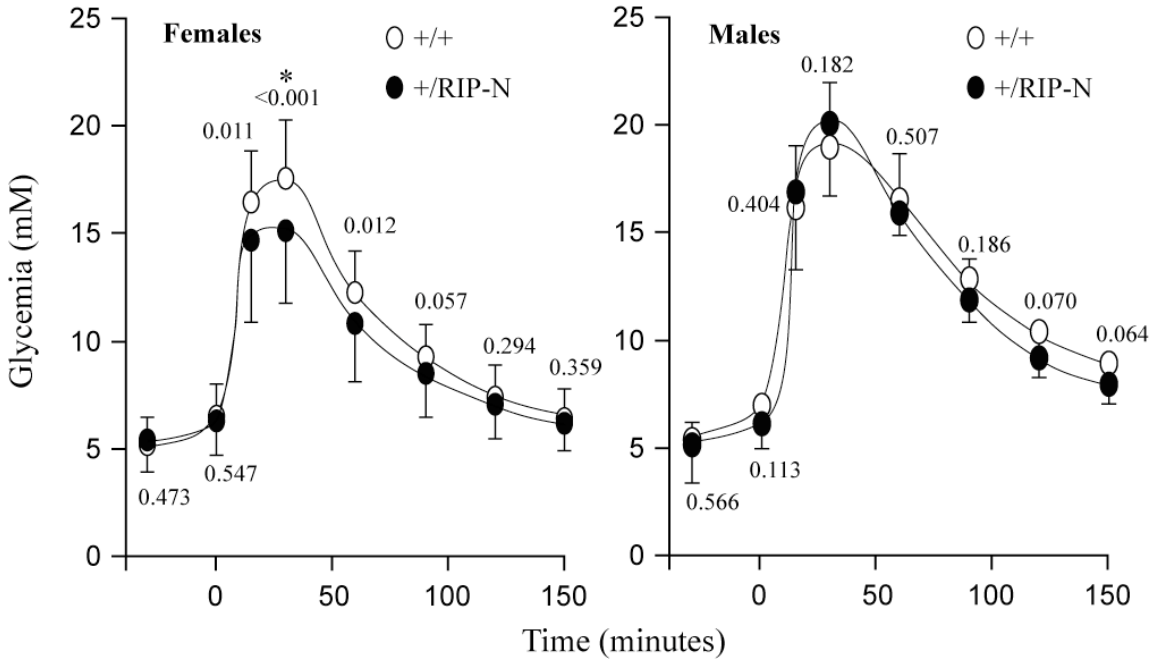

Figure 4. Glycemia and glucose tolerance of RIP-N mice.
A. Non-fasting glycemia of wild-type and RIP-N males and females was determined as described in the methods.
B. Mice were subjected to an intraperitoneal glucose tolerance test (IPGTT) to analyse their response to hyperglycaemic conditions. Results correspond to the mean ± SD of 6 independent experiments.

4.2.5 RIP-N transgenic mice are protected against streptozotocin-induced diabetes.

Multiple low dose-streptozotocin injections in mice induce islet inflammation, ultimately leading to β cell loss and diabetes [30]. This model is thought to mimic the development of type 1 diabetes in humans [31]. Using this protocol, it was found that RIP-N mice only developed moderate diabetes compared to control mice (Figure 5). This indicates that the presence of fragment N in β cells increase their resistance *in vivo* to diabetes-inducing conditions.

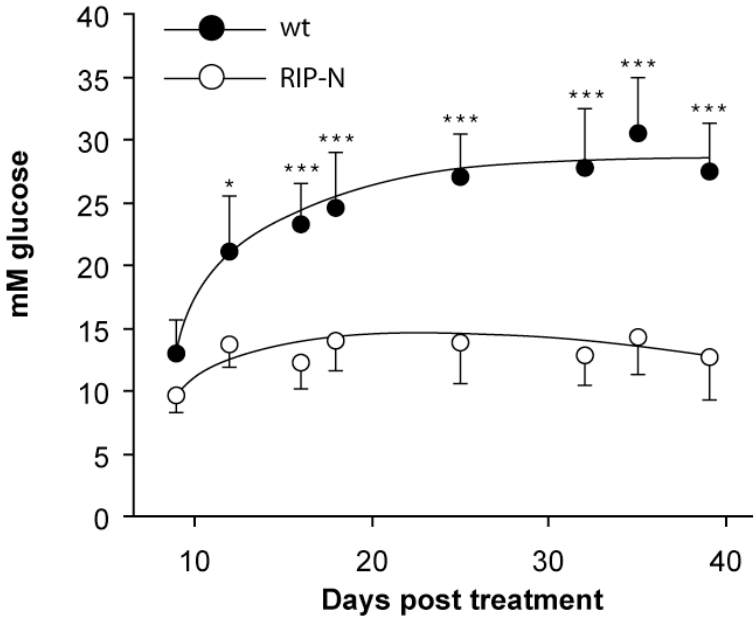

Figure 5. Resistance of RIP-N mice to streptozocin-induced diabetes.
Wild-type and RIP-N females (nine each) were subjected to a multiple low-dose injections of streptozocin to induce type 1-like diabetes (see materials and methods). Glucose blood levels were then determined at the indicated times. The results are expressed as the mean ± SD. This experiment has been repeated two more times with similar results.

4.3 Discussion

Apoptosis, which is the cause of β cells death in patients with type 1 diabetes [32], might also participate in the loss of β cell mass observed in type 2 diabetes [33-36]. The notion, however, that there is a decrease in β cell mass in type 2 diabetes has been controversial for a number of years. Nevertheless, if one considers those studies using well-preserved pancreases obtained from autopsies, it appears that there is a 3-10 fold increase in the rate of β cell apoptosis in type 2 patients compared to control subjects [37]. These results indicate that failure to compensate for insulin resistance could result from decreased β cell mass mediated by apoptosis.

Understanding the pathways leading to β cell death and β cell protection might therefore be of crucial importance to find new approaches to treat diabetic patients. Procedures to block β cell death could not only potentially inhibit the development of diabetes but might also be useful in the context of islet transplantation where apoptosis has been shown to adversely

affect the number of islets that can be implanted in patients. Here we present an *in vivo* model - the RIP-N transgenic mice - where the N-terminal fragment of RasGAP (called fragment N) effectively protects pancreatic β cell against apoptosis without affecting their ability to appropriately secrete insulin in physiological conditions.

Hyperlipidaemia, a risk factor for the development of diabetes [38], can cause β cell apoptosis [39, 40]. Islets isolated from RIP-N mice underwent less apoptosis in conditions mimicking hyperlipidemia (i.e. high concentrations of palmitate) compared to control islets. Hyperglicemia, which leads to β cells dysfunction and death [6], also induced less apoptosis in fragment N-expressing islets. Finally, RIP-N transgenic islets were more resistant to IL1β, TNFα, and IFNγ-induced death. Interestingly, these inflammatory cytokines, known to be involved in the development of type 1 diabetes, have also been shown to be produced at high concentrations in diabetic-prone obese patients [41, 42]. These observations suggest that the protective signals elicited by fragment N can counteract pro-diabetic conditions (e.g. hyperglycemia, hyperlipidemia, presence of inflammatory cytokines) that are deleterious for β cells.

Islet transplantation can restore insulin independence in patients with unstable forms of type 1 diabetes [21, 22]. This promising therapeutical approach suffers however from a shortage of donor pancreatas. The situation is worsened by the fact that there is up to 70% of the transplanted islet mass that fails to engraft in the host as a result of apoptosis [43]. It is in fact estimated that, unless this loss through apoptosis is severely reduced, islet transplantation might not become a widely accepted treatment modality [44]. A critical parameter that negatively influences β cell survival in the islet transplantation procedure is the prolonged hypoxia experienced by the islets during their revascularization in the liver of the host [45, 46]. When exposed to hypoxia, islets isolated from RIP-N mice showed a marked reduction in apoptosis compared to control islets. This indicates that expression of

fragment N in islet cells can potentially increase the efficacy of islet transplantation by reducing hypoxia-induced cell death.

Much work on the cellular mechanisms controlling cell death and survival has been performed within the last few years. This knowledge has been used to manipulate β cells in order to increase their survival capacities. One strategy was based on Akt because it is a potent anti-apoptotic kinase in many cell types [47]. Transgenic mice expressing an active form of Akt (myr-Akt) in β cells in mice have larger β cell and bigger islets [20]. These transgenic mice are resistant to experimentally induced diabetes but, paradoxically, their β cells have a much increased basal apoptotic rate [20]. Conceivably, this higher apoptotic rate is compensated by increased β cell renewal to maintain an adequate β cell mass. As NFκB activation can induce β cell death [6] and because Akt stimulates NFκB [12], the increased apoptosis response observed in myr-Akt-expressing β cells likely results from the stimulation of the NFκB pathway. Indeed, prevention of NFκB activation using a dominant-negative IκB mutant allows mice to resist streptozotocin-induced diabetes [48] [19]. NFκB inhibition might however not always be protective against diabetes as indicated by the increased susceptibility of NOD mice to develop diabetes when their β cells express the dominant-negative IκB mutant [19]. Additionally, it has been shown that expression of a dominant-negative IκB mutant in β cells in mice can inhibit glucose-stimulated insulin secretion [29].

The RIP-N mice appear to lack some of the defects associated with the models described above. The activation of Akt by fragment N in the β cells of RIP-N mice is not accompanied by an increased basal apoptotic rate, most likely because fragment blocks Akt from stimulating NFkB. Moreover, in contrast to mice expressing an active form of Akt in β cells, RIP-N mice do not display islet and β cell hyperplasia. Finally, RIP-N mice have no defect in glucose-induced insulin-secretion. Transgenic mice over-expressing proteins of the IAP

(inhibitor of apoptosis) family specifically in the β cells have been generated. Similarly to RIP-N mice, their β cells are less susceptible to apoptosis and this is not accompanied by alterations in islet morphology and function [49]. It will therefore be important to define if there is a link between fragment N and IAPs that could explain the protective function of fragment N in β cells. A detailed characterization at the molecular level of the pathways regulated by fragment N might ultimately lead to the identification of new strategies to preserve β cell mass.

4.4 Materials and Methods

4.4.1 Cell Culture.

Isolated islets were maintained in RPMI 1640 medium (catalog number 61870; Invitrogen) containing 10% decomplemented fetal calf serum (catalogue number 10270; Invitrogen), 10 mM HEPES (catalog number H-3537; Sigma), 2 mML-glutamine (catalog number G-7513; Sigma), 1 mM sodium pyruvate (catalog number S-8636; Sigma) and penicillin (100 units/ml)/streptomycin (100 μg/ml) (catalogue number and 15140; Invitrogen) at 37 °C and 5% CO_2.

4.4.2 Chemicals and Antibodies

The anti-phospho-(serine 473)-Akt rabbit polyclonal IgG antibody was from Cell Signaling Technology (catalogue number 9271). The monoclonal antibody specific for the hemagglutinin (HA) tag was purchased as ascites from BabCo (Richmond, CA; catalogue number MMS-101R). This antibody was adsorbed on HeLa cell lysates to decrease nonspecific binding [23]. The anti-RasGAP antibody directed at the Src homology domains of RasGAP was from Alexis (catalogue number ALX-210-860). The anti-insulin guinea pig polyclonal IgG antibody (catalogue number 4010-01) and the anti-glucagon rabbit polyclonal IgG antibody (catalogue number 4030-01F) were from Linco Research Inc. The

anti mouse Ki67 rat monoclonal IgG antibody, the EnVision+ system horse radish peroxidase (HRP)-labelled polymer anti-rabbit or anti-mouse antibodies and the liquid DAB+ substrate chromogen system were from Dakocytomation Denmark A/S (catalogue number M7249, K4003, K4001 and K3468, respectively). The Anti-TdT rabbit polyclonal antibody was from AbD Serotec (catalogue number AHP597H). The FITC-conjugated goat anti-guinea pig IgG polyclonal antibody (catalogue number 106-095-003) and the Cy3 goat anti-mouse IgG polyclonal antibody (catalogue number 115-165-003) were from Jackson ImmunoResearch Europe.

Glucose was from Merck (catalogue number 1.08342). Streptozocin, cisplatin, hydrogen peroxide and palmitate were from Sigma (catalogue number S0130, P4394, 349887 and P9767-5G, respectively). Cytokines (TNFα, interleukin-1β, and interferon-γ) were from Alexis (catalogue number ALX-520-002-C010, ALX-520-001-C010, and PBL-11500-2, respectively).

4.4.3 Apoptosis Assay

The extent of apoptosis was assessed by scoring the number of cells with pycnotic nuclei after Hoechst 33342 staining [25].

4.4.4 Hypoxia experiment

The isolated islets were placed in the culture compartment (50 µl) of an airtight stainless steel chamber and maintained under strictly controlled metabolic conditions on a thermostabilized stage. The culture compartment was separated from the gas compartment by a thin (15 µm) transparent and gas-permeable silicone membrane (RTV 141, Rhône-Poulenc, Lyon, France).

After a period of stabilization of 90 min under normoxia (17% O_2), islets were incubated in a hypoxic (0.7% O_2) or normoxic atmosphere for 240 min.

4.4.5 Mouse islet isolation

Islets were isolated after collagenase digestion as described [25].

4.4.6 PCR

The presence of the transgene was detected by PCR amplification of genomic DNA isolated from tail biopsies (see "Southern Blot" section). Sense (ACTCCAAGTGGAGGCTGAGA) and anti-sense (TCCTTCCACAAACCCATAGC) primers were used to amplify a transgenic-specific band of 204 bps. As an endogenous control for the PCR reaction, the sense (AGGAACACACCATCATCCAGG) and anti-sense (GGGGAGAACTTGTCAATGAAACA) primers were used to amplify an 804 bp-band from the MHC class II I-Eα gene. Touchdown PCR was performed as follows: one 5 minute-incubation at 94° C; 10 cycles using the following conditions: 30 seconds at 94° C, 30 seconds at 65° C for the first cycle or at a temperature decremented by 1°C in each subsequent cycle, and 45 seconds at 72° C; 25 cycles using the following conditions: 30 seconds at 94° C, 30 seconds at 55° C; 45 seconds at 72° C; a final elongation of 7 minutes at 72° C. The reactions were performed using *Taq* DNA Polymerase (Roche Applied Science, catalogue number 11647679001). The PCR products were analyzed on 1.5 % agarose gel containing ethidium bromide.

4.4.7 Insulin quantitation

The mice were euthanized by cervical dislocation and after a midline abdominal incision, pancreas was removed, placed in 2 ml of acid/ethanol (75% ethanol 1.5 % concentrated HCl) and homogenized using a Polytron PT 1200 homogenizer (Kinematica AG) until the pancreas was completely disaggregated. Once homogenized, 2 ml of acid/ethanol were further added to the samples and insulin was extracted by gentle rocking at 4° C overnight. Finally samples were centrifuged at 700 x *g* for 3 minutes and the supernatant was recovered. Insulin content, on the supernatant, was then quantified as previously described [25].

4.4.8 Immuno-cytochemistry

For immunofluorescence studies, 6-7 week old mice were anesthetized and heart-perfused for 5 minutes with PBS and with PBS/4% paraformaldehyde for 15 minutes. Pancreatas were extracted and post-fixed in PBS/4% paraformaldehyde for 2 more hours and incubated overnight in PBS/30% sucrose (sucrose used here as a cryoprotectant). The following day, pancreatas were frozen in liquid nitrogen and kept at -80° C until sectioned. Frozen pancreatas were fully embedded in Tissue-Tek® Optimal Cutting Temperature Compound (Sakura Finetek Europe B.V.; catalogue number #4583) and 20 μm sections were obtained with a Leica CM3050 S Cryostat and mounted on SuperFrost® Plus slides (Menzel GmbH & Co KG; catalogue number J1800AMNZ). Sections were washed three times 15 minutes with PBS and incubated one hour with the antibody diluent (AD) solution (10% goat serum/0.3% Triton X-100/2% BSA in PBS). Slides were incubated overnight with the appropriate dilution of the primary antibody. The following day, slides were washed three times with PBS for 15 minutes and incubated one hour with the proper dilution of the secondary antibody. The slides were further washed three times for 15 minutes in PBS, mounted and, 3 hours later, pictures were taken with a Zeiss AxioVis C1 microscope.

4.4.9 Immuno-histochemistry

Mice were euthanized by cervical dislocation. Pancreatas were removed, fixed in PBS/4% paraformaldehyde and paraffin embedded. Eight μm sections were de-paraffined in xylene and re-hydrated in graded alcohols and distilled water. During the re-hydration steps, endogenous peroxidase activity was blocked with methanol/hydrogen peroxide 1% for 15 minutes. For TdT staining, antigen retrieval treatment was performed for 2 minutes at 121° C in 50 mM Tris-HCl, 1 mM EDTA (pH 9). Sections were blocked for 10 minutes with 10% goat serum in 50 mM Tris-HCl, 1 mM EDTA (pH 7.6) and rinsed in the same buffer. Primary antibodies were applied for 1 hour in 50 mM Tris-HCl, 1 mM EDTA, 0.5% BSA

(pH 7.6). The secondary HRP-coupled antibody (EnVision+ System, DakoCytomation) was applied for 30 minutes. A visualization reagent (3,3'-diaminobenzidine; DAB) was applied for 5 minutes and rinsed off in tap water. Sections were counterstained by Harris's haematoxylin, re-hydrated and mounted. All the steps were performed at room temperature. Pictures were taken with a Zeiss AxioVis C1 microscope.

4.4.10 Western Blot Analysis

Cells were lysed in monoQ-c buffer [23]. The primary antibodies were revealed with a 1/5'000 dilution of an Alexa Fluor 680–conjugated anti-rabbit antibody (Molecular Probes, Eugene, OR; catalogue number A21109) or an IRDye 800–conjugated anti-mouse antibody (Rockland, Gilbertsville, PA; catalogue number 610-132-121) and subsequently visualized with the Odyssey infrared imaging system (LICOR Biosciences, Bad Homburg, Germany).

4.4.11 Southern Blot.

DNA was purified from 2 to 5 mm mice tail biopsies. Briefly, tails were digested overnight at 56° C in 750 µl digestion buffer (100 mM NaCl; 10 mM Tris-HCl pH 8; 25 mM EDTA pH 8; 0.5 % SDS; 0.1 mg/ml proteinase K). The following day, samples were mixed 5 minutes at maximum speed in an Eppendorf Thermomixer Comfort mixer. Two hundred µl of a saturated solution of NaCl was added, the samples were mixed for 5 minutes at maximum speed in an Eppendorf Thermomixer Comfort mixer and centrifuged at maximum speed for 5 minutes in a benchtop Eppendorf centrifuge. The intermediate phase (~750 µl) was recovered and 500 µl of isopropanol was added. Samples were mixed and centrifuged as mentioned above. Finally the DNA pellet was washed with cold 70% ethanol and resuspended in 90 µl of Tris-EDTA buffer (10 mM Tris; 1 mM EDTA; pH 8.0).

DNA (30 µl) was digested with *Eco*RI overnight and separated on a 0.8 % agarose gel. The gel was later washed sequentially in 0.25 M HCl, for 10 minutes, 0.4 M NaOH for 30 minutes, in neutralizing solution (1.5 M NaCl; 0.5 M Tris-HCl pH 7.2; 1 mM EDTA pH 8)

for 20 minutes and 5 minutes in 20x SSC (3 M Sodium Chloride; 0.3 M Sodium Citrate, pH 7.0).

The gel was transferred by capillarity overnight in 20x SSC to an Amersham Hybond™-N+ membrane (GE Healthcare; catalogue number RPN303B). The following day, the membrane was briefly washed in 2x SSC, air-dried and UV-fixed with 120 mJ (UV Stratalinker 2400; Stratagene). The membrane was then probed overnight in hybridization solution (0.5 M Sodium Phosphate pH 7.2; 7% SDS, 1mM EDTA and 1% BSA) with a probe corresponding to a 0.7 kb *Bam*HI/*Eco*RI fragment from the RIP-vmos.xf3 plasmid that contains the RIP1 promoter. The probe was labelled by random priming (Random Primed DNA Labelling Kit, catalogue number 1 004 760; Roche Applied Science). The probe recognizes a 2.8 kb transgene specific band and two 1.8 and 0.7 kb endogenous bands corresponding to the Ins1 and Ins2 promoters. Finally, the membrane was washed twice in washing Solution (40 mM Sodium Phosphate pH 7.2; 1% SDS; 5 mM EDTA and 0.5 % BSA) and visualized using a BioRad® Personal Molecular Imager FX™ System.

4.4.12 Transgenic lines.

The transgenic construct (RIP-N.xf3) bears fragment N of RasGAP under the control of the rat insulin promoter (RIP). It was obtained by ligation of a blunt-ended BamHI/SalI 1.4 kb fragment from plasmid N-D157A.bs (obtained by ligation of a blunt-ended 1.4 kb *Bam*HI/*Xho*I fragment from plasmid N-D157A.dn3 into the pBS II SK + plasmid [Stratagene] opened with *Eco*RV) with a blunt-ended *Xba*I/*Hind*III 4 kb fragment from RIP-vMos.xf3 plasmid. The correctness and functionality of the plasmid were controlled by sequencing and transfection into insulinoma cell lines. Finally, a *Bam*HI 2.8 kb fragment from RIP-N.xf3 was microinjected into FVB/N oocytes at the Transgenic Animal Facility of the Lausanne University. Four independent RIP-N expressing founders were obtained. Only the data pertaining to founder #1 are described here.

4.4.13 Blood glucose level measurements and intraperitoneal glucose tolerance test (IPGTT).

Blood glucose content of mice under feeding or fasting (16 hours) conditions was determined with an Accu-Check Compact Plus glucometer (Roche Diagnostics). For the IPGTTs, fasted (16 hours) animals were injected intraperitoneally with 2 mg/kg glucose. Blood glucose levels were determined from a blood drop taken after a short incision of the tail tip at increasing time intervals (-30, 0, 15, 30, 60, 90, 120. 150 minutes) following glucose injection.

4.4.14 Streptozotocin-induced diabetes.

Type 1-like diabetes was induced by multiple low dose streptozotocin injections. Briefly, 4 hour-fasted female RIP-N mice were injected intraperitoneally for 5 consecutive days with 50 mg streptozotocin per kg of mice. Streptozotocin was prepared and diluted in citrate buffer pH 4.5 (sodium citrate 25 mM, citric acid 23 mM) just before injection. Blood glucose levels were assessed biweekly.

4.4.15 Statistical Analysis.

All the statistical analyses were done with Microsoft Office Excel 2003 SP1 using the two-tailed unpaired Student's t test. Significance is indicated by an asterisk when $p < 0.05/n$, two asterisk when $p < 0.01/n$ and three asterisks with $p < 0.001/n$, where p is the probability derived from the t test analysis and n is the number of comparisons done (Bonferroni correction).

4.5 References

1. Liadis, N., et al., *Caspase-3-dependent beta-cell apoptosis in the initiation of autoimmune diabetes mellitus.* Mol. Cell. Biol., 2005. **25**(9): p. 3620-9.
2. Maedler, K. and M. Donath, *Beta-cells in type 2 diabetes: a loss of function and mass.* Horm Res, 2004. **62 Suppl 3**: p. 67-73.
3. Donath, M. and P. Halban, *Decreased beta-cell mass in diabetes: significance, mechanisms and therapeutic implications.* Diabetologia, 2004. **47**(3): p. 581-9.

4. Alnemri, E., et al., *Human ICE/CED-3 protease nomenclature.* Cell, 1996. **87**(2): p. 171.
5. Yan, N. and Y. Shi, *Mechanisms of apoptosis through structural biology.* Annu. Rev. Cell Dev. Biol., 2005. **21**: p. 35-56.
6. Donath, M., et al., *Mechanisms of beta-cell death in type 2 diabetes.* Diabetes, 2005. **54 Suppl 2**: p. S108-13.
7. Moritz, W., et al., *Apoptosis in hypoxic human pancreatic islets correlates with HIF-1alpha expression.* FASEB J, 2002. **16**(7): p. 745-7.
8. Ilieva, A., et al., *Pancreatic islet cell survival following islet isolation: the role of cellular interactions in the pancreas.* J Endocrinol, 1999. **161**(3): p. 357-64.
9. Efanova, I., et al., *Glucose and tolbutamide induce apoptosis in pancreatic beta-cells. A process dependent on intracellular Ca2+ concentration.* J. Biol. Chem., 1998. **273**(50): p. 33501-7.
10. Delaney, C., et al., *Cytokines induce deoxyribonucleic acid strand breaks and apoptosis in human pancreatic islet cells.* Endocrinology, 1997. **138**(6): p. 2610-4.
11. Lawlor, M. and D. Alessi, *PKB/Akt: a key mediator of cell proliferation, survival and insulin responses?* J. Cell. Sci., 2001. **114**(Pt 16): p. 2903-10.
12. Ozes, O., et al., *NF-kappaB activation by tumour necrosis factor requires the Akt serine-threonine kinase.* Nature, 1999. **401**(6748): p. 82-5.
13. Romashkova, J. and S. Makarov, *NF-kappaB is a target of AKT in anti-apoptotic PDGF signalling.* Nature, 1999. **401**(6748): p. 86-90.
14. Yang, J. and C. Widmann, *The RasGAP N-terminal fragment generated by caspase cleavage protects cells in a Ras/PI3K/Akt-dependent manner that does not rely on NFkappa B activation.* J. Biol. Chem., 2002. **277**(17): p. 14641-6.
15. Giannoukakis, N., et al., *Protection of human islets from the effects of interleukin-1beta by adenoviral gene transfer of an Ikappa B repressor.* J. Biol. Chem., 2000. **275**(47): p. 36509-13.
16. Heimberg, H., et al., *Inhibition of cytokine-induced NF-kappaB activation by adenovirus-mediated expression of a NF-kappaB super-repressor prevents beta-cell apoptosis.* Diabetes, 2001. **50**(10): p. 2219-24.
17. Baker, M., et al., *Expression of a dominant negative inhibitor of NF-kappaB protects MIN6 beta-cells from cytokine-induced apoptosis.* J Surg Res, 2001. **97**(2): p. 117-22.
18. Donath, M., et al., *Inflammatory mediators and islet beta-cell failure: a link between type 1 and type 2 diabetes.* J Mol Med, 2003. **81**(8): p. 455-70.
19. Kim, S., et al., *NF-kappaB prevents beta cell death and autoimmune diabetes in NOD mice.* Proc. Natl. Acad. Sci. U.S.A., 2007. **104**(6): p. 1913-8.
20. Tuttle, R., et al., *Regulation of pancreatic beta-cell growth and survival by the serine/threonine protein kinase Akt1/PKBalpha.* Nat. Med., 2001. **7**(10): p. 1133-7.
21. Shapiro, A., *Islet transplants and impact on secondary diabetic complications: does C-Peptide protect the kidney?* J. Am. Soc. Nephrol., 2003. **14**(8): p. 2214-6.
22. Shapiro, A., S. Nanji, and J. Lakey, *Clinical islet transplant: current and future directions towards tolerance.* Immunol. Rev., 2003. **196**: p. 219-36.
23. Yang, J. and C. Widmann, *Antiapoptotic signaling generated by caspase-induced cleavage of RasGAP.* Mol. Cell. Biol., 2001. **21**(16): p. 5346-58.
24. Yang, J., et al., *Impaired Akt activity down-modulation, caspase-3 activation, and apoptosis in cells expressing a caspase-resistant mutant of RasGAP at position 157.* Mol. Biol. Cell, 2005. **16**(8): p. 3511-20.
25. Yang, J., et al., *Expression of an uncleavable N-terminal RasGAP fragment in insulin-secreting cells increases their resistance toward apoptotic stimuli without*

affecting their glucose-induced insulin secretion. J. Biol. Chem., 2005. **280**(38): p. 32835-42.
26. Gannon, M., et al., *Analysis of the Cre-mediated recombination driven by rat insulin promoter in embryonic and adult mouse pancreas.* Genesis, 2000. **26**(2): p. 139-42.
27. Gorogawa, S., et al., *Insulin secretory defects and impaired islet architecture in pancreatic beta-cell-specific STAT3 knockout mice.* Biochem. Biophys. Res. Commun., 2004. **319**(4): p. 1159-70.
28. Wendel, H., et al., *Survival signalling by Akt and eIF4E in oncogenesis and cancer therapy.* Nature, 2004. **428**(6980): p. 332-7.
29. Norlin, S., U. Ahlgren, and H. Edlund, *Nuclear factor-{kappa}B activity in {beta}-cells is required for glucose-stimulated insulin secretion.* Diabetes, 2005. **54**(1): p. 125-32.
30. O'Brien, B., et al., *Beta-cell apoptosis is responsible for the development of IDDM in the multiple low-dose streptozotocin model.* J Pathol, 1996. **178**(2): p. 176-81.
31. Like, A. and A. Rossini, *Streptozotocin-induced pancreatic insulitis: new model of diabetes mellitus.* Science, 1976. **193**(4251): p. 415-7.
32. Mathis, D., L. Vence, and C. Benoist, *beta-Cell death during progression to diabetes.* Nature, 2001. **414**(6865): p. 792-8.
33. Rhodes, C., *Type 2 diabetes-a matter of beta-cell life and death?* Science, 2005. **307**(5708): p. 380-4.
34. Wilkin, T., *The accelerator hypothesis: weight gain as the missing link between Type I and Type II diabetes.* Diabetologia, 2001. **44**(7): p. 914-22.
35. Maedler, K., et al., *FLIP switches Fas-mediated glucose signaling in human pancreatic beta cells from apoptosis to cell replication.* Proc Natl Acad Sci USA, 2002. **99**(12): p. 8236-41.
36. Maedler, K., et al., *Glucose induces beta-cell apoptosis via upregulation of the Fas receptor in human islets.* Diabetes, 2001. **50**(8): p. 1683-90.
37. Butler, A., et al., *Beta-cell deficit and increased beta-cell apoptosis in humans with type 2 diabetes.* Diabetes, 2003. **52**(1): p. 102-10.
38. Carr, M. and J. Brunzell, *Abdominal obesity and dyslipidemia in the metabolic syndrome: importance of type 2 diabetes and familial combined hyperlipidemia in coronary artery disease risk.* J Clin Endocrinol Metab, 2004. **89**(6): p. 2601-7.
39. Haber, E., et al., *New insights into fatty acid modulation of pancreatic beta-cell function.* Int Rev Cytol, 2006. **248**: p. 1-41.
40. Biarnés, M., et al., *Beta-cell death and mass in syngeneically transplanted islets exposed to short- and long-term hyperglycemia.* Diabetes, 2002. **51**(1): p. 66-72.
41. Hotamisligil, G., et al., *Increased adipose tissue expression of tumor necrosis factor-alpha in human obesity and insulin resistance.* J. Clin. Invest., 1995. **95**(5): p. 2409-15.
42. Hotamisligil, G., N. Shargill, and B. Spiegelman, *Adipose expression of tumor necrosis factor-alpha: direct role in obesity-linked insulin resistance.* Science, 1993. **259**(5091): p. 87-91.
43. Paraskevas, S., et al., *Cell loss in isolated human islets occurs by apoptosis.* Pancreas, 2000. **20**(3): p. 270-6.
44. Korsgren, O., et al., *Current status of clinical islet transplantation.* Transplantation, 2005. **79**(10): p. 1289-93.
45. Carlsson, P., et al., *Markedly decreased oxygen tension in transplanted rat pancreatic islets irrespective of the implantation site.* Diabetes, 2001. **50**(3): p. 489-95.

46. Emamaullee, J. and A. Shapiro, *Factors influencing the loss of beta-cell mass in islet transplantation.* Cell transplantation, 2007. **16**(1): p. 1-8.
47. Datta, S., A. Brunet, and M. Greenberg, *Cellular survival: a play in three Akts.* Genes Dev., 1999. **13**(22): p. 2905-27.
48. Eldor, R., et al., *Conditional and specific NF-kappaB blockade protects pancreatic beta cells from diabetogenic agents.* Proc. Natl. Acad. Sci. U.S.A., 2006. **103**(13): p. 5072-7.
49. Dohi, T., et al., *Inhibition of apoptosis by survivin improves transplantation of pancreatic islets for treatment of diabetes in mice.* EMBO Rep., 2006. **7**(4): p. 438-43.

Chapter 5 - Discussion

5 DISCUSSION AND PERSPECTIVES.

5.1 General Discussion

The work performed in our laboratory during the last years permitted us to describe the role played by RasGAP in the context of apoptosis. At caspase levels that do not induce apoptosis, RasGAP is first cleaved at position 455 and two fragments are generated (fragment N and fragment C) [1]. Surprisingly, cells unable to cleave RasGAP were rendered more sensitive to stress-induced apoptosis. Fragment N protects cells against apoptosis via the activation of the Ras/PI3K/Akt pathway. In addition, fragment-N is also able to inhibit NFκB activity. When caspase levels increase to a level that induces apoptosis, fragment N is further cleaved at position 157. This cleavage abrogates fragment N anti-apoptotic properties and generates two smaller fragments, named N1 and N2. Interestingly, fragment N2 was found to sensitize cancer cells to genotoxin-induced apoptosis [1, 2].

In the present work we show that the activation of the Ras/PI3K/Akt pro-survival pathway mediated by fragment N relies on the presence of the uncleaved form of RasGAP. This fact shows, once more, that RasGAP can act as Ras effector. The role played by RasGAP in the activation of the fragment-N mediated survival pathway could be to act as a hypothetical scaffold protein that would bring Ras and its effectors in close proximity. RasGAP is found in high molecular weight complexes ([3] and unpublished data from our laboratory) and is cleaved at surprisingly low caspase activity levels. Considering these two facts together, we can think of a high molecular complex containing RasGAP and other proteins involved in the anti-apoptotic pathway. This complex could be located in close proximity to caspase activation sites, therefore forming a "caspase-activity sensing complex". If this complex exists, it does not seem to be indispensable for mouse survival, since knock-in mice expressing a caspase-insensitive RasGAP mutant ($RasGAP^{D455A/D455A}$) are viable and exhibit

normal development and homeostasis under normal conditions. RasGAP$^{D455A/D455A}$ mice were not differentially affected by sub-lethal doses of γ-radiation or chronical injections of sub-lethal doses of cisplatin compared to wt mice. This might indicate that other safeguard mechanisms exist. However, some stress responses might rely on this pathway, since RasGAP$^{D455A/D455A}$ mice showed increased heart hypertrophy following transaortic constriction-mediated haemodynamic overloading. Nonetheless, fragment-N anti-apoptotic properties can be used for therapeutical purposes. As we showed in chapter 4, over-expression of fragment-N in pancreatic ß-cells protected them against stress-induced apoptosis and protected the mice against experimentally induced diabetes.

5.2 Perspectives.

5.2.1 Fragment-N mediated Akt activation relies on full length RasGAP.

The numerous questions raised by the implication of RasGAP in the anti-apoptotic response mediated by its cleavage fragments, require numerous answers. The presence of RasGAP in supra-molecular complexes, induced by low stress conditions, is currently being tested using gel filtration. This method has previously being notably used to identify and characterize the apoptosome [4] and inflammasome [5]. Using this method, the presence of RasGAP in high molecular fractions, induced by stress, is determined by western blot of fractions obtained after chromatographic separation of cell lysates. High molecular weight fractions containing RasGAP would be then subjected to immunoprecipitation with an anti-RasGAP antibody and the proteins associated with it identified by mass spectroscopy.

Even though the structure of the C-terminal domain of RasGAP is currently known, nothing (except the SH3 domain structure [6]) is known about the structure of the N-terminal domain. The structures of both RasGAP and fragment-N are going to be determined by X-ray crystallography to understand the role played by RasGAP N-terminal fragment in the

interaction with other proteins and the possible conformational changes mediated by caspase cleavage.

5.2.2 RasGAP uncleavable knock-in.

RasGAP cleavage does not seem to be involved in the regulation of caspase activity in haematopoietic cell development. However, RasGAP$^{D455A/D455A}$ derived splenocytes showed an increased proliferative rate (measured by MTT assay) when stimulated with an anti-CD3 antibody. Nevertheless, these results should be confirmed. Further experiments, should aim at identifying the nature of the proliferating population (since splenocytes are a mixed cell population) and clarify whether the increased proliferative rate is due to increased proliferation or increased apoptosis in the less proliferating cells.

Preliminary experiments in which transaortic constriction was performed in RasGAP$^{D455A/D455A}$ and RasGAP$^{wt/wt}$ mice, showed increased heart hypertrophy in the RasGAP$^{D455A/D455A}$ mice. These results should be further confirmed and the biochemical and histological characterizations performed. The results of the biochemical characterization would allow understanding the role played by RasGAP cleavage in this process. We can hypothesize that increased apoptosis in RasGAP$^{D455A/D455A}$ hearts would induce proliferation as a compensatory mechanism, leading to an increased hypertrophy.

The capacity of fragment-N to modulate NFκB activity [2] will be tested *in vivo*. The role of NFκB during inflammation has been described as a positive feedback signal, inducing the expression of pro-inflammatory cytokines upon inflammatory signalling. The role of fragment-N NFκB inhibition will be studied in a model of heart inflammatory stress. If the role played by fragment-N NFκB inhibition is important, RasGAP$^{D455A/D455A}$ mice should have an exacerbated inflammatory response. Similar experiments can be performed by stressing the mice with lipopolysaccharide and following cytokine production, a direct indicator of NFκB activity.

5.2.3 Fragment-N protects against diabetes.

The anti-apoptotic properties of fragment-N have proven to be a useful therapeutic tool in the context of diabetes. Fragment-N is able to efficiently protect islets against stress-induced apoptosis and mice against experimental diabetes. We have shown that fragment-N can be useful in the context of islet transplantation because it protects islet cells against hypoxia and cytokine-induced apoptosis, two important factors responsible for ß-cell demise prior transplantation. However, islet transplantation experiments should be performed to validate that fragment-N effectively enhances islet transplantation success rate and consequently diminishes the number of islets necessary for the procedure.

Even if fragment-N protects islet, its practical use during transplantation procedure, would be very difficult to set up (mainly through viral infections). The understanding of the protective pathway induced by it is indispensable to be able to modulate these protective pathways. To dissect the survival pathways modulated by fragment N, microarray analysis should be performed. In addition this could lead the discovery of new downstream therapeutic targets.

5.3 References

1. Yang, J. and C. Widmann, *Antiapoptotic signaling generated by caspase-induced cleavage of RasGAP*. Mol. Cell. Biol., 2001. **21**(16): p. 5346-58.
2. Yang, J. and C. Widmann, *The RasGAP N-terminal fragment generated by caspase cleavage protects cells in a Ras/PI3K/Akt-dependent manner that does not rely on NFkappa B activation*. J. Biol. Chem., 2002. **277**(17): p. 14641-6.
3. Chow, A., A. Davis, and D. Gawler, *Identification of a novel protein complex containing annexin VI, Fyn, Pyk2, and the p120(GAP) C2 domain*. FEBS Lett., 2000. **469**(1): p. 88-92.
4. Cain, K., et al., *Caspase activation involves the formation of the aposome, a large (approximately 700 kDa) caspase-activating complex*. J. Biol. Chem., 1999. **274**(32): p. 22686-92.
5. Martinon, F., K. Burns, and J. Tschopp, *The inflammasome: a molecular platform triggering activation of inflammatory caspases and processing of proIL-beta*. Mol. Cell, 2002. **10**(2): p. 417-26.
6. Ross, B., et al., *High resolution crystal structures of the p120 RasGAP SH3 domain*. Biochem. Biophys. Res. Commun., 2006. **353**(2): p. 463-8.

Chapter 6 – Methods

SOP 1.0
Transfection (calcium-phosphate)

Reagents

1. HEPES buffer (2X) pH 7.05 (23°C):

1.1. Important note: always calibrate the pH meter before starting preparing the Hepes buffer.
1.2. Composition.

Chemicals	Final concentration	Source/Company	Code/quantities
NaCl	280 mM	Fluka	71380 (1 kg)
KCl	10 mM	Fluka	60130 (1 kg)
Na_2HPO_4	1.5 mM	Merck	1.06586.0500 (500 g)
D-glucose•H_2O	12 mM	Merck	1.08342.1000 (1 kg)
HEPES	50 mM	Fluka	54461 (250 g)

1.3. Recipe.

Chemicals	For 500 ml
NaCl	8 g
KCl	0.38 g
Na_2HPO_4	0.1 g
D-glucose•H_2O	1.1 g
HEPES	5 g
Adjust pH with NaOH (1 N, then 0.1 N) to 7.05 (23°C)	See 1.4

1.4. Add ddH_2O to about 450 ml, then adjust to pH 6.8-6.9 with 1 N NaOH, and finally to pH 7.05 with 0.1 N NaOH. Complete to 500 ml with ddH_2O. Control that the pH is still at 7.05.
1.5. Sterilize through a 0.22 μm 500 ml Stericups (Millipore #SCGPU05RE). Under a sterile hood, aliquot in 50 ml tubes (40 ml per tube). Write the lot number and the date on the tubes **(the lot number should be indicated in your laboratory book)**. Store at –20°C.

2. Others

Chemicals	Source/Company	Code/quantities	Solvent	[stock]	Storage	Sterile
NaOH	Fluka	#71690 (500 g)	ddH_2O	10 N	Room temp.	no
Chloroquine	Sigma	C6628 (25g)	PBS	25 mM	-20°C	yes
$CaCl_2$•$2H_2O$ (MW 147.02)	Acros	207780010 (1 kg)	ddH_2O	2.5 M	4°C	yes
Gelatin	Fluka	48722 (500 g)	PBS	0.1%	4°C	yes
DMEM, glutamax I, 4.5 g/l glucose, sans sodium pyruvate	Gibco	61965026 (500 ml)				
Newborn calf serum (NBCS), heat inactivated	Gibco	26010041 (500 ml)				

2.1. Preparation of NaOH solutions.
NaOH can cause irreversible damage to the eyes. It is thus mandatory to wear glasses when preparing or using NaOH solutions. The preparation of 10 N NaOH involves a highly exothermic reaction, which can cause breakage of glass container. Prepare this solution with extreme care in plastic beakers. To 80 ml of H_2O, slowly add 40 g of NaOH pellets, stirring continuously. As an added precaution, place the beaker on ice. When the pellets have dissolved completely, adjust the volume to 100 ml with H_2O. Store the solution in a plastic container at room temperature (plastic containers are to be used because NaOH slowly dissolves glassware). Sterilization is not necessary.

2.2. Preparation of a 25 mM chloroquine solution.
In a 50 ml Falcon tube, add 0,645 gr of chloroquine and complete to 50 ml with ddH_2O. Transfer to a 50 ml syringe and sterilize through a 0.22 μm filter (Millex – GV filters [Millipore #SLGV025LS]). Under a sterile hood, aliquote in 15 ml tubes (10 per tube). Write the lot number and the date on the tubes **(the lot number should be indicated in your laboratory book)**.

2.3. Preparation of a 2.5 M $CaCl_2$ solution.
In a 50 ml Falcon tube, add 18.4 g of $CaCl_2 \bullet 2H_2O$ and complete to 50 ml with ddH_2O. Transfer to a 50 ml syringe and sterilize through a 0.22 μm filter (Millex – GV filters [Millipore #SLGV025LS]). Under a sterile hood, aliquote in 15 ml tubes (10 per tube). Write the lot number and the date on the tubes **(the lot number should be indicated in your laboratory book)**.

2.4. Preparation of a PBS/0.1% gelatin solution (500 ml).
Add 0.5 g gelatin and 50 ml PBS 10X to 450 ml ddH_2O in a glass bottle. Autoclave and store at 4°C.

Procedure

Day 0.
1. Plate cells in appropriate medium (use gelatinized dishes if required).

Cells	Number per 10 cm dish	Number per well (6 well-plates)	medium	Gelatinized dish
HEK 293 and derived cell lines	$2 \cdot 10^6$	350'000	DMEM; 10% NBCS	yes
COS cells	?????		DMEM; 10% NBCS	no

1.1. Gelatinization of the dishes.
Place the indicated volume of PBS/0.1% gelatin in the dish (tilt the plate to cover the entire surface with the solution). Wait at least 10 min. Just before adding the cells to the plates, aspirate the PBS/0.1% gelatin (do not allow the plates to dry).

Dish size	Volume of PBS/01% gelatin
10 cm	2-5 ml
6 well plates	0.5 ml

Day 1.

2. Prewarm the HEPES 2X buffer in a 37°C water bath (at least 20 min). In case the buffer is thawed, mix very well before using.

3. Add the DNA in the indicated volume of H_2O. Add the corresponding volume of 2.5 M calcium solution. Mix **10 times** by pipetting the solution up and down. Allow 20-30 min the solution to equilibrate.

Cells	Dish size	Volume of medium in the dish	DNA amount	Volume of water in which the DNA is added	Volume of 2.5 M calcium to be added
HEK293	10 cm	10 ml	5-20 µg	450 µl	50 µl
	6 well plate	2 ml	2 µg	90 µl	10 µl
	12 well plate	?	?	?	?
	24 well plate	?	?	?	?

4. Add 25 µM chloroquine to the cell culture medium (not necessary to change the medium). Note: if the cells are grown in RPMI medium (e.g. HeLa cells), you have to replace it with DMEM because RPMI medium is not compatible with the present transfection technique.

Dish size	Volume of medium	Volume of stock
10 cm	10 ml	10 µl
6 well plates	2 ml	2 µl

5. Place the plates back in the incubator for at least 10 min.

6. Add the indicated volume of prewarmed (37°C) 2X HEPES buffer to the DNA/calcium solution, mix 5 times by pipetting the solution up and down. Incubate for 1 minute exactly (starting from the moment the HEPES has been added to the DNA; not from the time when the mixing is finished). Put the DNA-HEPES mix in the culture medium (rock the plate left to right and up and down 2 times).

Dish size	Volume of HEPES 2X to be added
10 cm	500 µl
6 well plate	100 µl

7. Incubate the cells at 37°C for 8-16 hours (**always mention this time of incubation in your laboratory book**). Replace the transfection medium with normal culture medium containing penicillin and streptomycin [use a 1:100 dilution of a Penicillin-Streptomycin Glutamine 100X solution (10'000 units/ml penicillin G; 10 mg/ml streptomycin sulfate; 29,2 mg/ml L-glutamine; 10 mM sodium citrate; 0.14% NaCl {GibcoBRL #10378-016})] to avoid contamination (the DNA used for the transfection is generally not sterile!).

8. Expected transfection efficiencies (count at least 500 cells).

Cells	Transfection efficiency
HEK293	30-80%
COS	30-40%

9. **In your laboratory book, always mention how long after step 7 were the cells analyzed**.

References

1. Jordan et al. - Nucl. Acid Res. (1996) **24**:596 (#3461

Apparatus

Transfer tank located in the drawers next to Christian's office door. It is the transparent tank containing red-black electrode module inside. Gel cassetes and sponges are either in the drawer above the one containing the tanks or above the sink in the middle of the lab.

Materials and reagents

3. Plastic sheets, commercial Enhanced chemiluminescence (ECL) solution and other reagents.

3.1. Materials and reagents.

Materials and reagents	Source/Company	Code/quantities
Plastic sheets Kapak Tubular Roll Stock [9.5''x250' #5 Scotchpak (2 Mil)].	Kapak Parkdale Drivewe, Minneapolis, Minnesota 55416 • 1681	
Tris	Sigma	T1503 5Kg
Tween	Acros	p7949 100ml
Milk		
ECL reagent Supersignal West Femto Substrate	Pierce	#34095
Ponceau S	Acros	161470250 (25 g)

3.2. **Ponceau S Staining Solution [0.1%(w/v) Ponceau S in 5% (v/v) acetic acid]**

- 1g Ponceau S
- 50ml acetic acid
- Make up to 1 liter with ddH_2O
  Store at 4^oC. Do not freeze.

  Alternative recipe:0.2% (w/v) Ponceau S in 3% (v/v) acetic acid.

3.3. **Tris-buffer saline (TBS; 18 mM HCl, 130 mM NaCl, 20 mM Tris pH 7.2)**

- 30ml HCl
- 152g NaCl
- 48g Tris base
- Up to 1L dH_2O

3.4. TBS/tween

- 19L dH_2O
- 1L 20X TBS
- 0.1% Tween (final concentration)

3.5. TBS/milk

- 5% powdered milk (25g for 500ml of TBS/tween)
- TBS/tween
- Alternatively some primary antibodies work better if they are diluted in 5% BSA (5%BSA in TBS/tween)

4. Home-made ECL solution.

4.1. Composition of the stocks.

Chemicals	Stock concentration	Final concentration	Source/Company	Code/quantities
Luminol (3-aminophthalydrazide)	250 mM (1 g in 22.7 ml DMSO). Make 1.5 ml aliquotes	1.25 mM	Sigma	A-8511 (1 g)
P-coumaric acid	90 mM (0.5 g in 33.3 ml DMSO). Make 660 µl aliquotes.	0.2 mM	Acros	12109-0250 (25 g)
Tris	1 M pH 8.5	100 mM	Boehringer Mannheim	708976 (1 kg); IBCM stock
H_2O_2 30%	30%	0.01%	Merck	1.07210.0250 (250 ml)

Solution 1: 2.5 mM luminol and 0.4 mM coumaric acid in 100 mM Tris pH 8.5.
Solution 2: 0.02% H_2O_2 in 100 mM Tris pH 8.5.

5. *Home-made enhanced ECL solution* ***Note: for the moment this is not working (use the above recipe instead)***.

5.1. Composition of the stocks.

Chemicals	Stock concentration	Final concentration	Source/Company	Code/quantities
Luminol (3-aminophthalydrazide)	250 mM	1.25 mM	Sigma	A-8511 (1 g)
p-iodophenol	(in DMSO)	50 µM		
Tris	1 M pH 8.5	100 mM	Boehringer Mannheim	708976 (1 kg); IBCM stock
H_2O_2 30% (8.82 M)	30%	2 mM	Merck	1.07210.0250 (250 ml)

Procedure

1. General remarks.
   1.1. The conditions of incubation of the blots have to be adapted for each antigen and each antibody used. Therefore, the procedures presented in the following sections have to be considered as general guidelines and should not be assumed to work in all cases. Indications of possible improvements when the conditions are not found optimal will be mentioned.
   1.2. Always centrifuge the tubes containing the antibodies before usage.
   1.3. In principle, do not incubate two blots in the same bag.
   1.4. Never touch the blot with bare hands. Use gloves and move the blots with tweezers.
   1.5. The following procedure should be considered only for the small gels (see SOP12.1).

2. Migration on gels.

Percentage of acrylamide	Separation
8%	40-200 kDa
10%	30-200 kDa
12%	20-200 kDa
4-20%	7-250 kDa
8-16%	15-250 kDa

3. Transfer to membranes.
   3.1. After migration, proteins are transferred to nitrocellulose filters (Schleicher and Schuell, BA83 0.2μm, no. 401380) or PVDF membranes. Instruction on how to do this can be found in the same drawer as the material used for the transfer and for the SDS-PAGE (see SOP 12.1).
   3.2. Transfer buffers.

David has recently tested the two following buffers. According to him, transfer buffer II works better.

Composition of transfer buffer I.

Chemicals	Stock solution	Final concentration	Source/Company	Code/quantities
CAPS	1M pH11	10 mM	Acros	172621000 (100 g)
Methanol		10%	Fluka	65543 (5 l)

CAPS 1M stock solution (500 ml): 110 g CAPS (MW 221.3) and 20 g NaOH in water. The pH should be 11. Store in the dark at 4°C.
Prepare the transfer buffer (5 liters) directly in the transfer tank (50 ml CAPS 1M, 500 ml methanol, and water up to 5 liters).
Methanol evaporation ensures that the buffer does not heat too much. Therefore the transfer buffers cannot be used too many times. Without methanol, the buffer would boil during the transfer!
Transfer o/n at 600 mA.

Composition of the transfer buffer II.

Chemicals	10X stock (1 liter)	Final concentration (1X transfer buffer)	Source/Company	Code [quantities]
Tris	30.2 g	1 mM	Biosolve ltd	20092388 [4 kg]
Glycine	144 g	8 mM	ACROS	120070050 [5 kg]
SDS	10 ml of a 10% solution in water	0.001%	Biosolve ltd	19822359 [0.5 kg]

Prepare the transfer buffer 1X (5 liters) directly in the transfer tank.
Add 500 ml of the 10X buffer, 1 liter of methanol and water up to 5 liters.
Transfer 5 hours at 660 mA.

Currently the situation with the transfer buffers is like this: they are located above the sink were other materials for the transfer can also be found (sponges, etc.), There are several bottles of 10x transfer buffer. In order to make 1x transfer buffer, mix 100 ml of the 10X preparation with 700ml of water and 200ml of some alcohol (methanol or ethanol).

3.3 After preparing the transfer tank, place the top on and plug it into a power supply machine (make sure that the plus and minus plugs are connected right: you do not want your proteins to be released on the wrong side directly into the transfer buffer). Transfer is usually preformed at 250 mA (constant amperage) for one hour or one hour and twenty minutes.

3.4 Check if the protein markers have been transferred (one should see the markers on the membrane and not on the gel).

4. This protocol should be used when there are no particular problems to get a strong signal

4.1. Ponceau S Stain for Western blots.

Background. *This is a rapid and reversible staining method for locating protein bands on Western blots. Sensitivity is somewhat less than Coomassie blue and produces reddish pink stained bands; minor components may be difficult to resolve. The stain is useful because it does not appear to have a deleterious effect on the sequencing of blotted polypeptides and is therefore one method of choice for locating polypeptides on Western blots for blot-sequencing. The stain binds strongly to nylon-based filter media but is fine for nitrocellulose and PVDF membranes. Incubate the membrane for up to an hour in staining solution with gentle agitation. Rinse the membrane in distilled water until the background is clean. The stain can be completely removed from the protein bands by continued washing. Stain solution can be re-used up to 10 times.* **How we use it in the laboratory**. Incubate the blot in Ponceau for 2-3 min to visualize the proteins and to determine whether the transfer was homogeneous. With a pen, mark the position of the molecular weight markers. The blots are then subjected to the following incubations.

4.2. wash 3x 20 min at room temperature with TBS/0.1% Tween 20 (TBS/Tween; found in the big tank next to the sink near the entrance of the laboratory).

4.3. 45-60 min at room temperature with TBS/5% powdered milk (TBS/milk).

4.4. overnight with the primary antibody (in TBS/milk) at 4°(in a cold room).

4.5. 3x 20 min at room temperature with TBS/Tween.

4.6. 45 min at room temperature with TBS/milk.

4.7. 45 min with the secondary antibody (in TBS/milk) at room temperature (if the secondary antibody bears a fluorochrome sensitive to light [e.g. antibodies required for the odyssey detection; see SOP 17], make sure that incubation is performed in a black box).

4.8. 3x 20 min at room temperature with TBS/tween (in the dark).

5. Detection of the secondary antibodies on films.

5.1. This method should be used only for antibodies and antigens that do not generate strong signals. If this is not the case, detect the secondary antibodies with the BioRad Fluor-S imager (refer to SOP 2.0) or even better with the Odyssey apparatus (see SOP 17).
5.2. Check that the developer has been turned on and is ready to be used.
5.3. Prepare a cassette that should contain a fluorescent ladder (to position your film on the blot later on).
5.4. Wash a glass plate thoroughly (first with soap, rinse with water and finally with ethanol).
5.5. Prepare the ECL reagent by mixing equal volumes of solutions I and II. You need about 1 ml for each 10 cm^2 of your blot.
5.6. Cut some Kappak plastic sheet that will be used to contain your blot during the exposure to films. Seal it but leave one side open.
5.7. Take the blot with tweezers and touch some absorbing paper with one of its corner to remove the liquid in excess. Place the blot on the glass plate with the transferred proteins up. Pour the ECL reagent on the blot. Check that the whole surface is covered and wait one minute.
5.8. With tweezers, transfer the blot in the Kappak bag. Remove the bubbles and seal the bag. Using absorbing paper, remove the liquid on the exterior of the bag. Place the bag in the cassette as close as possible to the fluorescent ladder. Tape the bag on one side.
5.9. Immediately, go to the dark room with the sealed blot, the films and a cassette. Place a film on the blot. Close the cassette. Wait one minute. Remove the first film that you insert in the developer. While the first film develops, place a second one on the blot and close the cassette. When the first film comes out, check the intensity of the signal. If it is weak, expose the second film for 5-15 min. If it is too strong, develop the second film immediately (it will of course be too dark too) and expose a third film to 5-15 seconds. If the film has to be exposed for 1-2 seconds, tape it on the other side of the cassette. This will ensure that when you close the lids, the film will not move. Note again that if the signal is strong, you should not use this technique (see point 3.1).
5.10. Keep all the films (the overexposed ones are often used to position the molecular weight markers). All the films should be labeled (**do it immediately**) with the date, the experiment number, the exposure time, the type of ECL used, and the experimental conditions for each lane. Also try (when possible) to identify the bands on your blots.

6. Detection of the secondary antibodies with the BioRad Fluor-S imager.
6.1. Refer to SOP 2.0.
6.2. In this case also, the images obtained should be labeled: date, the experiment number, the exposure time, the type of ECL used, and the experimental conditions for each lane. Also try (when possible) to identify the bands on your blots.
7. Quantitation of the ECL signal.
7.1. In principle, quantitation should not be performed using films because the signal on films is not linear (you need more that one photon to active the silver grains) and saturates rapidly.
7.2. If possible, quantitation should be performed using the BioRas Fluor-S imager. Please refer to SOP 2.0.

8. Detection of the secondary antibodies using the Odyssey system (Licor).
8.1. Refer to SOP 17.
9. No signal
9.1. Increase the incubation with the antibodies: o/n incubation with the first antibody and 2-4 hours with the secondary antibody. Perform the incubations at 4°C.
9.2. Reduce the "stringency" of the incubation buffer. Milk containing buffer can possibly quench a fraction of the antibody. The following buffers are ranked from highest to lowest stringency: milk-containing buffer, BSA containing-buffer, tween-containing buffer, PBS or Tris buffer.
10. How to store antibodies.

It is possible to reuse antibodies many times and this should be done whenever the antibody is rare and not available commercially. The solution containing the antibody needs to contain 0.05% azide (NaN_3) and 10 mM EDTA.

11. Very important: after completion of the Western blot procedure, always store the nitrocellulose membranes in Kappak bags at -20°C for further potential use.

References

1. Widmann et al. Biochem. J. (1995) **310**:203 (#3461)
2. Yang et al. Mol.Cell Biol. (2001) 21:5346 (#3666)

SOP 9
Maxiprep

Reagents

Chemicals/medium	Source/Company	Code/quantities
JETstar maxi	Genomed	20 prep (#220020)
Isopropanol		
Glycerol		
Tris		
EDTA		

TE: Tris 10 mM pH 7.4, EDTA 1 mM.

Bacteria culture

1. For most plasmids, inoculate 250 ml of LB with the appropriate antibiotic (see SOP 8.0) with:
   - a tip that has touched a colony on an Agar plate.
   - a few ml of a mini-prep culture
   - a chunk of a glycerol stock taken with a yellow tip
2. Incubate o/n at 37°C in a shaker.
3. If required, take 1 ml of the culture to prepare a glycerol stock (put this one ml in an Eppendorf tube, centrifuge in an Eppendorf centrifuge at 4'000 rpm for 5 min, discard the supernatant and resuspend the pellet in 300-500 µl of a sterile 10% glycerol solution; store at –70°C).

Maxi prep

1. Principle.
   The procedure employs a modified alkaline/SDS method to prepare the cleared lysate. After neutralization, the lysate is applied onto a JETstar column and the plasmid DNA is bound to the anion exchange resin. Washing the resin removes RNA and all other impurities. Afterwards, the purified plasmid is eluted from the column and finally concentrated by alcohol precipitation. The supplier says that the JETstar purified plasmid DNA is of a higher quality than 2 x CsCl purified plasmid DNA. The expected yield for a maxi column is between 300-500 µg of DNA.
2. Centrifuge the cultures in 250 ml bottles at 5'000 rpm for 5-10 min at 4°C using the GSA rotor in the Sorvall RC-5B centrifuge. Check that the rotor is clean before and after use. Clean if necessary and always remove any liquid present.
3. Place the column on the "blue cow". Add 30 ml of solution E4 in the column and let flow by gravity.
4. Note: RNAse must be added to solution E1 prior to its first use. Just poor the lyophilized RNAse powder into bottle E1 and mix. Add the sticker indicating that the RNAse has been added, the date and your name. Discard the supernatant. Resuspend the pellet in 10 ml of solution E1.
5. Add 10ml of solution E2 and mix gently. Incubate 5min at room temp on a rocker (Rocker lnotech; shake 9, timer 5, frequency 17).
6. Add 10 ml of solution E3 and mix immediately by inverting the bottle 5 times. Transfer to a 50 ml blue Falcon tube (do not use yellow Falcon tube since they are more fragile and may break during the centrifugation). Centrifuge at 9'000 rpm for 10 min at 20°C using the SLA 600TC rotor in the Sorvall RC-5B centrifuge.
7. Poor the supernatant on the column and let flow by gravity. Wash the resin with 60 ml of solution E5.
8. Place the column on a 50 ml blue Falcon tube and secure the column on the tube with tape. Add 15 of solution E6 and let flow by gravity.
9. Add 10.5 of isopropanol. Mix and incubate on ice for at least 1 hour (alternatively, the tube can be stored o/n at –20°C).

10. Centrifuge at 10'000 rpm for 30 min at 4°C using the SLA 600TC rotor in the Sorvall RC-5B centrifuge. Discard the supernatant being very careful not to loose the pellet that is not always firmly adherent (sometimes not at all).
11. Add about 20 ml of 70% ethanol. Centrifuge at 10'000 rpm for 10 min at 4°C using the SLA 600TC rotor in the Sorvall RC-5B centrifuge. Discard the supernatant as above. Aspirate all the residual drops with a long white tip.
12. Resuspend the pellet in 500 µl of TE.
13. Measure the concentration with the spectrophotometer using a 1/100 dilution in a quartz cuvette. One OD at 260 nm corresponds to 50 µg/ml of DNA. The ratio between the OD at 260 nm and the OD at 280 nm should be between 1.8 and 2.0.
    Write down the concentration of the maxi prep in the plasmid files as well as on the tube.

Materials and reagents

1. coverslips keep in ethanol 100%

Materials and reagents	Source/Company	Code/quantities
PBS 10 X	?	?
0.2% TX-100 in PBS		
PBS 1X, 3% paraformaldehyde, 3% sucrose		
Gelatin	Fluka	48722 (500 g)
Mounting medium		
Antibody		

1.1. Preparation of a PBS/0.1% gelatin solution (500 ml).
Add 0.5 g gelatin and 50 ml PBS 10X to 450 ml ddH_2O in a glass bottle. Autoclave and store at 4°C.

2. List of antibodies

Name of Ab	Name of epitope or antigen	Origin of Ab	Source	Company or source	Dilution

---

Procedure

Preparation of coverslips

Growing cells on coverslips

1. In a sterile hood, take a coverslip from the ethanol bottle with tweezers. Set fire to the ethanol by passing quickly the coverslip over the flame. When all the ethanol has burnt and evaporated, place it in the appropriate culture plastic-ware. If required, coat the wells and the coverslips with PBS/0.1% gelatin for at least 10 minutes. Remove the PBS/gelatin if present and add the cells to the wells. Transfect or infect the cells if required.

Immunocytochemistry

1. Fill the required number of wells of 6-well plates with ~3ml PBS 1X (these 6-well plates can be used over and over). With tweezers, transfer the coverslips to the 6-well plates (face up). This can be performed under a sterile hood with sterile devices if the rest of the cells (i.e. cells not on the coverslips) have to be kept in culture.
2. After this step, the procedure can be continued on the bench. Use ~20°C solutions (solutions that have been kept at room temperature).
3. Aspirate the PBS 1X and put gently 3ml of PBS 1X, 2% paraformaldehyde, 3% sucrose. Incubate 15 min in the dark *(fixation step)*.
4. Wash very carefully with 3 ml PBS 1X.
5. Add very carefully 3ml 0.2% TX-100 in PBS 1X. Incubate the coverslips 10 min in the dark. (*permeabilization of the membrane*)
6. Wash very carefully with 3 ml PBS 1X.

7. Put 3 ml of sterile filtered serum-containing medium for 15 min in the dark (old sera can be used; filtrate the medium through 0.2 μm Millipore filter). These media are kept in the cold room. Take what is needed for the experiment (do not forget to include volumes used to dilute the antibodies) under a sterile hood and work according to cell culture standards.
8. Place some parafilm on a **clean** portion of the bench. Stretch the parafilm and fix it on the table with tape.
9. Dilute the first antibody in filtered medium and place 50 μl drops on the parafilm (1 drop per coverslip).
10. Take the coverslips with tweezers, remove the excess medium by touching a Kleenex tissue with the edge of the coverslip, and place the coverslip on the drop, face down.
11. Cover the coverslips with a lid (typically the top part of a foam box used for the shipping of frozen biological goods) with paper tapped on the interior side that must be moistened with water to reduce the extent of evaporation of the medium containing the antibodies. Incubate one hour.
12. Prepare a small becher containing PBS 1X.
13. Place 50 μl drops containing the second antibody (or any kind of labeling reagent) on a stretched parafilm (see #8-9).
14. Take the coverslips with tweezers, remove the excess medium by touching a Kleenex tissue with the edge of the coverslip, hold the coverslip ~5 seconds in the PBS-containing becher, remove the excess liquid and place the coverslip on the drop, face down. Cover with a lid as described in #11 and incubate for a further hour.
15. Take the coverslips with tweezers, remove the excess medium by touching a Kleenex tissue with the edge of the coverslip and place the coverslips face-up into the 6-well plate still filled with the filtered serum-containing medium.
16. Perform 6 incubations with PBS 1X in the dark. The incubations should last at least 20 min (preferably 30 min). If the coverslips float up (which happens especially during the last washes), push them to the bottom of the wells with the tweezers.
17. Clean the required number of slides to mount the coverslips.
18. For each coverslip, place 2 μl of mounting medium on the slide (up to four coverslips can be mounted per slide).
19. Take the coverslips with tweezers, remove the excess medium by touching a Kleenex tissue with the edge of the coverslip and place the coverslips face-down onto the drops of mounting medium.
20. With a long white tip connected to the vaccum, remove the excess of mounting medium trying not to move the coverslips.
21. Put some nail polish around the coverslips.
22. Let the nail polish dry a few hours (typically o/n).
23. Gently remove the dried PBS on the coverslips with a wet piece of Kleenex tissue.
24. The coverslips can now be analyzed with the appropriate imaging system.

IMPORTANT NOTE

The viral supernatants produced by these methods might, depending upon your retroviral insert, contain potentially hazardous recombinant virus. The user of these systems must exercise due caution in the production, use and storage of recombinant retroviral virions, especially those with amphotropic and polytropic host ranges. This consideration should be applied to all genes expressed as amphotropic and polytropic pseudotyped retroviral vectors. Appropriate guidelines should be followed in the use of these recombinant retrovirus production systems.

The user is strongly advised NOT to create retroviruses capable of expressing known oncogenes in amphotropic or polytropic host range viruses.

According to the Swiss Legislation all the manipulations done using lentiviruses, must be performed in a P2 security Laboratory.

For details and authorization for using the P2 Lab, contact Sylvain Lengacher at the Institute of Physiology (tel. 021 692 55 46, email: Sylvain.Lengacher@unil.ch)

For some additional information concerning the Lentiviral Systems you can check the following websites.

Garry Nolan's Lab website at Stanford University: http://www.stanford.edu/group/nolan/

Didier Trono's Lab website at Geneva University: http://www.tronolab.com/

Reagents.

Hexadimethrine bromide (Polybrene), Fluka (Sigma Cat. N° 52495)
Sucrose, Fluka (Sigma Cat. N° 84100)
Paraformaldehyde 95 %, (Sigma Cat. N° 441244)
Penicillin-Streptomycin Glutamine 100x solution, (GibcoBRL Cat N° 10378-016)
0.45 µm filters, Millex-HN, 0.45um, 25mm, stérile, 50/PK (Milian Cat N° SLHN025NS)
0.22 µm filters, Millex-GN, 0.22um, 25mm, stérile, 50/PK (Milian Cat N° SLGN025NS)
Chloroquine (Sigma Cat. N°C6628).
Laminin, mouse (1 mg) (BD Bioscience Cat. N° 354232)
Poly-D-Lysine (20 mg) (BD Bioscience Cat. N° 354210)
Biocidal ZF (1 l) (WAK Chemie Cat N° WAK-ZF-1)

Solutions.

1X Phosphate Buffered Saline (PBS)

NaCl,	8 g
KCl,	0.2 g
Na_2PO_4,	1.44 g
KH_2PO_4	0.24 g
H_2Odd	800ml

Adjust pH to 7.4 with HCl.
Adjust volume to 1 liter with additional distilled H_2O. Sterilize by autoclaving.

Tris-EDTA (TE) buffer. (10 mM Tris; 1 mM EDTA; pH 8.0)

1 M Tris pH 8.0	1 ml
0.5 M EDTA pH 8.0	0.2 ml
H_2Odd	98.8 ml

Autoclave

Polybrene 5 mg/ml (10 ml).
Dissolve 5 mg of Polybrene in 10 ml of PBS. Filter through a 0.22 µM filter, aliquot in eppendorf tubes (1 ml per tube) and store either at 4°C or at -20°C.

Chloroquine 25 mM (50 ml).
Dissolve 399.8 mg of Chloroquine in 50 ml of PBS. Filter through a 0.22 µM filter, aliquot in 15 ml falcon tubes (10 ml per tube) and store at -20°C.

Sodium Acetate 3 M pH 5.2 (100 ml).
To 24.6 gr of sodium acetate (Sigma Cat. N° S-2889), add 90 ml of nanopure water. Adjust the pH to 5.2 (with glacial acetic acid) and complete to 100 ml.

Fixation Solution (2% Paraformaldehyde 3% Sucrose).

a. Weigh 0.2 gr paraformaldehyde in a 15 ml tube.
b. Add 6 ml PBS.
c. Warm up to 60˚C and vortex.
d. Add drops of 0.5 M NaOH, warm up to 60° C and vortex until it dissolves.
e. Add 0.3 gr of Sucrose and make up the volume to 10 ml with PBS.
f. Make sure the final solution is neutral.

Procedure

Note: for details on the transfection protocol, refer to SOP001 *Transfection (calcium-phosphate)*.

Day 0.

1. Prepare five 10 cm gelatinized Petri dishes containing 2 - 2.5x10^6 HEK293T cells in 10 ml medium.

Gelatinization of the dishes.

Place between 2 to 5 ml of PBS/0.1% gelatin in the dish [See SOP001] (tilt the plate to cover the entire surface with the solution). Wait at least 10 min. Just before adding the cells to the plates, aspirate the PBS/0.1% gelatin (do not allow the plates to dry).

Day 1.

2. Prewarm all the solutions in a 37°C water bath (at least 20 min). In case the buffer is thawed, mix very well before using.
3. Add 25 µM chloroquine (10 µl of the 25 mM solution) to the cell culture medium (not necessary to change the medium). Place the plates back in the incubator for at least 10 min.

The addition of chloroquine to the medium appears to increase retroviral titer by approximately two fold. This effect is presumably due to the lysosomal neutralizing activity of the chloroquine (3). It is extremely important that the length of chloroquine treatment does not exceed 12 hours. Longer periods of chloroquine treatment have a toxic effect on the cells causing a decrease in retroviral titers.

4. In a 15 ml Falcon tube prepare the following master mix:

	Volume or quantities
H_2O	Variable
pCMV delta R8.91	**37,5 µg**
pMD.G	**12,5 µg**
Lentiviral vector (e.g. Prom.lti) encoding the gene of interest	**50 µg**
$CaCl_2$	250 µl
2xHepes	2500 µl
FINAL VOLUME	5 ml

All the plasmid should be prepared using Qiagen or Genomed Maxiprep kits and ethanol precipitated. In case the yield of the plasmid is not very high it should be purified using the CsCl purification method.

- Ethanol Precipitation:

a- Carefully calculate the volume of your DNA solution.
b- Add 1/10 volume of 3 M Sodium Acetate pH 5.2, mix well.
c- Add 2 volumes of cold absolute ethanol.
d- Keep at -20° C for at least 1 hour.
e- Centrifuge 10' at maximum speed.
f- Discard supernatant and wash pellet with ethanol 70 % three times.
g- Air dry and resuspend in TE.
h- Measure DNA concentration.

5. Mix well, by passing 5 times the solution through a 5 ml pipette.
6. Exactly 60 seconds after mixing the 2xHepes with the $CaCl_2$-DNA mixture, add 1 ml precipitate per plate.
7. Incubate for 6-8 hours in an incubator (37°C - 5% CO_2).
8. Remove medium, wash once with PBS and put fresh medium containing penicillin and streptomycin to avoid contamination (the DNA used for the transfection is generally not sterile!).
9. 48 hours after the transfection, collect the supernatant of the plates in a 50 ml Falcon Tube.
10. Centrifuge for 5' at 1500 rpm (~400 *g*) at 4°C to pellet the detached cells (ALC PK 130 centrifuge, rotor N° T535).
11. Filter the cleared virus-containing supernatant through a 0.45 µm filter, wrapping everything in a towel humidified with biocidal to avoid aerosols.
12. Once the virus is filtered, aliquot in 15 ml falcon tubes.

Note: The size of the aliquots may change according the use you will give to your virus.

13. Keep the virus at -80°C.

Freezing does not appear to cause more than a 2-fold drop in titer, as long as the cells do not undergo more than one freeze/thaw cycle. If the cells undergo more than one freeze/thaw cycle, there is a significant drop in retroviral titer.

14. If the virus encodes for a protein that can be detected, calculate functional titer by immunocytochemistry (See SOP011 *Immunocytochemistry*), as detailed below [for siRNA encoding lentiviruses you may calculate your functional titer by monitoring by western blot the conditions that lead to the best decrease of the targeted proteins, (See SOP006.1 *Western Blot*)].

1. Laminin-Polylysin coating

PolyLysine.

Comes as 20 mg/vial. Add sterile H_2O to the vial to a final volume of 1 ml to make a 1 mg/ml stock solution (in a 50 ml falcon tube). Make 1 ml (=1 mg) aliquots. Store at -20 C.

Laminin.

Comes as 1 mg/vial. Add sterile H_2O to the vial to a final volume of 1 ml to make a 1 mg/ml stock solution. Make 100 µl (=100 µg) aliquots. Store at -70 C.

Coating Coverslips.

1. Thaw 1 tube of polylysine and laminin solution.
2. Add laminin, poly-lysine to 25 ml of sterile H_2O.
3. Use 50 µl solution for each coverslips. Place at 37° C for 2 hrs.
4. Rinse 3x with PBS, and use to plate cells.

2. Plate the appropriate number of cells (according to your cells type) in six-well dishes, with two laminin-coated coverslips in each well.

Cells	Number per well (6 well-plates)	Medium	Coating
GAP $^{+/+}$ and derived cell lines	$3\text{-}5 \cdot 10^4$	DMEM; 10% NBCS	Polylysin /Laminin
HEK 293 and derived cell lines	$35 \cdot 10^4$	DMEM; 10% NBCS	Polylysin /Laminin
β-Tc-Tet and derived cell lines	10^5	DMEM (without L-Glu); 15% Horse Serum (Heat decomplemented); 2,5% FCS; 2 mM L-Glu; 10 mM Hepes pH 8; 1 mM Na-Pyruvate	Polylysin /Laminin

3. Incubate cells at 37°C, for 12-18 hours.

Important: infect cells when they are not more than 50% confluent.

4. The following day, thaw the frozen virus at 37°C (shake often) and once nearly completely thawed, keep on ice. The virus should stay at 0°C all the time.
5. Add various amounts of viruses according to the table below, add 2 µl of a 5 mg/ml polybrene stock solution and complete with fresh medium to 3 ml.

Cell #	**0 ml**	**0.25 ml**
0.5 ml	**1 ml**	**2 ml**

6. Immediately thereafter, seal the plates with parafilm and centrifuge them 45' at 2'500 rpm (~800 *g*) (ALC PK 130 centrifuge, rotor N° T537).
7. Incubate overnight in incubator (37°C - 5% CO_2).

8. Change medium after 24 hours.
9. Remove medium 72 hs after infection and rinse once with 2 ml of PBS.
10. Fix cells by adding 1 ml of PBS-2% paraformaldehyde-3% Sucrose, for 15 minutes.
11. The following immunocytochemistry steps can be performed on the bench *(See SOP011)*.
12. Knowing the number of cells at the moment of infection and the smallest volume that leads to expression of the gene of interest in ~100% of the cells, you can estimate the number of infective particles per ml.

References

1. Jordan et al. - Nucl. Acid Res. (1996) **24**:596. For transfection.
2. Dull, T. et al. - J.Virol. 72.11 (1998): 8463-71. For 3rd generation lentiviral vectors.
3. Mulligan, R.C. and Berg, P. - PNAS 78, 2072-2076 (1981)

Apparatus

Hybridization oven. *Biometra OV 3 – C Lab*
Agarose gel electrophoresis system.

Materials and reagents

1. *Hybond N+ membrane (30 cm × 3 m) 1 roll*. (Amersham Biosciences Cat. N° RPN303B).
2. *Chromatography paper 3MM Chr (46x57 cm) 100 sheets.* (Whatman Cat. N° 3030917)
3. *Random primed labeling kit.* (Roche Applied Science Cat. N° 1004760)
4. *High Pure PCR purification kit (50 purifications).* (Roche Applied Science Cat. N° 1732668)
5. *[α-^{32}P]-dCTP 250 µCi.* (CHIMBAR Ref N° R00031).
6. *Hybridization bottle, 260 × 40 mm* (Amersham Biosciences Cat. N° RPN2516)
7. *Hybridization bottle, 170 × 40 mm* (Amersham Biosciences Cat. N° RPN2517)
8. *JETSORB Gel Extraction Kit, 150 Preps* (Genomed Cat N° 110150)

Materials and reagents	**Source/Company**	**Code/quantities**
NaCl	Fluka	IBCM Stock /1 kg
Ammonium Acetate 7.5 M	Sigma	A-2706 / 100 ml
UltraPure™ Phenol:Chloroform:Isoamyl Alcohol (25:24:1, v/v)	Gibco	15593-031 / 100 ml
SDS	CHIMBAR	C00495 / 4 kg
Proteinase K	Roche	3 115 828 / 5 ml
Sodium phosphate dibasic	Sigma	500 gr
Tris	CHIMBAR	C00511 / 4 kg
EDTA	Fluka	03620 / 1 kg
Phosphoric Acid	Acros	201140010 / 1 L
Albumin, Bovine	Sigma	A7906 / 100 gr
Sodium Citrate	Sigma	C-8532 / 5 kg

Digestion Buffer. (100 mM NaCl ; 10 mM Tris-HCl pH 8; 25 mM EDTA pH 8; 0.5 % SDS; 0.1 mg/ml Proteinase K)

5 M NaCl	200 µl
100 mM Tris-HCl pH 8	1 ml
0.5 M EDTA pH 8	500 µl
20 % SDS	250 µl
Proteinase K (16-20 mg/ml)	5.5 µl
H_2Odd up to	10 ml

Hybridization Solution. (0.5 M Sodium Phosphate pH 7.2; 7% SDS, 1mM EDTA and 1% BSA).

1 M Phosphate Buffer pH 7.2	150 ml
SDS 20 %	105 ml
0.5 M EDTA pH 8	0.6 ml
BSA	3 gr
H_2Odd up to	300 ml

Neutralizing solution. (1,5 M NaCl; 0.5 M Tris-HCl 7,2 and 1 mM EDTA pH 8)

5 M NaCl	300 ml
1 M Tris-HCl pH 7.2	500 ml
0.5 M EDTA pH 8	2 ml
H_2Odd up to	1000 ml

Washing Solution I (40 mM Sodium Phosphate pH 7.2; 1% SDS,; 5 mM EDTA and 0.5 % BSA)

1 M Phosphate Buffer pH 7.2	40 ml
20% SDS	50 ml
0.5 M EDTA pH 8	10 ml
BSA	5 gr
H_2Odd up to	1000 ml

20x SSC. (3 M Sodium Chloride; 0.3 M Sodium Citrate, pH 7.0)
Weight 175.5 gr of NaCl and 88.2 gr of Sodium Citrate, complete to 800 ml with nanopure water, adjust the pH with NaOH and once the pH adjusted complete to 1000 ml with nanopure water.

$NaHPO_4$1 M pH 7.2.
Weight 71 gr of Na_2HPO_4 and add 4 ml of 85% H_3PO_4. Complete with water and check pH. Other phosphate buffers can be prepared from this stock solution.

EDTA 0.5 M pH 8 (1 liter).
Weight 186.1g disodium EDTA-$2H_2O$ and add 800 ml distilled water. Stir vigorously (it takes forever! heat OR add NaOH to help dissolution, but in this case do not heat as NaOH is volatile. Adjust the pH to 8.0 with NaOH 10 M and later 1 M.

Tris-EDTA (TE) buffer. (10 mM Tris; 1 mM EDTA; pH 8.0)

1 M Tris pH 8.0	1 ml
0.5 M EDTA pH 8.0	0.2 ml
H_2Odd	98.8 ml

Autoclave

Procedure

1. General remarks.
   1.1. Always test more than one probe!!!!!!!!.

2. Genomic DNA purification (Current Protocols)
   2.1. Trypsinize and collect cells, centrifuge 10' at 500*xg* and discard supernatant.
   2.2. Resuspend cells with 1 to 10 ml of ice-cold PBS. Centrifuge 5' at 500*xg* and discard supernatant. Repeat this resuspension and centrifugation step.
   2.3. Resuspend cells in 1 volume of digestion buffer. (For <3x 10^7 cells use 0.3 ml digestion buffer. For larger number of cells use 1 ml digestion buffer/10^8 cells.
   2.4. Incubate the samples with shaking at 50° C for 12 to 18 hr.
   2.5. Thoroughly extract the samples with an equal volume of phenol/chloroform/isoamyl alcohol (24.5:24.5:1).
   2.6. Centrifuge 10' at 1700*xg* in a swinging bucket rotor *(Sigma centrifuge 4K15, rotor N° 11'140)*.
   2.7. If the phases are not well separated, add another volume of digestion buffer, omitting Proteinase K, and repeat the centrifugation.
   2.8. Transfer the aqueous (top) layer to a new tube and add ½ volume of 7.5 M ammonium acetate and 2 (original) volumes of 100% ethanol. Centrifuge 2' at 1700 x g.
   2.9. Rinse the pellet with 70% ethanol, decant ethanol and air dry the pellet.
   2.10. Resuspend DNA in TE buffer until dissolved. DNA may be shaken gently at room temperature or at 65° C for several hours to facilitate solubilization.
   2.11. Measure DNA concentration and quality.

The concentration of DNA is read by measuring the absorbance of a sample at 260 nm on a spectrophotometer. The OD260/OD280 ratio can be determined in order to assess the purity of the sample. If this ratio is 1.8 - 2.0, the absorption is probably due to nucleic acids. A ratio less than 1.8

indicates that there may be proteins and/or other UV absorbers in the sample, in which cases it is advisable to re-precipitate the DNA. A ratio higher than 2.0 indicates that the samples may be contaminated with chloroform or phenol and should be re-precipitated with ethanol.
DNA measures are estimated from the 260 nm readings. The values are in OD (optical density units) where 1 OD = 50 ng/µl. Therefore if you get a value of 0.2 OD, your concentration is 50*0.2 = 10 ng/µl. If you have made a dilution of your DNA you need to multiply again for the dilution factor.
For example, if you have used 2 µl of your DNA sample in 98 µl of water (dilution 1/50) you need to multiply the previous value by your dilution factor. Therefore a reading of 260 nm = 0.2 OD represents 10*50 = 500 ng/µl in your original DNA sample. In summary, with a 1/50 dilution, multiplication of the 260 nm OD by 2500 (50*50) will provide the final concentration.

3. Digestion.
   3.1. Digest your genomic DNA in the following conditions.

DNA	15 - 20 µg
Enzyme	10 U
Buffer 10x	4 µl
H_2Odd	up to 40 µl

Perform the digestion overnight at 37° C, preferentially in a bacterial incubator, to avoid evaporation.

3.2. Once the digestion is finished, check if the digestion was complete by taking 2 µl of the digestion, mixed with 4 µl of LB and loaded in a gel. Once the blue is in the middle of the gel, check the gel in the transiluminator and see whether there is a smear (indicating that the digestion indeed occurred).

If the digestion is complete continue with the following steps.

4. Transfer
   4.1. After fractionating the DNA by gel electrophoresis, use a razor blade to cut off a small triangular piece from the bottom right-hand corner of the gel for orientation purposes.
   4.2. Denature DNA as follows:
   - 10’ in 0.25 N HCl or until loading gel becomes yellow. (Depurination)
   - 30’ in 0.4 M NaOH. (Denaturation)
   - 20’ in 1.5 M NaCl; 0.5 M Tris-HCl pH 7.2; 1 mM EDTA pH 8. (Neutralization)
   - 5' in 20X SSC.

   4.3. While denaturing DNA, using gloves and a fresh scalpel, cut a piece of nylon membrane ~1 mm larger than the gel in each dimension. Also cut eight sheets of thick blotting paper (Whatman3MM paper) to the same size as the membrane.
   4.4. Float the membrane on the surface of a dish of H_2Odd until it wets completely from beneath, then immerse the membrane in 2x SSC and finally into the transfer buffer for at least 5 minutes. Using a clear scalpel blade cut a corner of the membrane to match the corner cut from the gel.
   4.5. Assembly of the Transfer Apparatus.

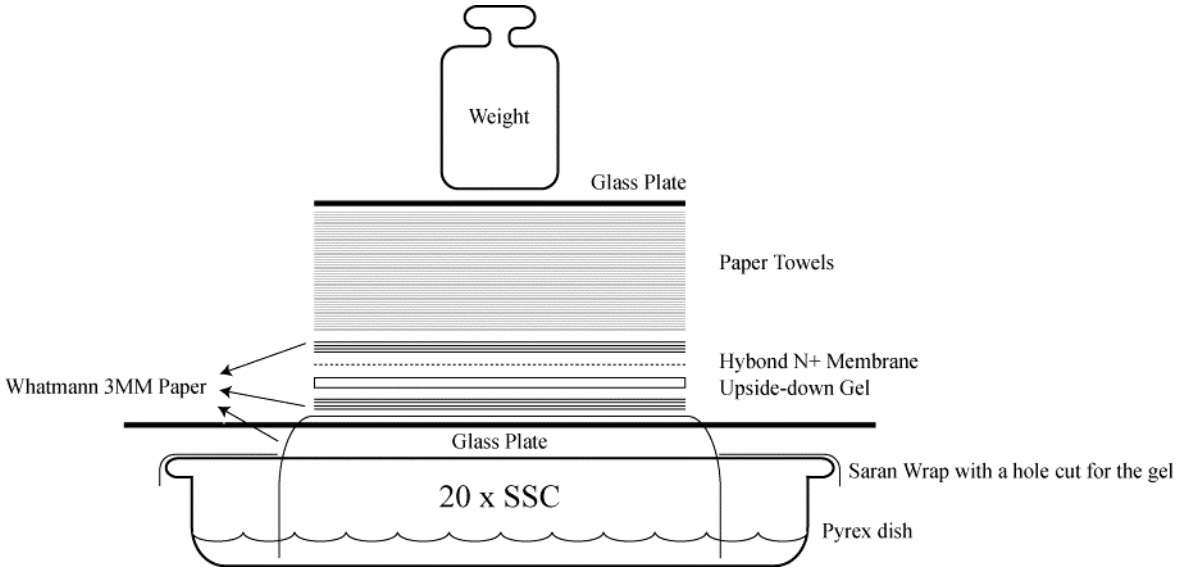

4.6. Place a piece of Whatman paper on a sheet of Plexiglas or glass plate to form a support that is longer and wider than the gel. The ends of the paper should drape over the edges of the plate. Place the support inside a baking dish.

4.7. Fill the baking dish with the transfer buffer. Once the Whatman paper is thoroughly wet, smooth out all air bubbles. Add 4 sheets of wet Whatman paper, and smooth out all air bubbles.

4.8. Place the gel upside-down on the support so that it is centered on the wet blotting paper.

4.9. Wet the gel with transfer buffer. Surround gel with plastic wrap or parafilm to prevent the paper towels to come in contact with the wet paper below the gel.

4.10. Place the wet membrane so that the cut corners are aligned. Try to avoid the formation of bubbles between the gel and the membrane.

4.11. Wet two of the Whatman papers in the transfer buffer and place them on top of the wet membrane. Roll a pipette across the surface of the membrane to smooth away any air bubbles.

4.12. Place the dry Whatman papers over the wet Whatman paper, and eliminate bubbles as before.

4.13. Cut or fold a stack of paper towels (5-8 cm high) just smaller than the blotting papers. Put a glass plate on top of the stack and weigh it down with a 400-g weight. Prevent evaporation of the transfer solution by sealing with plastic wrap or parafilm on either end of the tray.

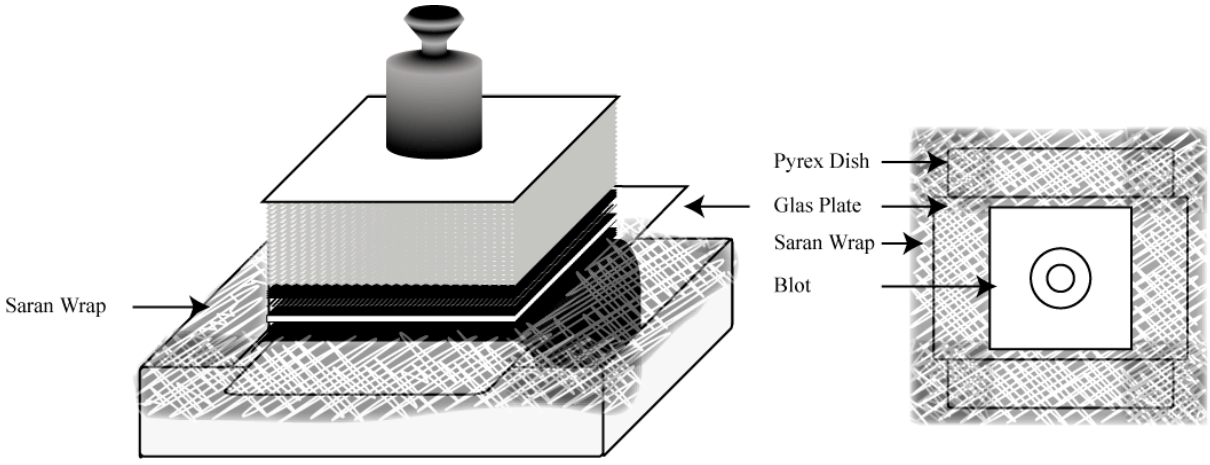

4.14. Transfer overnight.

4.15. Next day, peel the membrane. Before peeling the membrane indicate the positions of the wells in the membrane making small holes in the membrane with a needle.
4.16. Wash the filter/membrane briefly in 2 x SSC.
4.17. Air dry (approximately 30').
4.18. Fix the DNA to the membrane by crosslink (Autocrosslink 1200 J, using the Stratalinker® UV Crosslinker from Stratagene, located in Romano Regazzi's Lab). Any membrane not used immediately in hybridization reactions should be thoroughly dried, wrapped loosely in aluminium foil or blotting paper, and stored at room temperature, preferably under vacuum.

5. Probe labeling
5.1. Add to 25 ng template DNA (linear) sterile double distilled water to a final volume of 9 µl in an eppendorf microfuge tube.

Template DNA can be obtained from a PCR or the digestion of a plasmid. In both cases, the band should be purified from the gel using the **JETSORB Gel Extraction Kit from Genomed.**

Protocol:

1. Solubilization of agarose.
Excise the agarose gel slice, determine its weight and transfer the slice into a suitable tube. For each 100 mg gel slice add the following kit components:
- 300 µl buffer A1
- 10µl JETSORB suspension *(Before use, resuspend JETSORB carefully by vortexing)*

2. DNA Binding
Vortex and incubate the assay at 50°C for 15 min. Mix every 3 min during incubation. After this, centrifuge (30 sec / ³10,000 g) and remove the supernatant completely with a pipette.

3. High Salt Wash
Wash (resuspend) the pellet once with 300 µl of buffer A1. Centrifuge as before to recover JETSORB and remove the supernatant with a pipette. Resuspend the pellet by vortexing and/or flicking the tube.
Vortexing is only recommended for DNA fragments up to 5 kb.

4. Low Salt Wash
Wash (resuspend) the pellet with 300 µl of reconstituted buffer A2. Centrifuge as before and remove the supernatant with a pipette. Repeat step 4!

5. JETSORB Drying
Dry the JETSORB pellet by air or under vacuum.
Comments: Before DNA elution, the pellet must be free of ethanol. The pellet turns snow white when it is completely dry.

6. DNA Elution
Add 20 µl TE buffer (10 mM Tris/HCl, 1 mM EDTA, pH 8.0) or water, resuspend the pellet as before and incubate for 5 min at 50°C. Flick the tube once during incubation. Centrifuge as before and transfer the supernatant into a new tube.

5.2. Denature the DNA by heating in a boiling water bath for 10 min at 95°C and chilling quickly in an ice/water bath. ***Note*:** Complete denaturation is essential for efficient labelling
5.3. Add the following to the freshly denatured probe on ice:

Reagent	**Volume**
dNTPs Stock Mix	3 µl
Reaction mixture (vial 6)	2 µl
[α-32P]dCTP, 3000 Ci/ mmol,	5 µl
Klenow enzyme (vial 7)	1 µl

• Incubate at 37°C for 30 min.
5.4. Stop the reaction by adding 2 µl 0.2 M EDTA (pH 8.0) and/or by heating to 65 °C for 10 min.

Note: Longer incubation can increase the yield of labelled DNA.

6. Hybridization
   6.1. Put the membrane in the roller bottle and add 10 ml the hybridization solution for 1 small bottle (or 20 ml for a big bottle), pre-warmed at 65° C.
   6.2. Incubate at least 30' at 65° C in the oven.
   6.3. Denature double stranded probes by heating the probe for 5' at 100° C (in a thermal block or in boiling water) and chill rapidly on ice water. Add the probe.
   6.4. Incubate O/N at 65° C.
   6.5. Wash the membrane first with a few ml of Washing Solution, to eliminate the bulk radioactivity.
   6.6. Wash twice for 30' at the hybridization temperature with half filled bottle with Washing Solution (pre-warm the solutions)
   6.7. After the last wash, briefly wash the membrane in tap water, to eliminate the washing solution.
   6.8. Remove most of the liquid from the membrane by placing it on a pad of paper towels. Place the damp membrane on a sheet of Saran Wrap.
   6.9. Cover the membrane with a sheet of Saran Wrap, and expose the membrane to X-ray film for 16-24 hs at -70° C with an intensifying screen to obtain an auto radiographic image. Put at least two films, develop the first one, one or two days after, and keep one in case you need to expose longer.